AFFDL-TR-67-28

THE VIBRATION AND BUCKLING CHARACTERISTICS OF CYLINDRICAL SHELLS UNDER AXIAL LOAD AND EXTERNAL PRESSURE

WILLIAM F. BOZICH, CAPT., USAF

TECHNICAL REPORT AFFDL-TR-67-28

MAY 1967

AIR FORCE FLIGHT DYNAMICS LABORATORY
RESEARCH AND TECHNOLOGY DIVISION
AIR FORCE SYSTEMS COMMAND
WRIGHT-PATTERSON AIR FORCE BASE, OHIO

NOTICES

When Government drawings, specifications, or other data are used for any purpose other than in connection with a definitely related Government procurement operation, the United States Government thereby incurs no responsibility nor any obligation whatsoever; and the fact that the Government may have formulated, furnished, or in any way supplied the said drawings, specifications, or other data, is not to be regarded by implication or otherwise as in any manner licensing the holder or any other person or corporation, or conveying any rights or permission to manufacture, use, or sell any patented invention that may in any way be related thereto.

Copies of this report should not be returned to the Research and Technology Division unless return is required by security considerations, contractual obligations, or notice on a specific document.

200 - June 1967 - CO192 - 36-887

AFFDL-TR-67-28

THE VIBRATION AND BUCKLING CHARACTERISTICS OF CYLINDRICAL SHELLS UNDER AXIAL LOAD AND EXTERNAL PRESSURE

WILLIAM F. BOZICH, CAPT., USAF

ABSTRACT

The Galerkin method is applied to Flugge's differential equations for the vibration of a cylindrical shell under axial load and external pressure to obtain a 3N x 3N characteristic equation in matrix form. N is the number of terms in the assumed series of displacement functions for the u, v, and w displacements which can be selected to satisfy various boundary conditions. For the freely-supported cylinder, an exact solution exists, and the various assumed modes uncouple reducing the problem to the solution of a 3 x 3 characteristic equation for each mode.

The third order characteristic equation for the freely-supported cylinder was solved for a wide range of shell parameters. The natural vibration frequencies and buckling values for axial load and external pressure for all three eigenvalues associated with each mode are presented in a series of figures. The square of the vibration frequency for any mode was found to vary linearly with axial load, and approximately linearly with an external pressure loading for modes with two or more circumferential waves.

FOREWORD

This report was prepared by the Vehicle Dynamics Division, Air Force Flight Dynamics Laboratory, and represents an in-house effort initiated under Project No. 1370 "Dynamic Problems in Flight Vehicles," Task No. 137003, "Prediction and Prevention of Dynamic Aerothermoelastic Instabilities." The work was administered under the direction of the Air Force Flight Dynamics Laboratory, Research and Technology Division, Air Force Systems Command, Wright-Patterson Air Force Base, Ohio, with Capt. W. F. Bozich of the Aerospace Dynamics Branch acting as Project Engineer.

This work was initiated in order to develop a better understanding of the dynamic behavior of cylinders under initial stress. This investigation was conducted during the period June 1965 through August 1966. This report was released by the author for publication as an RTD Technical Report in August 1966.

This technical report has been reviewed and is approved.

Walter J. Mykytow

WALTER J. MYKYTOW
Asst. for Research & Technology
Vehicle Dynamics Division

TABLE OF CONTENTS

LIST OF ILLUSTRATIONS

LIST OF ILLUSTRATIONS (CONT'D)

LIST OF ILLUSTRATIONS (CONT'D)

LIST OF ILLUSTRATIONS (CONT'D)

SYMBOLS

Symbol	Definition
a	radius of cylinder
A	amplitude of axial displacement
A_j	constant associated with displacement in the x direction
B	amplitude of tangential displacement
B_j	constant associated with displacement in the ϕ direction
C	amplitude of radial displacement
C_j	constant associated with displacement in the z direction
$D = \frac{Eh}{(1-\nu^2)}$	stiffness parameter
D_{ij}	terms in the generalized stiffness matrix
E	modulus of elasticity
GJ	torsional rigidity
h	shell thickness
H_{ij}	same as D_{ij}, except $q_1 = 0$ in all terms
I_o	moment of inertia per unit length
I_{ij}	integral
K^{ij}	third order matrix (generalized stiffness)
$k = \frac{h^2}{12a^2}$	non-dimensional thickness to radius parameter
ℓ	length of shell
L_{ij}	differential operator
m	number of axial half-waves
n	number of circumferential waves
M^{ij}	third order matrix (generalized mass)
p	uniform normal pressure (positive inward)
$\bar{P}$	axial load on shell boundary (force/unit length)

SYMBOLS (CONT' D)

Symbol	Definition
$q_1 = \frac{\rho a}{D}$	non-dimensional pressure parameter (positive for external pressure)
q_{1o}	value of q_1 for buckling due to external pressure
$q_2 = \frac{P}{D}$	non-dimensional axial load parameter
q_{2o}	value of q_2 for buckling due to axial load
t	time
u	axial displacement (x direction)
$U_{(x)}$	assumed displacement function for u
v	tangential displacement (ϕ direction)
$V_{(x)}$	assumed displacement function for v
w	radial displacement (z direction)
$W_{(z)}$	assumed displacement function for w
x	axial coordinate
$X = \begin{Bmatrix} u \\ v \\ w \end{Bmatrix}$	matrix of displacements
$X_i = \begin{Bmatrix} A_i \\ B_i \\ C_i \end{Bmatrix}$	matrix of displacement coefficients
$\delta X = \begin{Bmatrix} \delta u \\ \delta v \\ \delta w \end{Bmatrix}$	variation of displacements
z	radial coordinate
$\gamma^2 = \frac{\rho a^2 (1-\nu^2)}{E}$	density parameter
ρ	density of shell material
ν	Poisson' s ratio
ϕ	circumferential coordinate
$\Phi\ (x)$	mode shape
ω	circular frequency

SYMBOLS (CONT' D)

Symbol	Definition
ω_0	value of circular frequency for the unloaded cylinder
$\lambda = \frac{m\pi a}{\ell}$	axial wavelength parameter
$\Delta = \gamma^2\omega^2 + q_2\lambda^2$	eigenvalue expression
$\overline{\Delta} = \gamma^2\omega^2 + q_2\lambda^2 + q_1 n^2$	eigenvalue expression
$[\ ]$	rectangular or square matrix
$\{\ \}$	column matrix
$\{\ \}^T$	row matrix

SECTION I

INTRODUCTION

In recent years thin shells have been used extensively for aerospace applications because of the high structural efficiency of this type of construction. Space capsules, boosters, space stations, and large fuel tanks for hypersonic cruise vehicles are examples of stiffened and unstiffened shell configurations. In many cases these shells are pressurized and subjected to some type of loading. These loads and internal pressure can have a significant effect on the vibration characteristics. The purpose of this investigation is to examine the combined effects of axial load and external pressurization on the vibration characteristics of thin cylindrical shells and present the results in a suitable form for use in design.

Arnold and Warburton (References 1 and 2) examined the vibration characteristics of freely-supported shells and plotted results for several radius to thickness ratios. They indicated that three natural frequencies exist for each modal pattern. The different frequencies are associated with motions that are primarily radial, longitudinal, or torsional. The lowest frequency is usually associated with motion which is primarily radial. Forsberg (Reference 5) obtained an exact solution for the cylindrical shell using Flugge's equations of motion with various homogeneous boundary conditions. Fung (References 7, 8, and 10) obtained analytical and experimental results for the effects of internal pressurization on the vibration characteristics of cylindrical shells. Fung and Sechler (Reference 9) and Weingarten, Morgan, and Seide (Reference 13) obtained results for the buckling of cylindrical shells subjected to internal pressurization and axial load. A recent paper by Herrmann and Shaw (Reference 11) on the vibration of thin shells under initial stress included the change in magnitude and direction of the applied load as a result of deformation and contains a comparison of experimental data with various shell theories.

This investigation applies the Galerkin method to Flugge's cylindrical shell equations to formulate a characteristic equation valid for arbitrary boundary conditions. By selecting a series of functions for each of the displacements u, v, and w various boundary conditions can be handled. For the special case of an unloaded, freely-supported cylinder, Arnold and Warburton (Reference 1) obtained an exact solution. This same solution was obtained by Flugge (Reference 4) for the buckling of a cylinder subjected to axial load and internal pressurization, and used by Herrmann (Reference 11) indicating that the same deflection mode shape satisfies the combined problem. When a series of functions of this form were substituted into the equations obtained in this investigation, it is shown that the terms in the series uncouple and Flugge's buckling results are obtained if the frequency is assumed to be zero. Vibration results comparable to those of Arnold and Warburton are obtained if the load parameters are assumed to be zero.

For this special case the axial load parameter and frequency parameter can be combined into a single eigenvalue expression. The eigenvalue spectrum for this case is plotted in nondimensional form for a wide range of shell parameters covering radial, longitudinal, and axial deformation modes. From these charts and tables the critical buckling conditions or vibration frequencies can be obtained for the freely-supported cylinder subjected to an axial load and external pressurization.

SECTION II

THEORETICAL DEVELOPMENT

The coordinate system used in the analysis is the same as that of Flugge and is given in Figure 1. The equations of motion for thin cylindrical shells including the effects of a uniform normal pressure and an axial load can be obtained by adding the inertia terms to Flugge's static equations given in Reference 4.

$$a^2\frac{\partial^2 u}{\partial x^2}+\frac{(1-\nu)}{2}\frac{\partial^2 u}{\partial \phi^2}+\frac{(1+\nu)}{2}a\frac{\partial^2 v}{\partial x\,\partial \phi}+\nu a\frac{\partial w}{\partial x}+k\left[\frac{(1-\nu)}{2}\frac{\partial^2 u}{\partial \phi^2}\right.$$

$$\left.-a^3\frac{\partial^3 w}{\partial x^3}+\frac{(1-\nu)}{2}a\frac{\partial^3 w}{\partial x\,\partial \phi^2}\right]-q_1\left(\frac{\partial^2 u}{\partial \phi^2}-a\frac{\partial w}{\partial x}\right)-q_2 a^2\frac{\partial^2 u}{\partial x^2}-\gamma^2\frac{\partial^2 u}{\partial t^2}=0 \quad (1)$$

$$\frac{(1+\nu)}{2}a\frac{\partial^2 u}{\partial x\,\partial \phi}+\frac{\partial^2 v}{\partial \phi^2}+\frac{(1-\nu)}{2}a^2\frac{\partial^2 v}{\partial x^2}+\frac{\partial w}{\partial \phi}+k\left[\frac{3}{2}(1-\nu)a^2\frac{\partial^2 v}{\partial x^2}\right.$$

$$\left.-a^2\frac{(3-\nu)}{2}\frac{\partial^3 w}{\partial x^2\,\partial \phi}\right]-q_1\left(\frac{\partial^2 v}{\partial \phi^2}+\frac{\partial w}{\partial \phi}\right)-q_2 a^2\frac{\partial^2 v}{\partial x^2}-\gamma^2\frac{\partial^2 v}{\partial t^2}=0 \quad (2)$$

$$\nu a\frac{\partial u}{\partial x}+\frac{\partial v}{\partial \phi}+w+k\left[\frac{(1-\nu)}{2}a\frac{\partial^3 u}{\partial x\,\partial \phi^2}-a^3\frac{\partial^3 u}{\partial x^3}-\frac{(3-\nu)}{2}a^2\frac{\partial^3 w}{\partial x^2\partial \phi}+a^4\frac{\partial^4 w}{\partial x^4}\right.$$

$$\left.+2a^2\frac{\partial^4 w}{\partial x^2\,\partial \phi^2}+\frac{\partial^4 w}{\partial \phi^4}+2\frac{\partial^2 w}{\partial \phi^2}+w\right]+q_1\left(a\frac{\partial u}{\partial x}-\frac{\partial v}{\partial \phi}+\frac{\partial^2 w}{\partial \phi^2}\right)+q_2 a^2\frac{\partial^2 w}{\partial x^2}+\gamma^2\frac{\partial^2 w}{\partial t^2}=0 \quad (3)$$

where

$$k=\frac{h^2}{12\,a^2}\ ,\quad q_1=\frac{pa}{D}\ ,\quad q_2=\frac{P}{D}\ ,\quad \gamma^2=\frac{\rho a^2(1-\nu^2)}{E}$$

The equations of motion can be written in the following matrix form

$$\left[L\right]\left\{X\right\}=0 \quad (4)$$

or

$$\begin{bmatrix} L_{11} & L_{12} & L_{13} \\ L_{21} & L_{22} & L_{23} \\ L_{31} & L_{32} & L_{33} \end{bmatrix}\begin{Bmatrix} u \\ v \\ w \end{Bmatrix}=0 \quad (5)$$

The differential operators L_{ij} can be written as follows after multiplying equations 1 and 2 by -1.

$$L_{11} = -a^2(1-q_2)\frac{\partial^2}{\partial x^2} + \left[q_1 - \frac{(1-\nu)}{2}(1+k)\right]\frac{\partial^2}{\partial \phi^2} + \gamma^2\frac{\partial^2}{\partial t^2} \tag{6}$$

$$L_{12} = -\frac{(1+\nu)}{2}a\frac{\partial^2}{\partial x\,\partial \phi} \tag{7}$$

$$L_{13} = -a(\nu+q_1)\frac{\partial}{\partial x} + ka^3\frac{\partial^3}{\partial x^3} - k\frac{(1-\nu)}{2}a\frac{\partial^3}{\partial x\,\partial \phi^2} \tag{8}$$

$$L_{21} = -\frac{(1+\nu)}{2}a\frac{\partial^2}{\partial x\,\partial \phi} \tag{9}$$

$$L_{22} = -a^2\left[\frac{(1-\nu)}{2}(1+3k) - q_2\right]\frac{\partial^2}{\partial x^2} - (1-q_1)\frac{\partial^2}{\partial \phi^2} + \gamma^2\frac{\partial^2}{\partial t^2} \tag{10}$$

$$L_{23} = -(1-q_1)\frac{\partial}{\partial \phi} + \frac{k(3-\nu)}{2}a^2\frac{\partial^3}{\partial x^2\partial \phi} \tag{11}$$

$$L_{31} = a(\nu+q_1)\frac{\partial}{\partial x} + \frac{k(1-\nu)}{2}\frac{a\partial^3}{\partial x\partial \phi^2} - \frac{ka^3\partial^3}{\partial x^3} \tag{12}$$

$$L_{32} = (1-q_1)\frac{\partial}{\partial \phi} - \frac{k(3-\nu)}{2}\frac{a^2\partial^3}{\partial x^2\partial \phi} \tag{13}$$

$$L_{33} = 1 + k\left[\frac{a^4\partial^4}{\partial x^4} + \frac{2a^2\partial^4}{\partial x^2\partial \phi^2} + \frac{\partial^4}{\partial \phi^4} + \frac{2\partial^2}{\partial \phi^2} + 1\right] + q_1\frac{\partial^2}{\partial \phi^2} + q_2a^2\frac{\partial^2}{\partial x^2} + \gamma^2\frac{\partial^2}{\partial t^2} \tag{14}$$

To obtain a solution by Galerkin's method, the equations of motion are multiplied by the variation of the displacements, δx, and the result integrated over the volume of the shell (Reference 12). Since the integration over the thickness has already been performed in deriving the equations, none of the factors is a function of z. It is therefore sufficient to integrate over the shell area. This can be written as follows:

$$\iint_A \{\delta x\}^T [L] \{x\}\, dA = 0 \tag{15}$$

The displacements u, v, and w are periodic in ϕ with period 2π. Simple harmonic motion is assumed and the displacements are written in the form of a product.

$$u = U(x)\cos n\phi\, e^{i\omega t} \tag{16}$$

$$v = V(x) \sin n\phi \, e^{i\omega t} \tag{17}$$

$$w = W(x) \cos n\phi \, e^{i\omega t} \tag{18}$$

The form of the solution given previously separates the various Fourier components in ϕ, since for each integer value of n the functions in ϕ satisfy the differential equations (Equations 1 to 3,. It is further assumed that U, V, and W can be expressed as a series of functions Φ which satisfy the appropriate boundary conditions for u, v, and w.

$$U(x) = \sum_{j=1}^{M} A_j \Phi_j^u (x) \tag{19}$$

$$V(x) = \sum_{j=1}^{M} B_j \Phi_j^v (x) \tag{20}$$

$$W(x) = \sum_{j=1}^{M} C_j \Phi_j^w (x) \tag{21}$$

A_j, B_j, and C_j in Equations 19 to 21 are arbitrary constants. The displacement X can now be written

$$\{X\} = \begin{Bmatrix} u \\ v \\ w \end{Bmatrix} = \begin{Bmatrix} \cos n\phi \, e^{i\omega t} \sum_{j=1}^{M} A_j \Phi_j^u (x) \\ \sin n\phi \, e^{i\omega t} \sum_{j=1}^{M} B_j \Phi_j^v (x) \\ \cos n\phi \, e^{i\omega t} \sum_{j=1}^{M} C_j \Phi_j^w (x) \end{Bmatrix} \tag{22}$$

The variation δX can be written

$$\delta X = \begin{Bmatrix} \delta u \\ \delta v \\ \delta w \end{Bmatrix} = \begin{Bmatrix} \cos n\phi \, e^{i\omega t} \sum_{i=1}^{N} \delta A_i \Phi_i^u (x) \\ \sin n\phi \, e^{i\omega t} \sum_{i=1}^{N} \delta B_i \Phi_i^v (x) \\ \cos n\phi \, e^{i\omega t} \sum_{i=1}^{N} \delta C_i \Phi_i^w (x) \end{Bmatrix} \tag{23}$$

Equations 22 and 23 are substituted into Equation 15 and the integrand is expanded.

$$\iint_A \left\{ \delta u \left[L_{11} u + L_{12} v + L_{13} w \right] + \delta v \left[L_{21} u + L_{22} v + L_{23} w \right] + \delta w \left[L_{31} u + L_{32} v + L_{33} w \right] \right\} dA = 0 \tag{24}$$

Substituting δu, δv, and δw from Equation 23 into Equation 24,

$$\iint_A \Big\{ \cos n\phi\, e^{i\omega t} \sum_{i=1}^{N} \delta A_i\, \Phi_i^u(x) \left[L_{11} u + L_{12} v + L_{13} w \right] + \sin n\phi\, e^{i\omega t} \sum_{i=1}^{N} \delta B_i\, \Phi_i^v(x) \left[L_{21} u + L_{22} v + L_{23} w \right] + \cos n\phi\, e^{i\omega t} \sum_{i=1}^{N} \delta C_i\, \Phi_i^w(x) \left[L_{31} u + L_{32} v + L_{33} w \right] \Big\} dA = 0 \tag{25}$$

Since δA_i, δB_i, and δC_i are arbitrary, the only way that the above equation can be identically zero is that each integral vanish individually (Reference 12).

$$\iint_A \cos n\phi\, e^{i\omega t}\, \delta A_i\, \Phi_i^u(x) \left[L_{11} u + L_{12} v + L_{13} w \right] dA = 0 \qquad i = 1, 2, \cdots N \tag{26}$$

$$\iint_A \sin n\phi\, e^{i\omega t}\, \delta B_i\, \Phi_i^v(x) \left[L_{21} u + L_{22} v + L_{23} w \right] dA = 0 \qquad i = 1, 2, \quad N \tag{27}$$

$$\iint_A \cos n\phi\, e^{i\omega t}\, \delta C_i\, \Phi_i^w(x) \left[L_{31} u + L_{32} v + L_{33} w \right] dA = 0 \qquad i = 1, 2, \quad N \tag{28}$$

Since δA_i, δB_i, δC_i, and $e^{i\omega t}$ are independent of the coordinates of dA, these can be taken out of the above integrals, to obtain

$$\iint_A \cos n\phi\, \Phi_i^u(x) \left[L_{11} u + L_{12} v + L_{13} w \right] dA = 0 \qquad i = 1, 2, \cdots N \tag{29}$$

$$\iint_A \sin n\phi\, \Phi_i^v(x) \left[L_{21} u + L_{22} v + L_{23} w \right] dA = 0 \qquad i = 1, 2, \quad N \tag{30}$$

$$\iint_A \cos n\phi\, \Phi_i^w(x) \left[L_{31} u + L_{32} v + L_{33} w \right] dA = 0 \qquad i = 1, 2, \quad N \tag{31}$$

The expressions for u, v, and w given by Equations 16 to 18 are substituted into Equations 29 to 31 with $dA = a\,d\phi\,dx$ and the integration performed on $d\phi$. From the orthogonality of sin $n\phi$ and cos $n\phi$ over the interval 0 to 2π,

$$\int_0^{2\pi} \sin^2 n\phi\, d\phi = \pi \tag{32}$$

$$\int_0^{2\pi} \cos^2 n\phi\, d\phi = \pi \tag{33}$$

$$\int_0^{2\pi} \sin n\phi \cos n\phi \, d\phi = 0 \tag{34}$$

By using this orthogonality condition, Equations 29 to 31 reduce to the following form:

$$I'_{11} + I'_{12} + I^i_{13} = 0 \qquad i = 1,2, \quad N \tag{35}$$

$$I'_{21} + I^i_{22} + I^i_{23} = 0 \qquad i = 1,2, \quad N \tag{36}$$

$$I^i_{31} + I'_{32} + I^i_{33} = 0 \qquad i = 1,2, \cdots N \tag{37}$$

Where the terms in Equations 35 to 37 are as follows:

$$I^i_{11} = \int_0^{\ell} \Phi^u_i(x) \left\{ -a^2 (1-q_2) \frac{d^2}{dx^2} + \left[\frac{(1-\nu)}{2} (1+k) - q_1 \right] n^2 - \gamma^2 \omega^2 \right\} U \, dx \quad i=1,2,\cdots N \tag{38}$$

$$I^i_{12} = \int_0^{\ell} \Phi^u_i(x) \left[-na \frac{(1+\nu)}{2} \frac{d}{dx} \right] V \, dx \qquad i = 1,2, \cdots N \tag{39}$$

$$I^i_{13} = \int_0^{\ell} \Phi^u_i(x) \left\{ -a \left[\nu + q_1 - \frac{(1-\nu)}{2} kn^2 \right] \frac{d}{dx} + ka^3 \frac{d^3}{dx^3} \right\} W \, dx \quad i=1,2,\cdots N \tag{40}$$

$$I^i_{21} = \int_0^{\ell} \Phi^v_i(x) \left[an \frac{(1+\nu)}{2} \frac{d}{dx} \right] U \, dx \qquad i = 1,2, \cdots N \tag{41}$$

$$I^i_{22} = \int_0^{\ell} \Phi^v_i(x) \left\{ n^2 (1-q_1) - a^2 \left[\frac{(1-\nu)}{2} (1+3k) - q_2 \right] - \frac{d^2}{dx^2} - \gamma^2 \omega^2 \right\} V \, dx \quad i=1,2, \cdots N \tag{42}$$

$$I^i_{23} = \int_0^{\ell} \Phi^v_i(x) \left[(1-q_1) n - \frac{a^2 (3-\nu)}{2} kn \frac{d^2}{dx^2} \right] W \, dx \qquad i = 1,2, \quad N \tag{43}$$

$$I'_{31} = \int_0^{\ell} \Phi^w_i(x) \left\{ a \left[\nu + q_1 - \frac{(1-\nu)}{2} n^2 k \right] \frac{d}{dx} - a^3 k \frac{d^3}{dx^3} \right\} U \, dx \quad i=1,2, \cdots N \tag{44}$$

$$I'_{32} = \int_0^{\ell} \Phi^w_i(x) \left[(1-q_1) n - \frac{a^2 n (3-\nu)}{2} k \frac{d^2}{dx^2} \right] V dx \quad i=1,2, \quad N \tag{45}$$

$$I'_{33} = \int_0^{\ell} \Phi^w_i(x) \left\{ 1 - n^2 q_1 + a^2 q_2 \frac{d^2}{dx^2} + k \left[a^4 \frac{d^4}{dx^4} - 2a^2 n^2 \frac{d^2}{dx^2} + (n^2-1)^2 \right] - \gamma^2 \omega^2 \right\} W \, dx \tag{46}$$

$$i = 1,2, \quad N$$

U, V, and W as given by Equations 19 to 21 are substituted into Equations 38 to 46. These expressions are substituted into Equations 35 to 37 with N = M to obtain the following form for the characteristic equation.

$$\begin{bmatrix} K^{11} & K^{12} & \cdots & K^{1N} \\ K^{21} & K^{22} & \cdots & K^{2N} \\ \vdots & \vdots & & \vdots \\ K^{N1} & K^{N2} & & K^{NN} \end{bmatrix} \begin{Bmatrix} Y_1 \\ Y_2 \\ \vdots \\ Y_N \end{Bmatrix} = \gamma^2\omega^2 \begin{bmatrix} M^{11} & M^{12} & \cdots & M^{1N} \\ M^{21} & M^{22} & \cdots & M^{2N} \\ \vdots & \vdots & & \vdots \\ M^{N1} & M^{N2} & & M^{NN} \end{bmatrix} \begin{Bmatrix} Y_1 \\ Y_2 \\ \vdots \\ Y_N \end{Bmatrix} \tag{47}$$

where the submatrices K^{ij} and M^{ij} can be written

$$K^{ij} = \begin{bmatrix} D_{11}^{ij} & D_{12}^{ij} & D_{13}^{ij} \\ D_{21}^{ij} & D_{22}^{ij} & D_{23}^{ij} \\ D_{31}^{ij} & D_{32}^{ij} & D_{33}^{ij} \end{bmatrix}, \quad M^{ij} = \begin{bmatrix} M_{11}^{ij} & 0 & 0 \\ 0 & M_{22}^{ij} & 0 \\ 0 & 0 & M_{33}^{ij} \end{bmatrix} \tag{48}$$

The terms in the D^{ij}, M^{ij}, and Y_j submatrices are,

$$D_{11}^{ij} = \int_0^{\ell} \Phi_i^u(x)\left\{-a^2(1-q_2)\frac{d^2}{dx^2} + \left[\frac{(1-\nu)}{2}(1+k) - q_1\right]n^2\right\}\Phi_j^u(x)\,dx \tag{49}$$

$$D_{12}^{ij} = \int_0^{\ell} \Phi_i^u(x)\left[\frac{-a(1+\nu)}{2}n\frac{d}{dx}\right]\Phi_j^v(x)\,dx \tag{50}$$

$$D_{13}^{ij} = \int_0^{\ell} \Phi_i^u(x)\left\{-a\left[\nu + q_1 - \frac{(1-\nu)}{2}kn^2\right]\frac{d}{dx} + \kappa a^3\frac{d^3}{dx^3}\right\}\Phi_j^w(x)\,dx \tag{51}$$

$$D_{21}^{ij} = \int_0^{\ell} \Phi_i^v(x)\left[\frac{a(1+\nu)n}{2}\frac{d}{dx}\right]\Phi_j^u\,dx \tag{52}$$

$$D_{22}^{ij} = \int_0^{\ell} \Phi_i^v(x)\left\{n^2(1-q_1) - a^2\left[\frac{(1-\nu)}{2}(1+3k) - q_2\right]\frac{d^2}{dx^2}\right\}\Phi_j^v(x)\,dx \tag{53}$$

$$D_{23}^{ij} = \int_0^{\ell} \Phi_i^v(x)\left[(1-q_1)n - \frac{a^2(3-\nu)}{2}kn\frac{d^2}{dx^2}\right]\Phi_j^w(x)\,dx \tag{54}$$

$$D_{31}^{ij} = \int_0^{\ell} \Phi_i^w(x)\left\{a\left[\nu + q_1 - \frac{(1-\nu)}{2}n^2k\right]\frac{d}{dx} - a^3k\frac{d^3}{dx^3}\right\}\Phi_j^u(x)\,dx \tag{55}$$

$$D_{32}^{ij} = \int_0^{\ell} \Phi_i^w(x)\left[(1-q_1)n - \frac{a^2n(3-\nu)}{2}k\frac{d^2}{dx^2}\right]\Phi_j^v(x)\,dx \tag{56}$$

$$D_{33}^{ij} \int_0^{\ell} \Phi_i^w(x)\left\{1-n^2 q_1 + a^2 q_2 \frac{d^2}{dx^2} + k\left[a^4 \frac{d^4}{dx^4} - 2a^2 n^2 \frac{d^2}{dx^2} + (n^2-1)^2\right]\right\} \Phi_j^w(x)\,dx \qquad (57)$$

$$M_{11}^{ij} = \int_0^{\ell} \Phi_i^u(x)\,\Phi_j^u(x)\,dx \qquad (58)$$

$$M_{22}^{ij} = \int_0^{\ell} \Phi_i^v(x)\,\Phi_j^v(x)\,dx \qquad (59)$$

$$M_{33}^{ij} = \int_0^{\ell} \Phi_i^w(x)\,\Phi_j^w(x)\,dx \qquad (60)$$

$$Y_j = \begin{Bmatrix} A_j \\ B_j \\ C_j \end{Bmatrix} \qquad (61)$$

A solution is obtained by selecting a series of displacement functions $\Phi^u(x)$, $\Phi^v(x)$, and $\Phi^w(x)$ for U(x), V(x), and W(x) respectively which satisfy the appropriate boundary conditions for the shell. Integrals (Equations 49 to 61) are evaluated and the various K^{ij} and M^{ij} matrices given by Equation 48 are formed and substituted into Equation 47 which can be solved by standard eigenvalue techniques.

If the series of displacement functions selected for $\Phi^u(x)$, $\Phi^v(x)$, and $\Phi^w(x)$ each form an orthogonal set, the generalized mass matrix M^{ij} in Equation 47 will be diagonal.

One set of functions which can be used for the series of assumed displacements Φ are the beam functions, which satisfy the following differential equation:

$$\frac{d^4\phi}{dx^4} - k\phi = 0 \qquad (62)$$

The functions, Φ, taken as the assumed modes, satisfy various combinations of the following boundary conditions at x = 0, and x = ℓ:

$$\Phi = 0 \qquad (63)$$

$$\Phi' = 0 \qquad (64)$$

$$\Phi'' = 0 \qquad (65)$$

$$\Phi''' = 0 \qquad (66)$$

The beam functions satisfying Equation 62 for various combinations of the boundary conditions (Equations 63 to 66) are orthogonal. Integrals of the beam functions and their derivatives have been evaluated by Felgar, and formulas for these integrals are given in Reference 3. In general, the terms in the matrix K^{ij} given by Equations 49 to 57 involve integrals of combinations of $\Phi^u{}_i(x)$, $\Phi^v{}_i(x)$, and $\Phi^w{}_i(x)$ which may be different functions. These are not tabulated. One approach would be to evaluate the various integrals in Equations 49 to 57 numerically. This would allow an independent choice of the function to represent each of the functions U(x), V(x), and W(x).

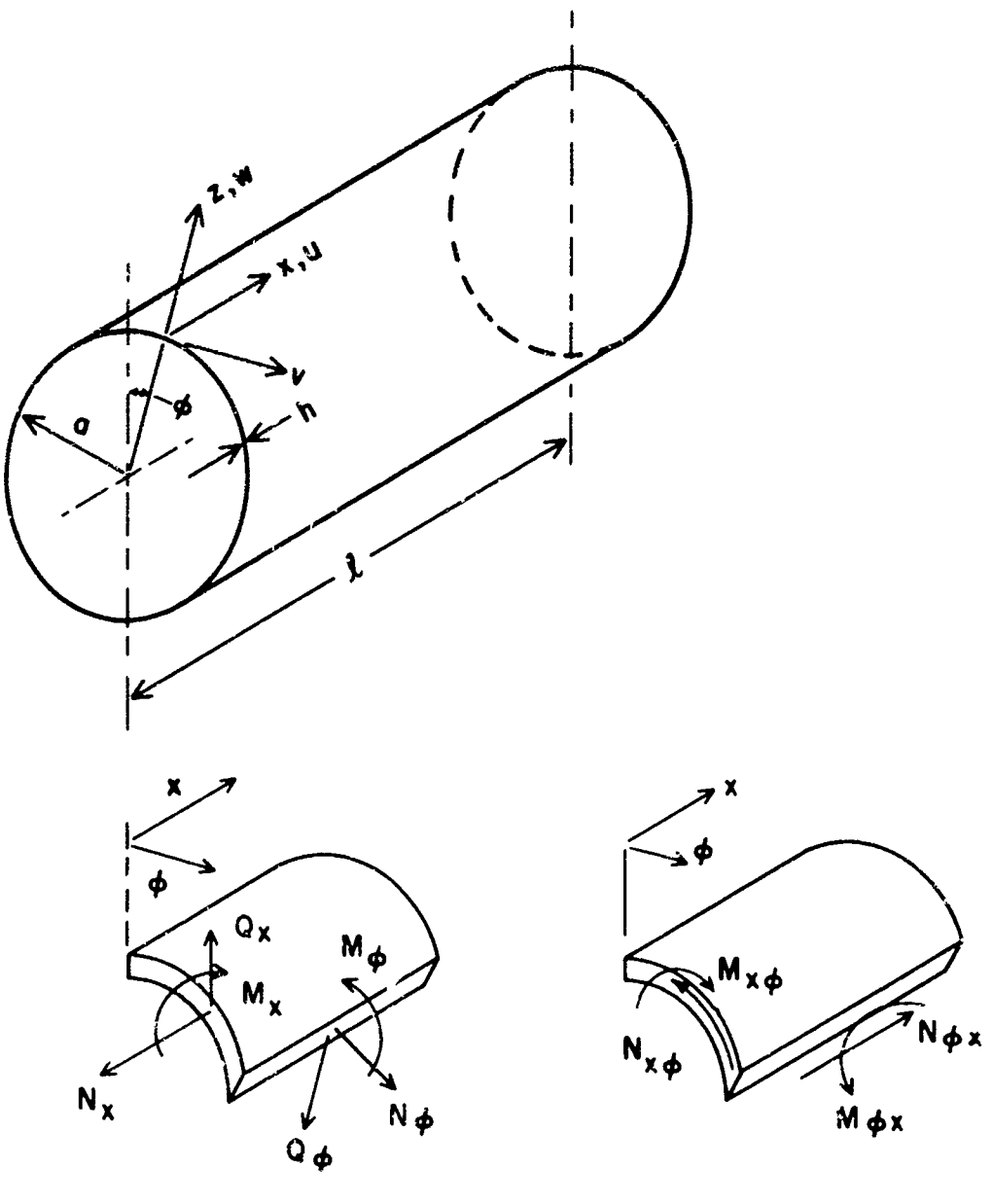

Figure 1. Cocrdinate System

SECTION III

SOLUTION FOR THE FREELY-SUPPORTED CYLINDER

An exact solution can be obtained for the vibration of a cylindrical shell with axial loads and internal pressurization for the following boundary conditions:

$$w = 0 \qquad \text{at} \quad x = 0, \ell \tag{67}$$

$$v = 0 \qquad \text{at} \quad x = 0, \ell \tag{68}$$

$$M_x = 0 \qquad \text{at} \quad x = 0, \ell \tag{69}$$

$$N_x = 0 \qquad \text{at} \quad x = 0, \ell \tag{70}$$

The boundary conditions corresponding to Equations 67 to 70 are satisfied if the functions U, V, and W satisfy the following conditions at $x = 0$ and $x = \ell$:

$$\frac{dU}{dx} = 0 \tag{71}$$

$$V = 0 \tag{72}$$

$$W = \frac{d^2 W}{dx^2} = 0 \tag{73}$$

These boundary conditions are satisfied by the following normalized displacement functions:

$$\Phi_m^u(x) = \sqrt{2} \cos \frac{m\pi x}{\ell} \tag{74}$$

$$\Phi_m^v(x) = \sqrt{2} \sin \frac{m\pi x}{\ell} \tag{75}$$

$$\Phi_m^w(x) = \sqrt{2} \sin \frac{m\pi x}{\ell} \tag{76}$$

The previous sine and cosine functions are orthonormal on the interval 0 to 2π and have the following properties:

$$\int_0^\ell \left(\sqrt{2} \cos \frac{i\pi x}{\ell}\right)\left(\sqrt{2} \cos \frac{j\pi x}{\ell}\right) dx = \begin{cases} \ell, & i = j \\ 0, & i \neq j \end{cases} \tag{77}$$

$$\int_0^\ell \left(\sqrt{2} \sin \frac{i\pi x}{\ell}\right)\left(\sqrt{2} \sin \frac{j\pi x}{\ell}\right) dx = \begin{cases} \ell, & i = j \\ 0, & i \neq j \end{cases} \tag{78}$$

$$\int_0^\ell \left(\sqrt{2} \sin \frac{i\pi x}{\ell}\right)\left(\sqrt{2} \cos \frac{j\pi x}{\ell}\right) dx = 0 \tag{79}$$

For this case the various integrals in Equations 49 to 60 are zero for $i \neq j$ and reduce to the following for $i = j = m$.

$$D_{11}^{mm} = a^2 (1 - q_2) \left(\frac{m\pi}{\ell}\right)^2 \ell + \left[\frac{(1-\nu)}{2}(1 + k) - q_1\right] n^2 \ell \tag{80}$$

$$D_{12}^{mm} = -a \frac{(1+\nu)}{2} \left(\frac{m\pi}{\ell}\right) n\ell \tag{81}$$

$$D_{13}^{mm} = -a\left[\nu + q_1 - \frac{(1-\nu)}{2} kn^2\right]\left(\frac{m\pi}{\ell}\right)\ell - ka^3\left(\frac{m\pi}{\ell}\right)^3\ell \tag{82}$$

$$D_{21}^{mm} = \frac{-a(1+\nu)}{2}\left(\frac{m\pi}{\ell}\right) n\ell \tag{83}$$

$$D_{22}^{mm} = n^2(1-q_1)\ell + a^2\left[\frac{(1-\nu)}{2}(1+3k) - q_2\right]\left(\frac{m\pi}{\ell}\right)^2\ell \tag{84}$$

$$D_{23}^{mm} = (1-q_1)n\ell + \frac{a^2(3-\nu)}{2}\left(\frac{m\pi}{\ell}\right)^2 kn\ell \tag{85}$$

$$D_{31}^{mm} = -a\left[\nu + q_1 - \frac{(1-\nu)}{2} n^2 k\right]\left(\frac{m\pi}{\ell}\right)\ell - a^3 k\left(\frac{m\pi}{\ell}\right)^3\ell \tag{86}$$

$$D_{32}^{mm} = (1-q_1)n\ell + \frac{a^2 n(3-\nu)}{2} k\left(\frac{m\pi}{\ell}\right)^2\ell \tag{87}$$

$$D_{33}^{mm} = \left[1 - n^2 q_1 + k(n^2-1)^2\right]\ell + (2a^2n^2k - a^2q_2)\left(\frac{m\pi}{\ell}\right)^2\ell + ka^4\left(\frac{m\pi}{\ell}\right)^4\ell \tag{88}$$

$$M_{11}^{mm} = \ell \tag{89}$$

$$M_{22}^{mm} = \ell \tag{90}$$

$$M_{33}^{mm} = \ell \tag{91}$$

The expressions given by Equations 80 to 91 are substituted into Equation 47 to obtain the following:

$$\begin{bmatrix} K^{11} & 0 & 0 \\ 0 & K^{22} & \cdot \\ \cdot & 0 & \cdot \\ \cdot & \cdot & \cdot \\ 0 & 0 & K^{NN} \end{bmatrix} \begin{Bmatrix} Y_1 \\ Y_2 \\ \cdot \\ \cdot \\ Y_N \end{Bmatrix} = \gamma^2\omega^2 \begin{bmatrix} M^{11} & 0 & 0 \\ 0 & M^{22} & \cdot \\ \cdot & C & \cdot \\ \cdot & & \cdot \\ 0 & 0 & M^{NN} \end{bmatrix} \begin{Bmatrix} Y_1 \\ Y_2 \\ \cdot \\ Y_N \end{Bmatrix} \tag{92}$$

or

$$\begin{bmatrix} (K^{11} - \gamma^2\omega^2 M^{11}) & 0 & \cdots & 0 \\ 0 & (K^{22} - \gamma^2\omega^2 M^{22}) & & \cdot \\ \cdot & & & \\ 0 & \cdots & & (K^{NN} - \gamma^2\omega^2 M^{NN}) \end{bmatrix} \begin{Bmatrix} Y_1 \\ Y_2 \\ \cdot \\ Y_N \end{Bmatrix} = 0 \tag{93}$$

Equation 93 is of a diagonal form and consists of the direct sum of 3 x 3 submatrices. This indicates that an exact solution exists for the assumed functions selected. For a non-trivial solution,

$$\begin{vmatrix} (K^{11} - \gamma^2 \omega^2 M^{11}) & & & \\ & (K^{22} - \gamma^2 \omega^2 M^{22}) & & \\ & & \ddots & \\ & & & (K^{NN} - \gamma^2 \omega^2 M^{NN}) \end{vmatrix} = 0 \qquad (94)$$

Applying the Laplace expansion to the above,

$$\left| K^{11} - \gamma^2 \omega^2 M^{11} \right| \left| K^{22} - \gamma^2 \omega^2 M^{22} \right| \cdots \left| K^{NN} - \gamma^2 \omega^2 M^{NN} \right| = 0 \qquad (95)$$

or

$$\left| K^{mm} - \gamma^2 \omega^2 M^{mm} \right| = 0 \qquad m = 1, 2, \quad N \qquad (96)$$

$$\left[K^{mm} - \gamma^2 \omega^2 M^{mm} \right] \left\{ Y_m \right\} = 0 \qquad m = 1, 2, \quad N \qquad (97)$$

The expressions for K^{ii} and M^{ii} are substituted into Equation 97. The resulting expression is divided by ℓ, and $\gamma^2\omega^2$ and q_2 $(\frac{m\pi}{\ell})$ are taken to the right-hand side. A non-dimensional wavelength parameter λ is introduced, and the following result is obtained:

$$\begin{bmatrix} D_{11}^m & D_{12}^m & D_{13}^m \\ D_{21}^m & D_{22}^m & D_{23}^m \\ D_{31}^m & D_{32}^m & D_{33}^m \end{bmatrix} \begin{Bmatrix} A_m \\ B_m \\ C_m \end{Bmatrix} = (\gamma^2\omega^2 - q_2 \lambda^2) \begin{Bmatrix} A_m \\ B_m \\ C_m \end{Bmatrix} \qquad m = 1, 2, \cdots N \qquad (98)$$

where

$$\lambda = \frac{m \pi a}{\ell} \qquad (99)$$

$$D_{11} = \lambda^2 + \left[\frac{(1-\nu)}{2} (1+k) - q_1 \right] n^2 \qquad (100)$$

$$D_{12} = D_{21} = - \frac{\lambda (1+\nu)}{2} n \qquad (101)$$

$$D_{13} = D_{31} = - \lambda \left[\nu + q_1 - \frac{(1-\nu)}{2} k n^2 \right] - k \lambda^3 \qquad (102)$$

$$D_{22} = n^2 (1 - q_1) + \lambda^2 \left[\frac{(1-\nu)}{2} (1+3k) \right] \qquad (103)$$

$$D_{23} = D_{32} = (1 - q_1)\, n + \frac{\lambda^2 (3 - \nu)}{2} kn \tag{104}$$

$$D_{33} = \left[1 - n^2 q_1 + k (n^2 - 1)^2\right] + 2n^2 k\lambda^2 + k\lambda^4 \tag{105}$$

In Equation 98 the vibration frequencies and axial load parameter are combined to form a single eigenvalue expression. This is discussed in more detail in Section IV.

If ω is assumed to be zero in Equation 98 these equations are identical to those given by Flugge in Reference 4 for the buckling of a cylindrical shell subjected to an axial load and internal pressure. If the axial load parameter q_2 and internal pressure parameter q_1 are assumed to be zero in Equation 98 these equations are comparable to those obtained by Arnold and Warburton (Reference 1). Small differences which occur are in terms containing the thickness to radius parameter k which is small for cylinders for which the thin shell equations apply.

Once the mode numbers are selected, the values of the D_{ij} terms can be evaluated for a given shell having the assumed boundary conditions and a given load of q_2. This is accomplished by assigning integer values to n and to m (in $\lambda = \frac{m\pi a}{\ell}$) which represent the number of circumferential waves and the axial half-waves respectively.

A solution can be obtained by solving Equation 98 by matrix iteration or by reducing Equation 98 to a determinant form and solving the resulting third order characteristic equation.

$$\left| D_{ij} - \Delta I \right| = 0, \qquad \Delta = (\gamma^2 \omega^2 + q_2 \lambda^2) \tag{106}$$

or

$$\begin{vmatrix} D_{11} - \Delta & D_{12} & D_{13} \\ D_{12} & D_{22} - \Delta & D_{23} \\ D_{13} & D_{23} & D_{33} - \Delta \end{vmatrix} = 0 \tag{107}$$

After expanding,

$$\Delta^3 - \Delta^2 (D_{11} + D_{22} + D_{33}) + \Delta (D_{11} D_{22} + D_{11} D_{33} + D_{22} D_{33} - D_{12}^2 - D_{13}^2 - D_{23}^2) - D_{11} D_{22} D_{33}$$

$$- 2D_{12} D_{13} D_{23} + D_{13}^2 D_{22} + D_{12}^2 D_{33} + D_{23}^2 D_{11} = 0 \tag{108}$$

Three values of Δ can be obtained from Equation 108 indicating that three frequencies exist for each of the assumed mode shapes. This result has been previously reported by Arnold and Warburton (Reference 2) and others. These various frequencies are associated with different values of the amplitude ratios $\frac{A}{C}$ and $\frac{B}{C}$. For one value of the frequency, usually the lowest, C > A, B and the motion is radial or in the z direction. The other two values of frequency are usually associated with motion that is tangential, B > A, C where the primary displacement is v, or longitudinal vibration, where A > B, C and the u displacement predominates. It is noted that for the cylindrical shell this coupling between displacements exists.

For the non-axisymmetric modes ($n \neq o$) the values of Δ can be determined from Equation 108 and the amplitude ratios $\frac{A}{C}$ and $\frac{B}{C}$ can be obtained from

$$\begin{bmatrix} D_{11}-\Delta & D_{12} & D_{13} \\ D_{12} & D_{22}-\Delta & D_{23} \\ D_{13} & D_{23} & D_{33}-\Delta \end{bmatrix} \begin{Bmatrix} A \\ B \\ C \end{Bmatrix} = 0 \tag{109}$$

Solving Equation 109 for the amplitude ratios yields

$$\frac{A}{C} = \frac{\frac{D_{13}}{D_{12}}(D_{22}-\Delta) - D_{23}}{D_{12} - \frac{(D_{11}-\Delta)(D_{22}-\Delta)}{D_{12}}} \tag{110}$$

$$\frac{B}{C} = \frac{\frac{D_{13}\,D_{23}}{D_{12}} - (D_{33}-\Delta)}{D_{23} - \frac{D_{13}}{D_{12}}(D_{22}-\Delta)} \tag{111}$$

A coupling between the three displacements u, v, and w exists for the non-axisymmetric modes.

For the special case of axisymmetric motion with $n = o$, the terms D_{12}, D_{21}, D_{23}, and D_{32} in Equation 98 are zero, and the tangential displacement v can be uncoupled from the axial and radial displacements. With $n = o$, Equation 98 can be written as two equations

$$\begin{bmatrix} D_{11}^m & D_{13}^m \\ D_{13}^m & D_{33}^m \end{bmatrix} \begin{Bmatrix} A_m \\ C_m \end{Bmatrix} = (\gamma^2\omega^2 + q_2\lambda^2) \begin{Bmatrix} A_m \\ C_m \end{Bmatrix} \tag{112}$$

$$m = 1, 2, \cdots N$$

$$\left[D_{22} - (\gamma^2\omega^2 + q_2\lambda^2)\right] B_m = 0 \tag{113}$$

$$m = 1, 2, \cdots$$

Setting the determinants of Equations 112 and 113 equal to zero and expanding gives:

$$\Delta^2 - (D_{11} + D_{33})\Delta + D_{11}D_{33} - D_{13}^2 = 0 \tag{114}$$

$$\Delta = D_{22} \tag{115}$$

Equation 115 represents the eigenvalue for pure torsional vibration, and Equation 114 coupled radial and axial vibration eigenvalues. The amplitude ratios for the latter are given by

$$\frac{A}{C} = \frac{-D_{13}}{(D_{11}-\Delta)} \tag{116}$$

SECTION IV

VIBRATION AND BUCKLING RESULTS FOR AXIAL LOADING

It was shown in Section III that for the specific case of a freely-supported cylinder, the various terms in the series of assumed modes uncouple, indicating that an exact solution was obtained. The frequency parameter $\gamma^2\omega^2$ was combined with the product of the axial load parameter q_2 and the square of the axial wave parameter λ to form a single eigenvalue expression $\Delta(\lambda, n)$.

$$\Delta(\lambda, n) = \gamma^2\omega^2 + q_2\lambda^2 \tag{117}$$

The expressions D_{ij} which make up the coefficients of the characteristic equation contain the shell parameters ν and k, the wave parameters n and λ, and external pressure parameter q_1. The parameters ω and q_2 appear only in the parameter Δ. When integer values are assigned to the number of circumferential waves n and axial half-waves m, the mode shape is, in effect, specified and solution of the appropriate characteristic equations yields the eigenvalues for that mode. Some typical mode shapes are shown in Figure 2. It is noted that for the boundary conditions considered, the eigenvalues $\Delta(\lambda, n)$ can be obtained without specifying a value for the axial load parameter q_2. The eigenvalues obtained depend on the internal pressure, however, since the coefficients of the characteristic equations contain the parameter q_1.

In this Section, the effects of internal pressure are neglected and q_1 is considered to be zero. If the parameter q_2 is zero, the eigenvalues obtained for the specified mode correspond to the values of the vibration frequency parameter $\gamma^2\omega^2$ for the shell with no axial loading. The circular frequency for the unloaded shell is ω_o.

$$\Delta(\lambda, n) = \gamma^2\omega_o^2 \tag{118}$$

From the three values of $\Delta(\lambda, n)$ associated with each mode, the vibration frequencies, ω_o, for radial, longitudinal, and torsional vibration having the specified mode shape can be determined for a zero value of axial load. These results correspond to those obtained in Reference 1.

The characteristic equation (Equation 108 or Equations 114 and 115) for the axisymmetric modes (n = 0) was solved for a range of radius to thickness ratios from 20 to 5000. For large values of the radius to thickness ratio ($\frac{a}{h}$ = 2000, 5000) and large values of $\frac{\ell}{ma}$, one of the roots was quite small ($\Delta << 1$). In this case, greater accuracy was obtained by solving the smallest eigenvalue using only the linear terms of Equation 108. The results are given in Figures 3 through 16 for the first eigenvalue which is radial deformation (C > A, B). Figure 17 gives the results for the second eigenvalue, and Figure 18 the results for the third eigenvalue. The results for the axisymmetric case (n = o) are given in Figure 19.

A single figure covers the range of radius to thickness ratios from 20 to 5000 for modes corresponding to the second and third eigenvalues. Since the results are independent of the radius to thickness ratio, bending effects are relatively unimportant as compared to stretching or membrane effects. The changes in the eigenvalue spectra with various values of radius to thickness for radial deformation indicate that these modes involve primarily bending effects.

Two curves are given for each radius to thickness ratio for radial deformation. In one case $\sqrt{\Delta}$ is plotted versus the axial wavelength parameter $\frac{\ell}{ma}$ for different values of n or number of circumferential waves, and in the other case $\sqrt{\Delta}$ is plotted versus n for different values of $\frac{\ell}{ma}$. For a given cylinder the ratio $\frac{\ell}{a}$ is fixed. By assigning integer values to m in the parameter $\frac{\ell}{ma}$ the values of $\sqrt{\Delta}$ for various modes can be determined from the figures. Since $\sqrt{\Delta}$ is equal to $\gamma\omega_o$ for $q_2 = 0$, the natural vibration frequencies for the unloaded shell can be obtained from these figures.

For modes having one circumferential wave (n = 1) the amplitude of the radial and tangential displacements corresponding to the lowest eigenvalue are approximately equal and greater than the axial displacement for values of $\frac{\ell}{ma} > 3.5$ and the deflection shape is similar to beam bending with little deviation from a circular cross-section. This is consistent with the results reported by Forsberg (Reference 6).

It was shown in Section III for the axisymmetric case (n = 0) that the torsional displacement uncouples from the radial and axial displacements. One of the eigenvalues corresponds to pure torsional vibration while the other two involve coupled radial and axial motion.

A simple expression for the torsional vibration can be obtained using Equations 115 and 103.

$$\Delta(\lambda, n) = \gamma^2 \omega_o^2 = \frac{\lambda^2 (1-\nu)(1+3k)}{2} \tag{119}$$

After solving ω_o and substituting γ, Equation 119 reduces to

$$\omega_o = \frac{m\pi}{\ell} \sqrt{\frac{E(1+3k)}{2\rho(1+\nu)}} \qquad m = 1, 2, \tag{120}$$

For small values of k, ($k \ll 1$), this can be written

$$\omega_o = \frac{m\pi}{\ell} \sqrt{\frac{E}{2\rho(1+\nu)}} \qquad m = 1, 2, \tag{121}$$

Equation 121 is the same result one would obtain for the torsional vibration of a clamped-clamped tube starting with the following differential equation

$$\frac{d^2 v}{dx^2} + \frac{\omega^2 I_o}{GJ} v = 0 \tag{122}$$

For the freely-supported cylindrical shell a boundary condition of zero tangential displacement was assumed at both ends of the shell which corresponds to clamped ends for torsion of a hollow shaft or tube.

The lowest eigenvalue for the axisymmetric modes is associated with radial deformation (C >A) for a value of $\frac{\ell}{ma} < 2$. The lowest eigenvalue is associated with torsional vibration for values of the parameter $\frac{\ell}{ma} > 2$. For values of $\frac{\ell}{ma}$ greater than a value approximately equal to π, the largest eigenvalue corresponds to radial deformation (C >A). The lowest frequency

of axisymmetric vibration for a freely-supported cylinder with $\frac{\ell}{ma} > \pi$ corresponds to pure torsional motion. The highest frequency corresponds to radial motion (Figure 19). This result was reported by Forsberg in Reference 6.

For small values of $\frac{\ell}{ma}$ and low values of n the second eigenvalue yields amplitude ratios (B>A, C) while modes having larger values of $\frac{\ell}{ma}$ and n have amplitude ratios (A>B, C). Thus the second eigenvalue corresponds to torsional vibration for some modes and axial vibration for other modes, as indicated in Figure 17. In Figure 18 a similar result is obtained for the third eigenvalue.

It can be seen from the figures that for the freely-supported cylinder under consideration, the lowest vibration frequency is associated with radial vibration for non-axisymmetric modes except for long cylinders with one circumferential wave. Among the various radial vibration frequencies the lowest value for the unloaded shell is obtained for one axial half-wave (m = 1). This leads to the largest value of $\frac{\ell}{ma}$. The number of circumferential waves associated with the lowest radial vibration frequency is a function of the shell geometry or length to radius ratio $\frac{\ell}{a}$ and radius to thickness ratio $\frac{a}{h}$. The larger the ratio of radius to thickness the greater the number of circumferential waves in the minimum frequency vibration mode.

For non-axisymmetric vibration frequencies corresponding to the second and third eigenvalues, the lowest frequencies are obtained for modes with one axial half-wave as in the case of radial vibration, and increase as the number of half-waves increase. The number of circumferential waves associated with the lowest frequency, however, for a given number of axial half-waves is one and the frequency increases as the number of circumferential waves increases. Thus for non-axisymmetric vibration corresponding to the second and third eigenvalues, the lowest frequencies are those for one circumferential wave, and one axial half-wave, and may involve either motion which is axial or torsional depending on the value of $\frac{\ell}{a}$ for a given shell. For cylinders with a value of $\frac{\ell}{a} < 2$ the second eigenvalue corresponds to torsional vibration and for cylinders with $\frac{\ell}{a} > 2$ to axial vibration (Figure 17).

If the frequency is assumed to be zero, the eigenvalues for any mode are the values of the buckling parameter q_2 for that mode. From these eigenvalues the axial loading for buckling given the symbol q_{20}, can be determined for the specified mode

$$\Delta\ (\lambda, n) = q_{20}\ \lambda^2 \tag{123}$$

The three eigenvalues $\Delta\ (\lambda, n)$ associated with each deflection mode correspond to buckling deformations which are radial, axial, or tangential. The lowest eigenvalue for non-axisymmetric modes is associated with buckling which involves radial deformation except for the modes with one circumferential wave.

Since the eigenvalues for a given mode shape can be obtained without specifying a value for q_2 the values $\Delta(\lambda, n)$ in Equation 123 for the buckling loads are the same as those for the circular frequency of an unloaded cylinder, Equation 118, or the vibration of a cylinder loaded below the buckling value, Equation 117. In addition the amplitude ratios A/C and B/C are the same for the various displacements.

Both sides of Equation 117 can be divided by $\Delta(\lambda, n)$ to obtain

$$1 = \frac{\gamma^2 \omega^2 + q_2 \lambda^2}{\Delta(\lambda, n)} \tag{124}$$

or

$$\frac{\gamma^2 \omega^2}{\Delta(\lambda, n)} = 1 - \frac{q_2 \lambda^2}{\Delta(\lambda, n)} \tag{125}$$

After substituting for $\Delta(\lambda, n)$ in Equation 125 from Equations 118 or 123 the following result is obtained:

$$\left(\frac{\omega}{\omega_0}\right)^2 = 1 - \frac{q_2}{q_{20}} \tag{126}$$

or

$$\omega^2 = \omega_0^2 \left(1 - \frac{q_2}{q_{20}}\right) \tag{127}$$

Equation 127 shows for a given cylinder, and for the values of $\Delta(\lambda, n)$ associated with a given deflection mode, that the square of the vibration frequency varies linearly with the axial load, or axial load parameter q_2. For positive values of q_2 (compressive loading) the square of the vibration frequency ω varies linearly from its value for no axial loading, ω_0, to zero at the buckling load $q_2 = q_{20}$. A compressive loading beyond this point would lead to imaginary frequencies and indicate that the cylinder was statically unstable for that deformation mode and loading. Negative values of q_2 correspond to a tensile loading and increase the natural vibration frequencies for a given mode.

The relationship between the vibration frequencies and axial load given by Equation 127 was obtainable because the deformation mode shape for natural vibrations and buckling are the same for the particular boundary conditions considered. The frequency and axial load parameters were combined into a single eigenvalue expression.

The lowest buckling mode, or minimum value of q_{20} is generally not associated with a mode shape having one axial half-wave as is the case for the minimum vibration frequency for no axial load. It is shown in Equation 123 that the minimum buckling load q_{20} is associated with the minimum value of $\frac{\Delta(\lambda, n)}{\lambda^2}$. For a given number of axial half-waves, m, the lowest vibration frequency and the lowest buckling load have the same number of circumferential waves, n.

The buckling values q_{20} for axial compression are obtained from Equation 123 after the eigenvalues have been obtained from Equation 108 for non-axisymmetric modes ($n \neq o$) and Equations 114 and 115 for axisymmetric modes. The buckling results obtained are the same as those of Flugge (Reference 4) since the equations are identical. Since only the buckling envelope is given in Reference 4 for various radius to thickness ratios, the complete buckling curves are plotted in Figures 20 through 36 for use with Equations 126 and 127.

The various eigenvalues were obtained from solution of the cubic equation except where the linear solution gave greater accuracy for the lowest root.

The buckling results for axial compression are plotted in Figure 20 for the axisymmetric modes. The results for buckling involving radial deformation are given in Figures 21 through 34 for radius to thickness ratios from 20 to 5000. Figure 35 is a plot of the buckling values corresponding to the second eigenvalue and Figure 36 is a plot of the buckling values corresponding to the third eigenvalue. As in the case of free vibration each plot for the second and third eigenvalue contains both torsional deformation and axial deformation. A single figure for each case covers the range of radius to thickness ratios from 20 to 5000 for these higher buckling values, indicating that bending effects are unimportant for these modes.

Since buckling modes with one circumferential wave have the lowest eigenvalue, as in the vibration case, the amplitude ratio for radial and tangential displacements approaches -1. These displacements are larger than the axial displacement for values of $\frac{\ell}{ma} > 3.5$. These buckling modes are similar to column buckling with little deviation from the circular cross section. In Reference 4 Flugge shows that the buckling values for this mode approach the Euler column values asymptotically for large values of $\frac{\ell}{ma}$.

For the case of axisymmetric buckling (n = 0) due to an axial load, Figure 20 shows that for values of $\frac{\ell}{ma} < 2$ the lowest buckling value is associated with radial deformation. If the values of $\frac{\ell}{ma} > 2$ the lowest axisymmetric buckling value involves torsional deformation. As in the vibration case, the torsional displacement uncouples from the radial and axial displacement for the axisymmetric modes. The expression for this pure torsional buckling due to axial load can be written.

$$q_{20} = \frac{P}{D} = \frac{(1-\nu)}{2}(1+3k) \tag{128}$$

For values of $k \ll 1$ this can be approximated

$$q_{20} \cong \frac{P}{D} = \frac{(1-\nu)}{2} \tag{129}$$

or

$$P = \frac{Eh}{2(1+\nu)} \tag{130}$$

in terms of the axial load per unit length on the cylinder boundary. In Equation 129 it is shown that the value of q_{20} for torsional buckling due to an axial load is a constant for a given cylinder. This also is shown in Figure 20.

While values of the buckling parameter q_{20} for various modes corresponding to the second and third eigenvalue are unimportant from a stability standpoint they are plotted in Figures 35 and 36 for use with Equation 126 or 127. As in the vibration case the minimum buckling values for the second and third eigenvalues, for the non-axisymmetric modes, occur for one circumferential wave and small values of $\frac{\ell}{ma}$ or a large number of axial half-waves.

The vibration frequencies for freely-supported cylinders with an axial load can be determined by using Figures 20 through 36 and Equation 126 or 127. These equations are valid for any of the three eigenvalues for a given deformation mode. For a given cylinder it would be necessary to select a mode of interest by assigning integer values to n and m, and calculating a value for $\frac{\ell}{ma}$. After determining whether radial, torsional, or axial vibration is of interest the values of ω_o and q_{20} can be determined from the appropriate charts for that

particular n and $\frac{\ell}{ma}$. The value of the parameter q_2 for the applied loading can be calculated and the new frequency ω or the frequency ratio $\left(\frac{\omega}{\omega_o}\right)$ can be calculated from Equation 126 or 127. If the shell is subjected to an axial tension loading, a negative value for q_2 is used in the formulas which yields an increase in frequency.

It can be seen that the greatest change in frequency occurs in those modes having the lowest buckling values q_{20}.

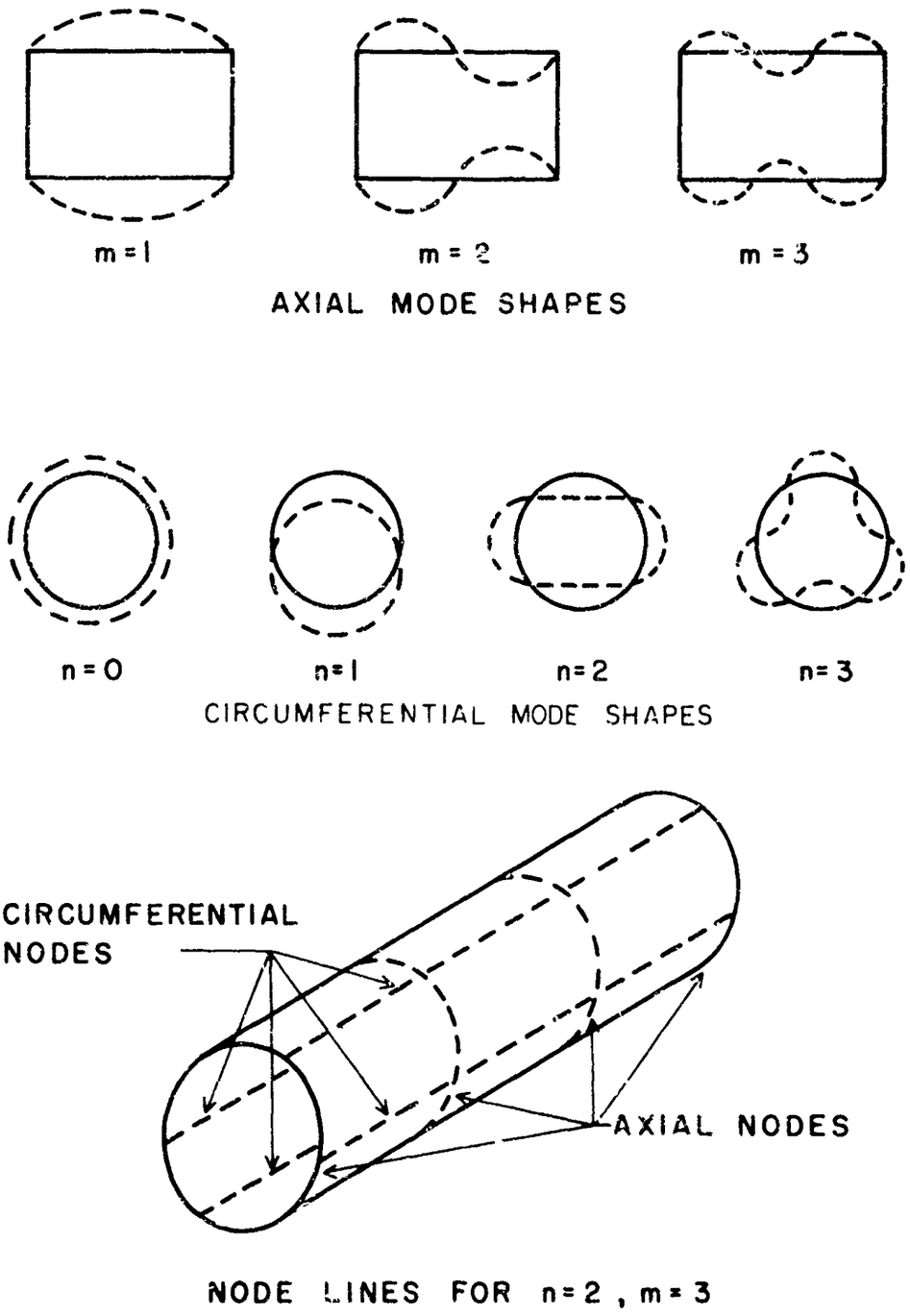

Figure 2. Deflection Modes

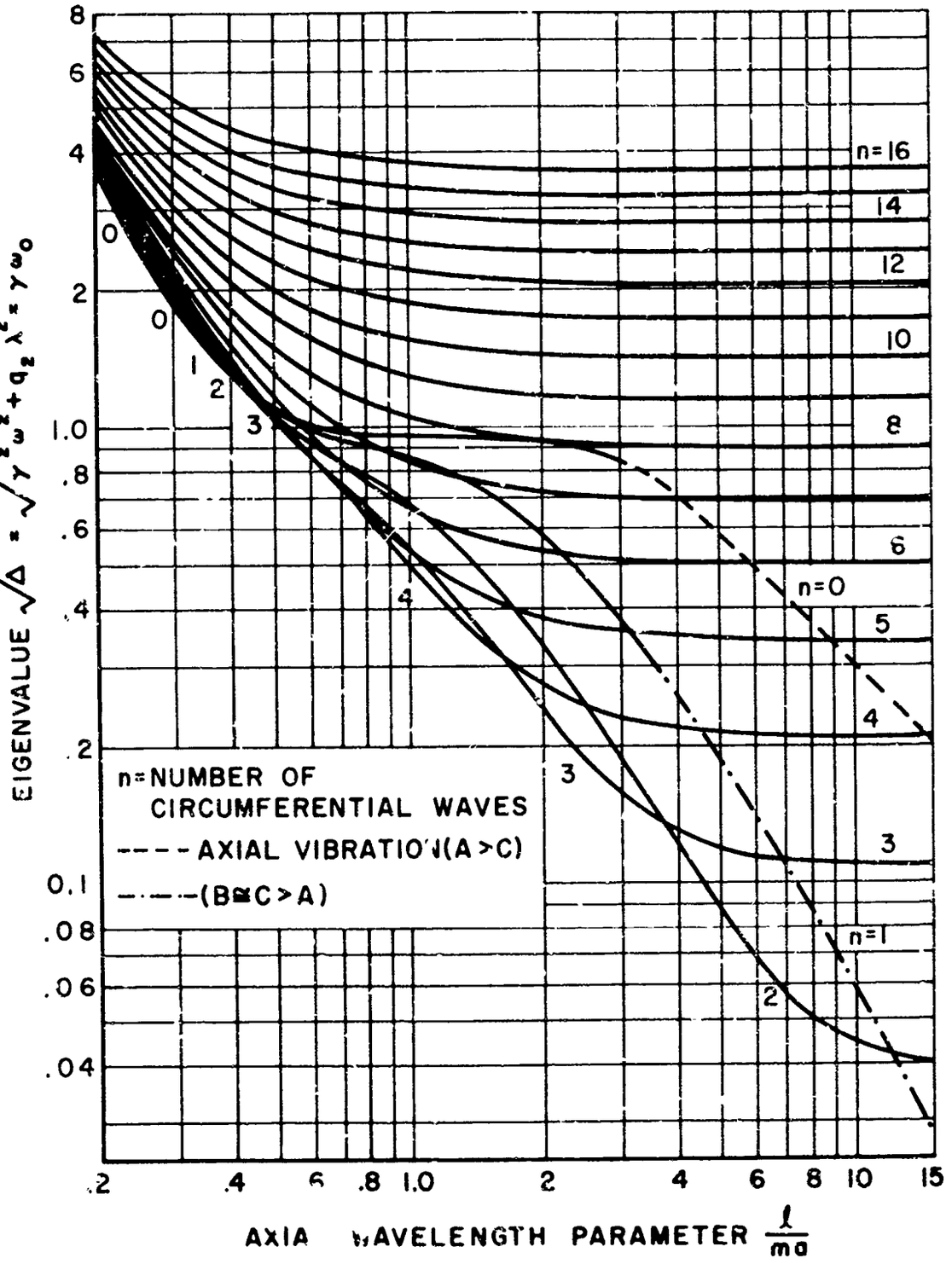

Figure 3. Radial Vibration Frequencies. $\frac{a}{h} = 20$. No external Pressure ($q_1 = 0$)

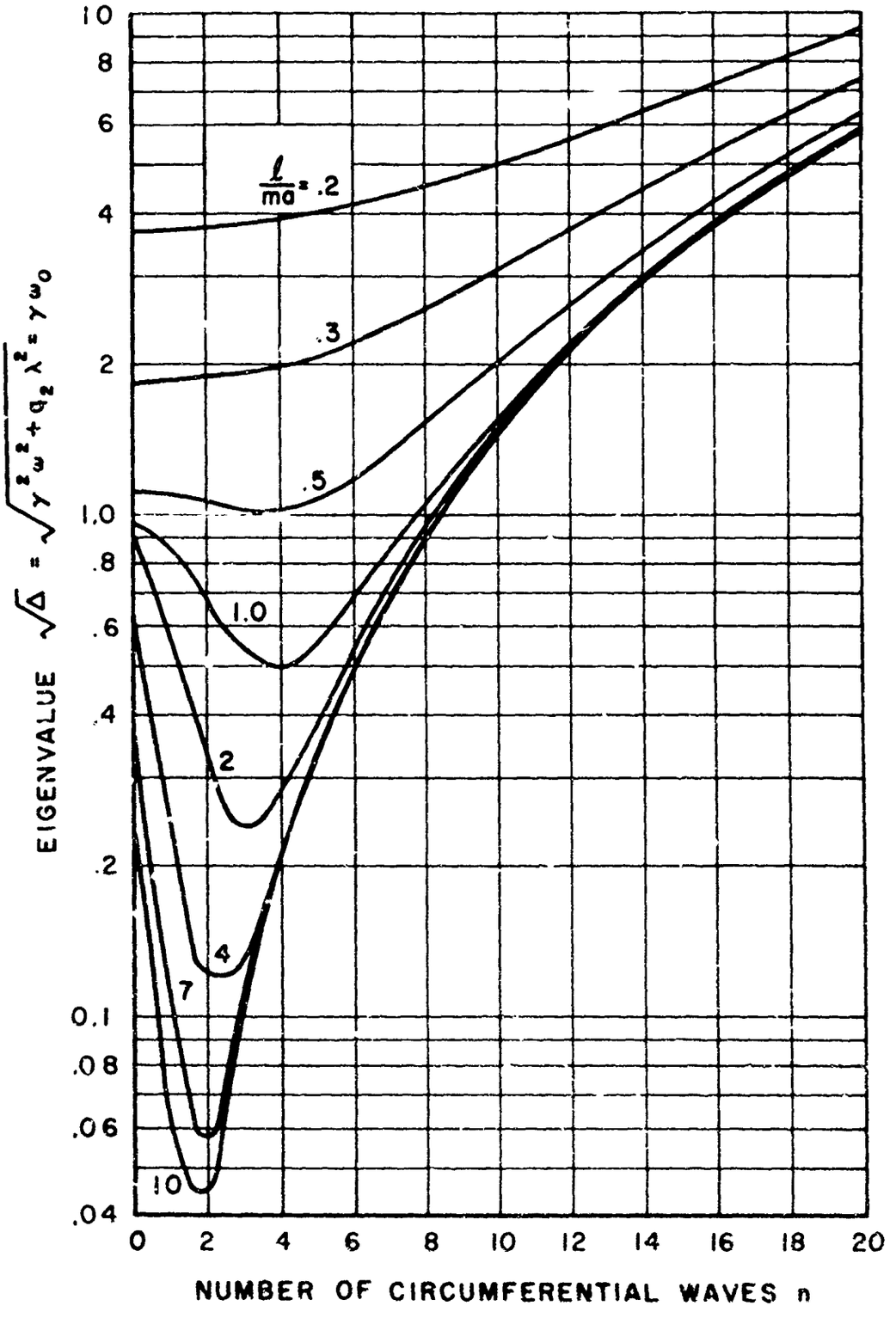

Figure 4. Radial Vibration Frequencies, $\frac{a}{h} = 20$. No external Pressure ($q_1 = 0$)

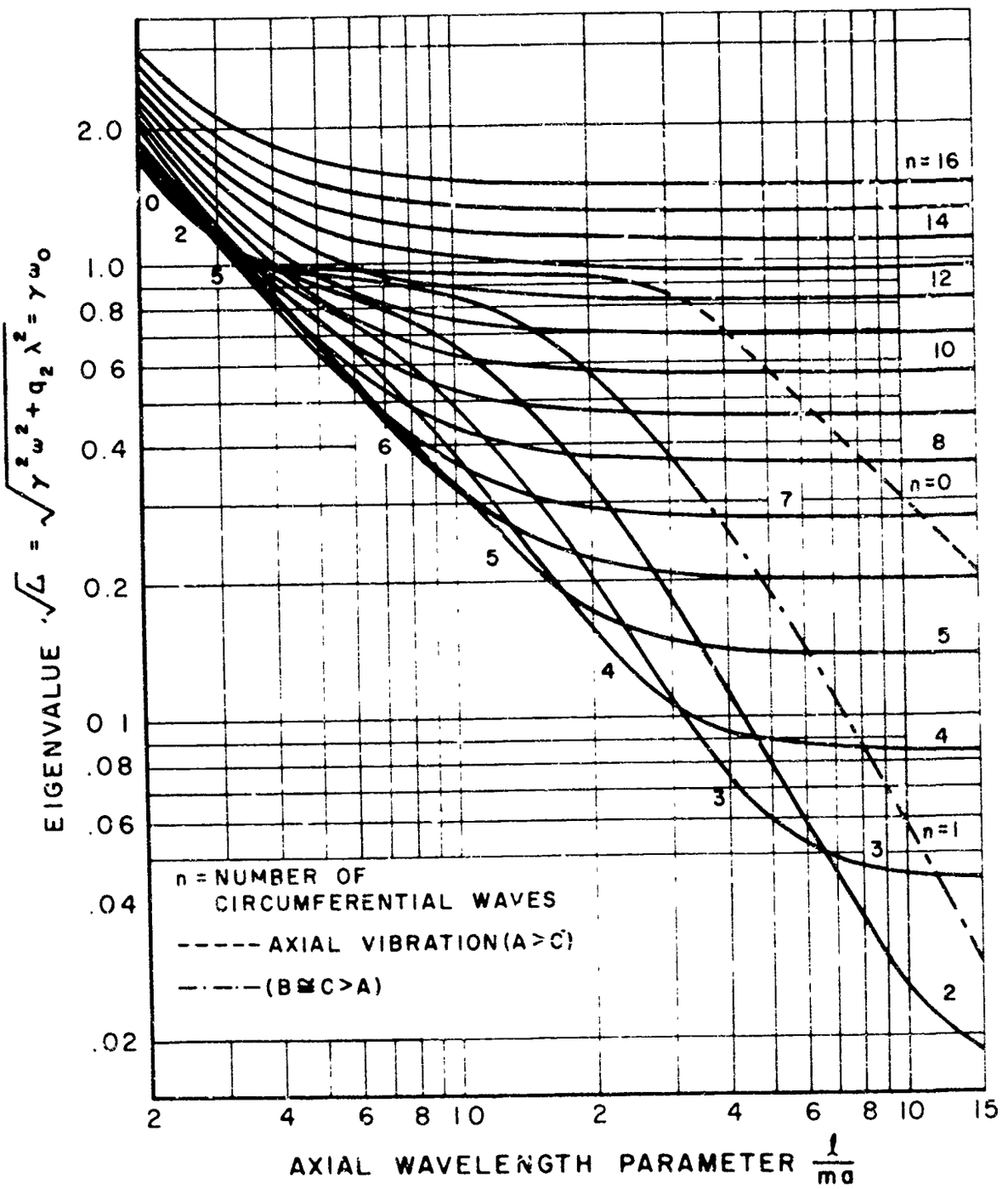

Figure 5. Radial Vibration Frequencies, $\frac{a}{h} = 50$, No External Pressure ($q_1 = 0$)

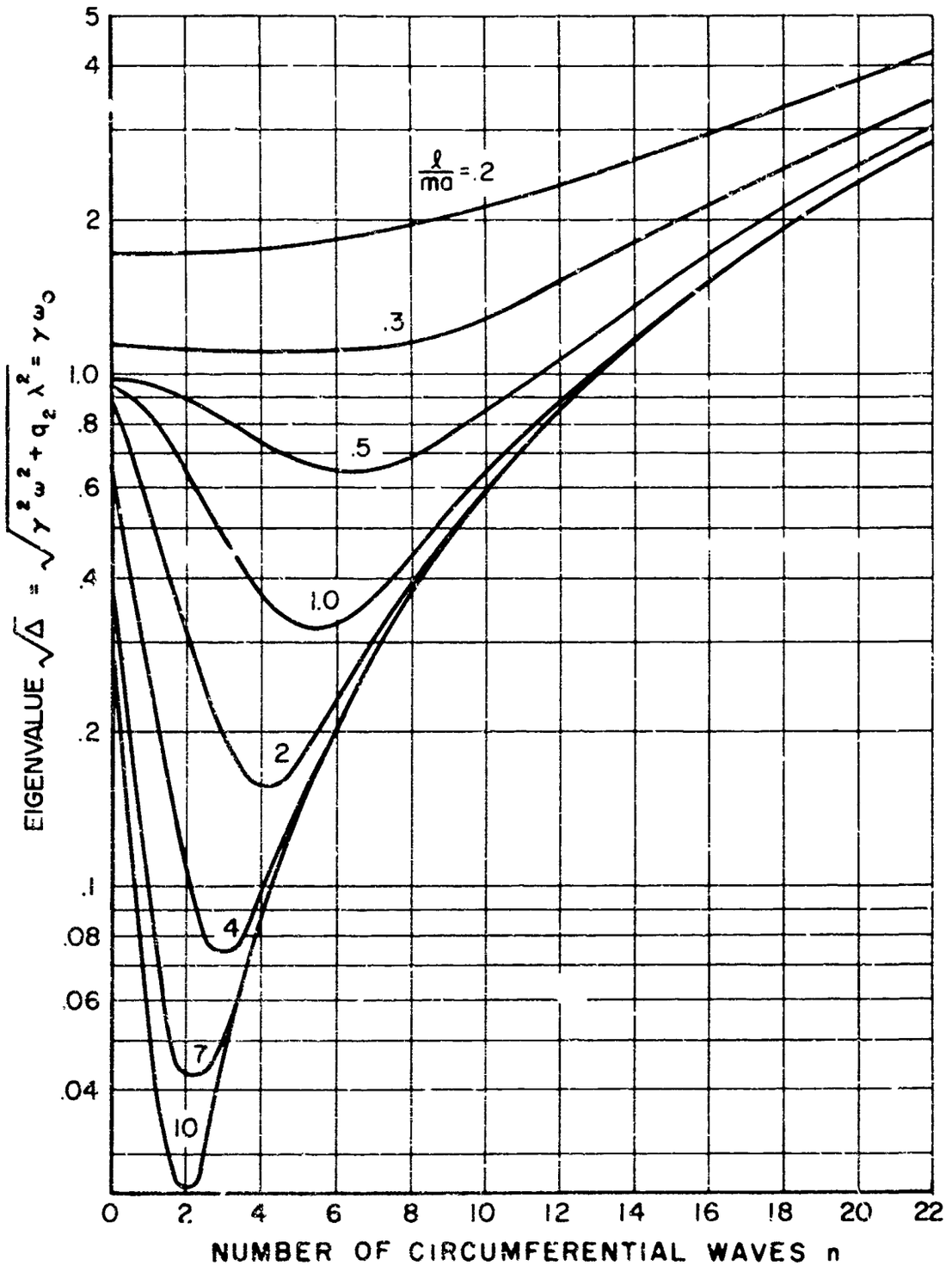

Figure 6. Radial Vibration Frequencies, $\frac{a}{h}=50$, No External Pressure ($q_1 = 0$)

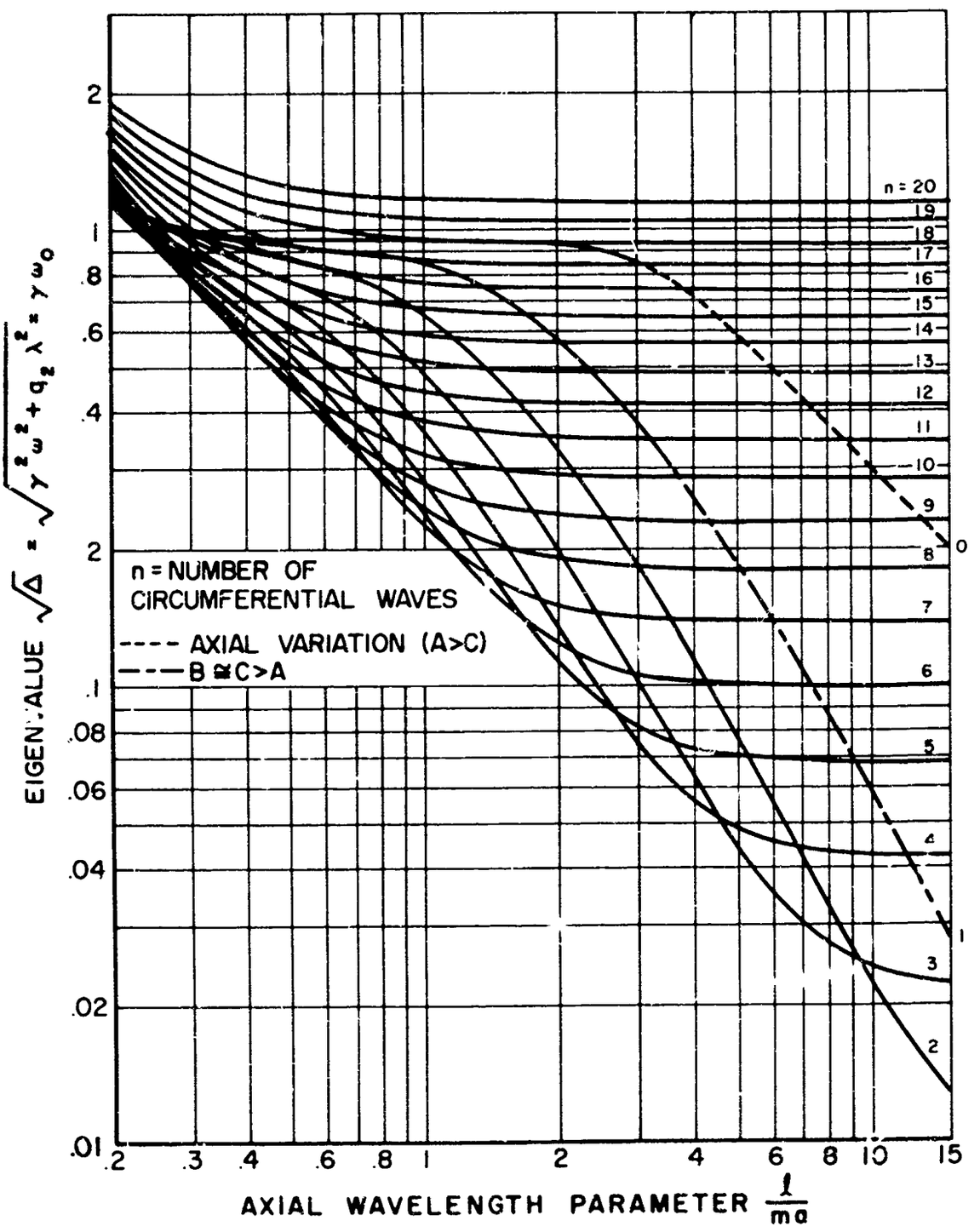

Figure 7. Radial Vibration Frequencies. $\frac{a}{h} = 100$. No External Pressure ($q_1 = 0$)

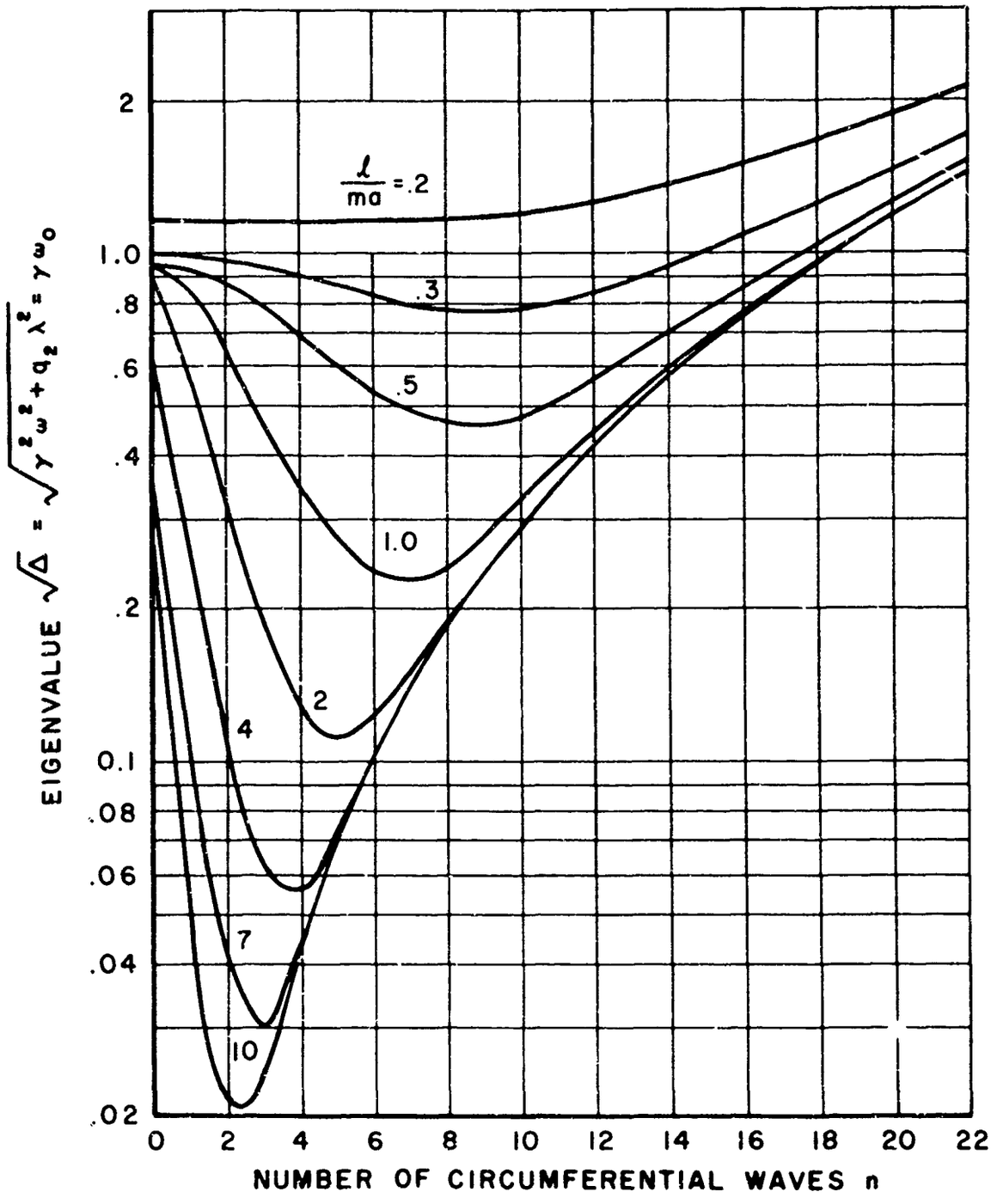

Figure 8. Radial Vibration Frequencies. $\frac{a}{h} = 100$. No External Pressure ($q_1 = 0$)

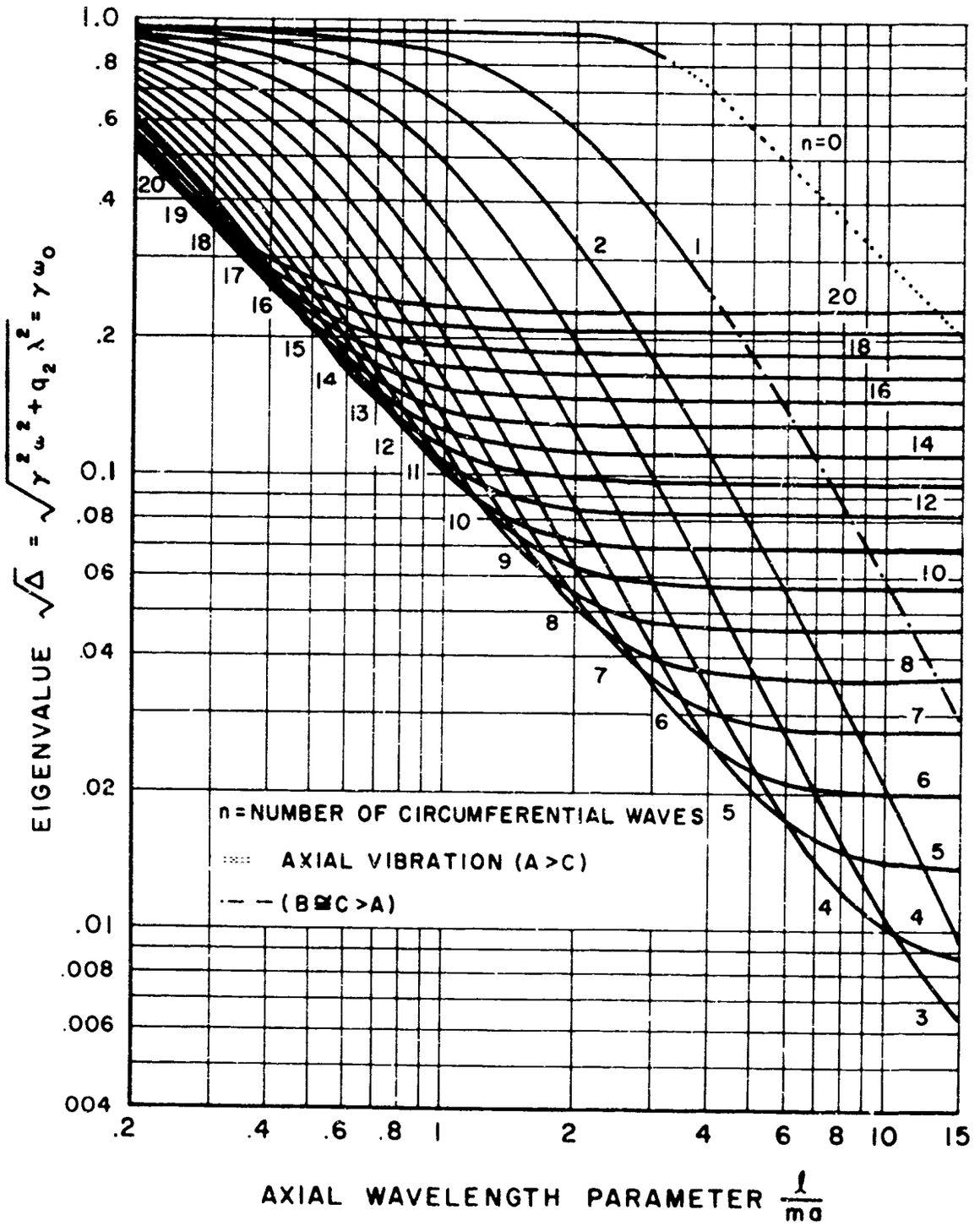

Figure 9. Radial Vibration Frequencies, $\frac{a}{h} = 500$, No External Pressure ($q_1 = 0$)

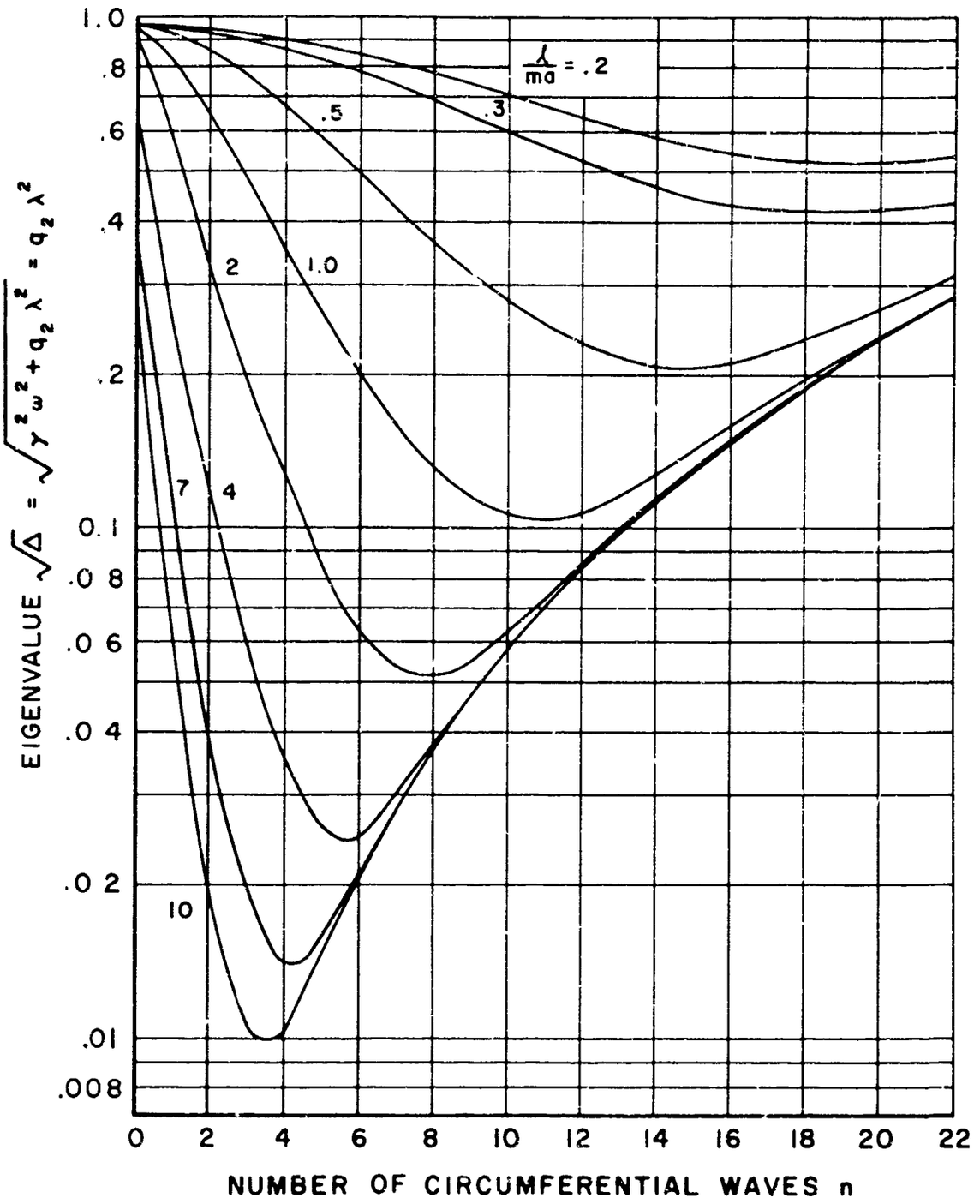

Figure 10. Radial Vibration Frequencies. $\frac{a}{h} = 500$. No External Pressure ($q_1 = 0$)

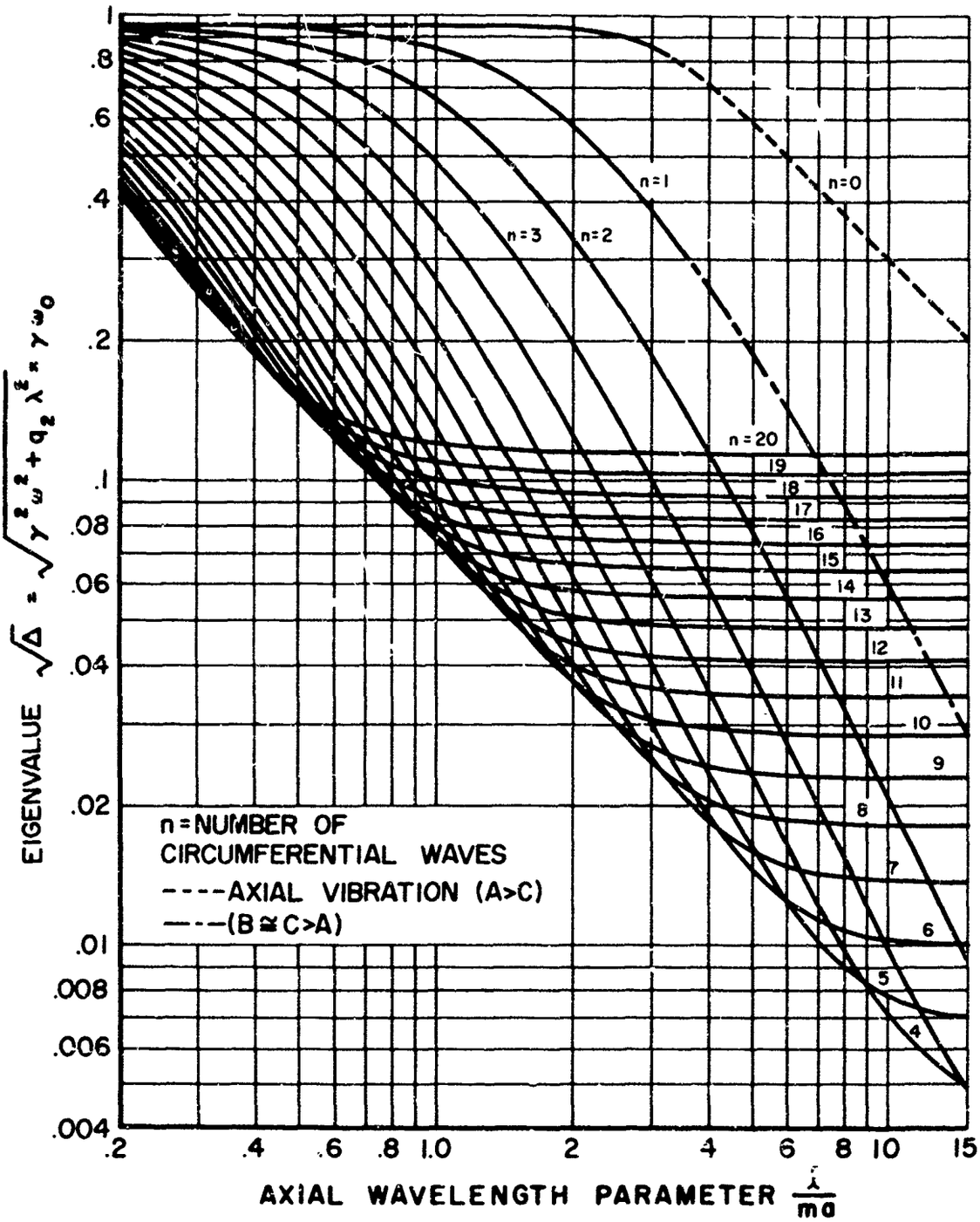

Figure 11. Radial Vibration Frequencies, $\frac{a}{h}$=1000. No External Pressure (q_1 = 0)

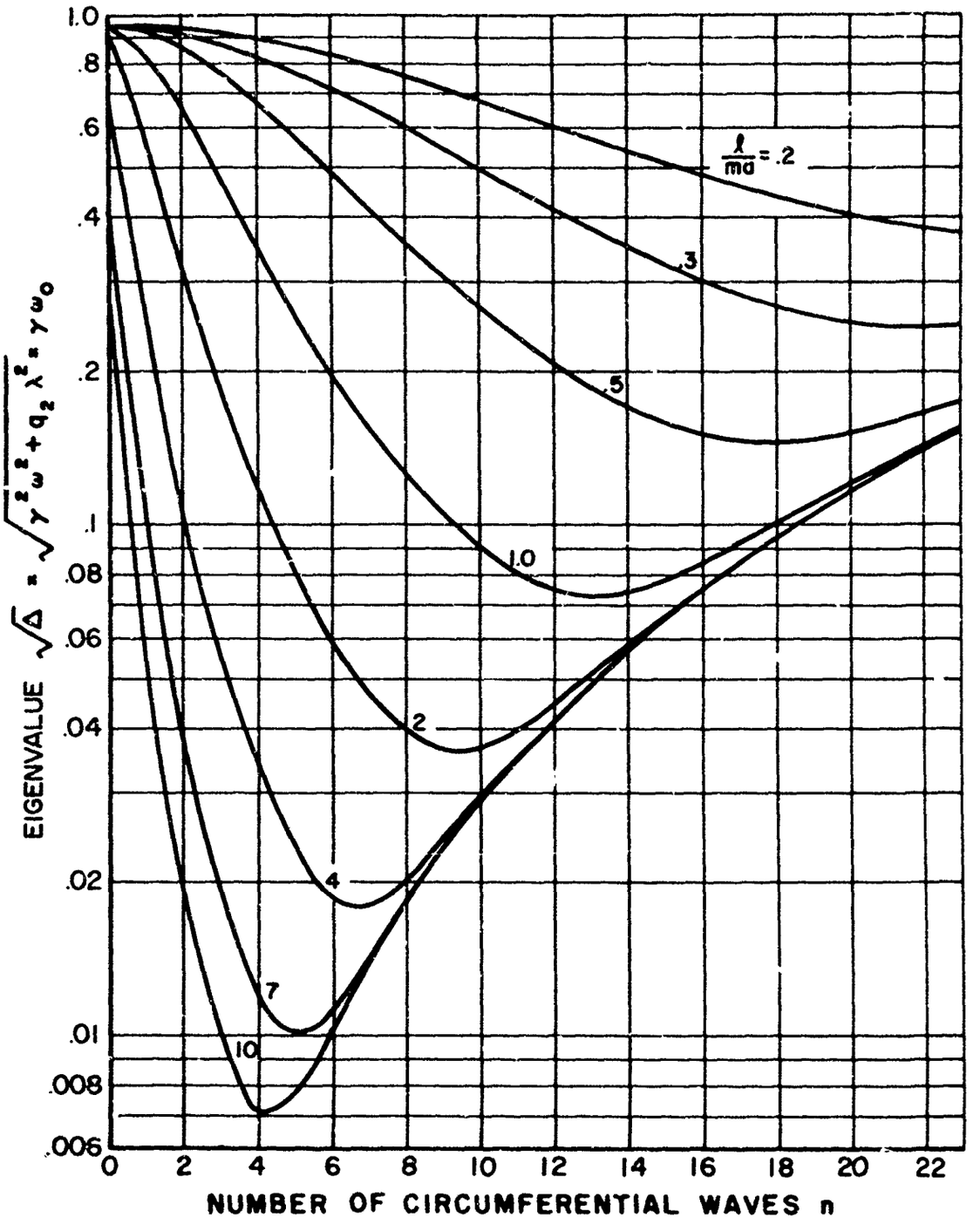

Figure 12. Radial Vibration Frequencies. $\frac{a}{h} = 1000$. No External Pressure ($q_1 = 0$)

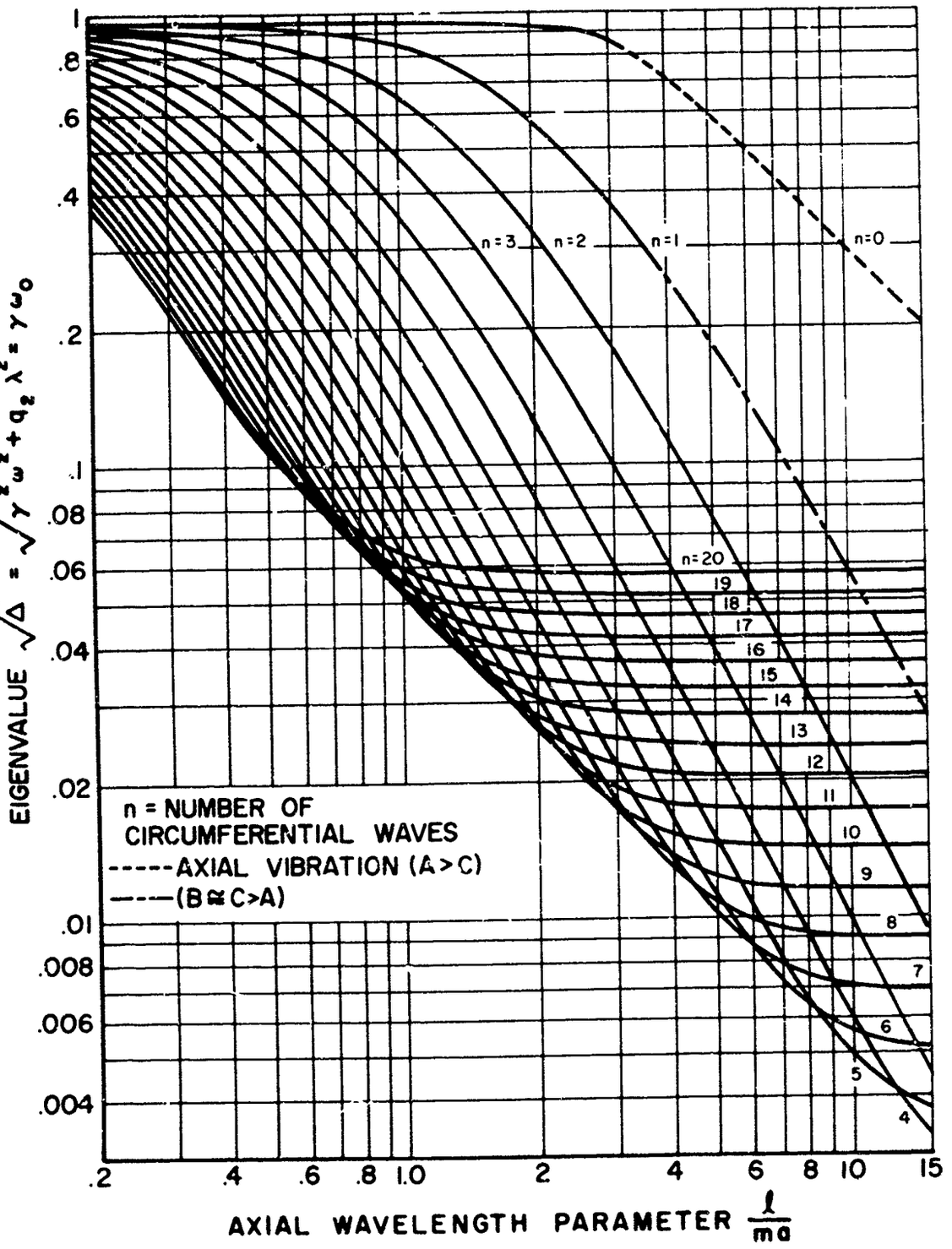

Figure 13. Radial Vibration Frequencies. $\frac{a}{h} = 2000$. No External Pressure ($q_1 = 0$)

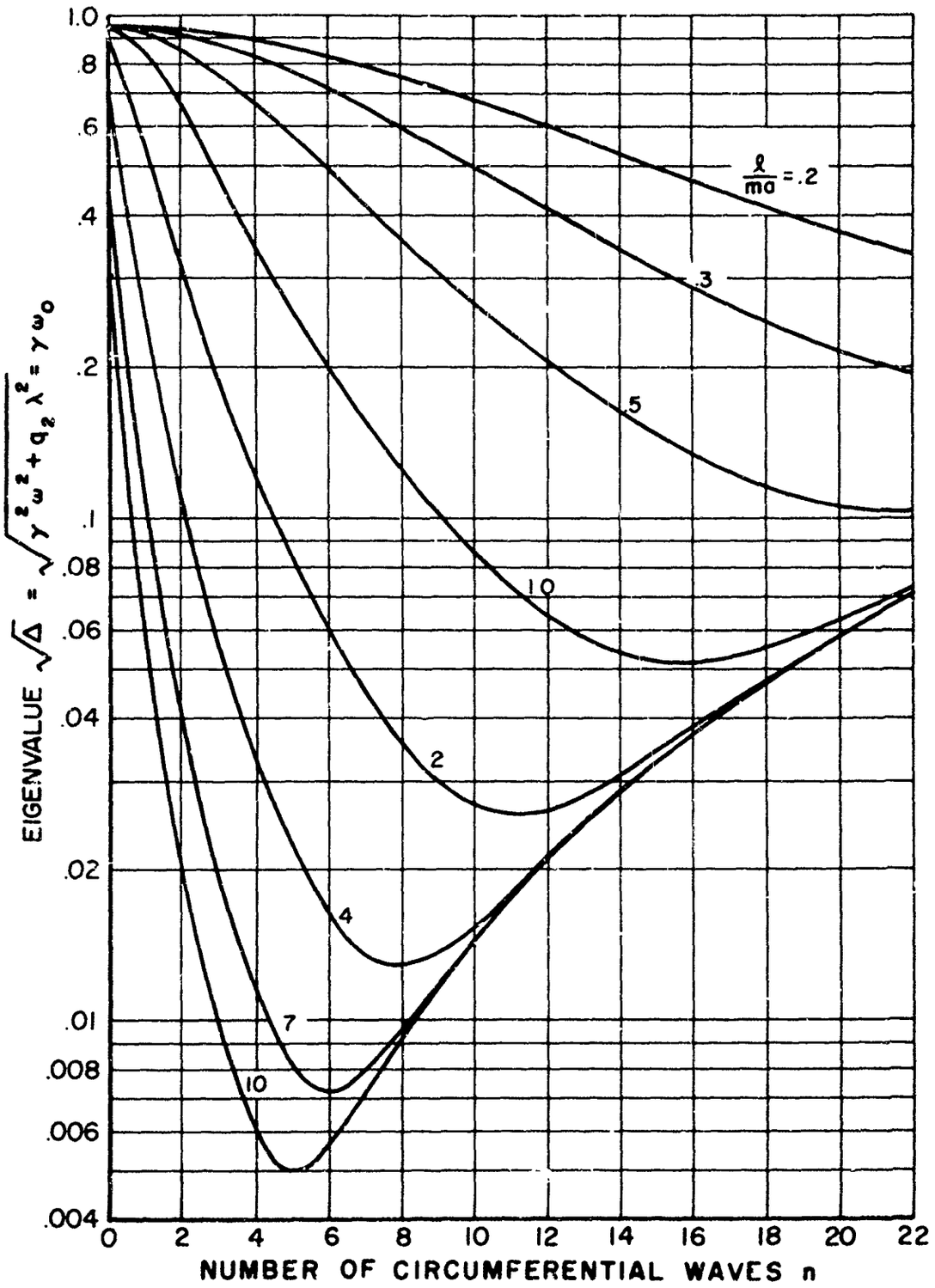

Figure 14. Radial Vibration Frequencies. $\frac{a}{h}$=2000. No External Pressure (q_1 = 0)

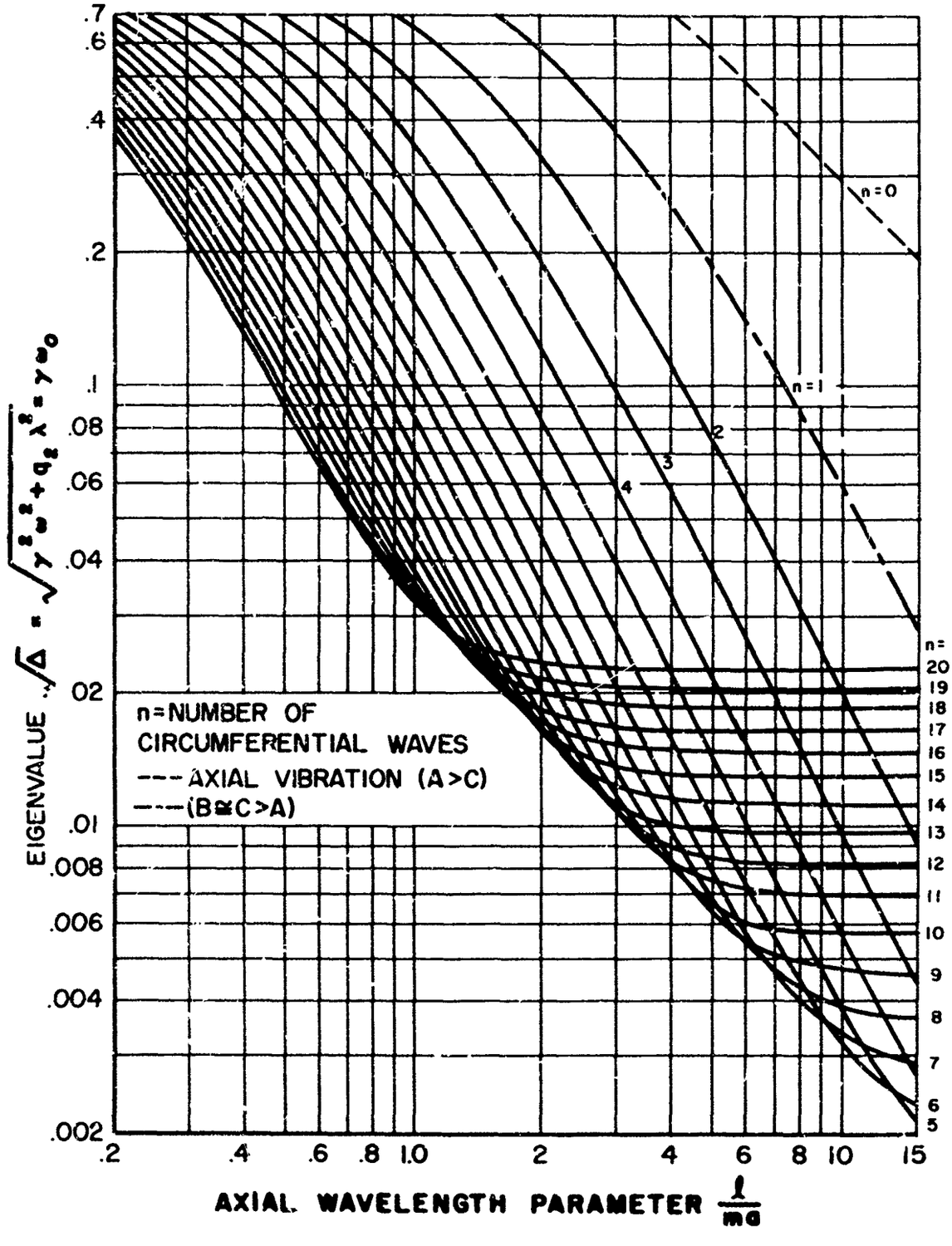

Figure 15. Radial Vibration Frequencies. $\frac{a}{h}$=5000. No External Pressure (q_1 = 0)

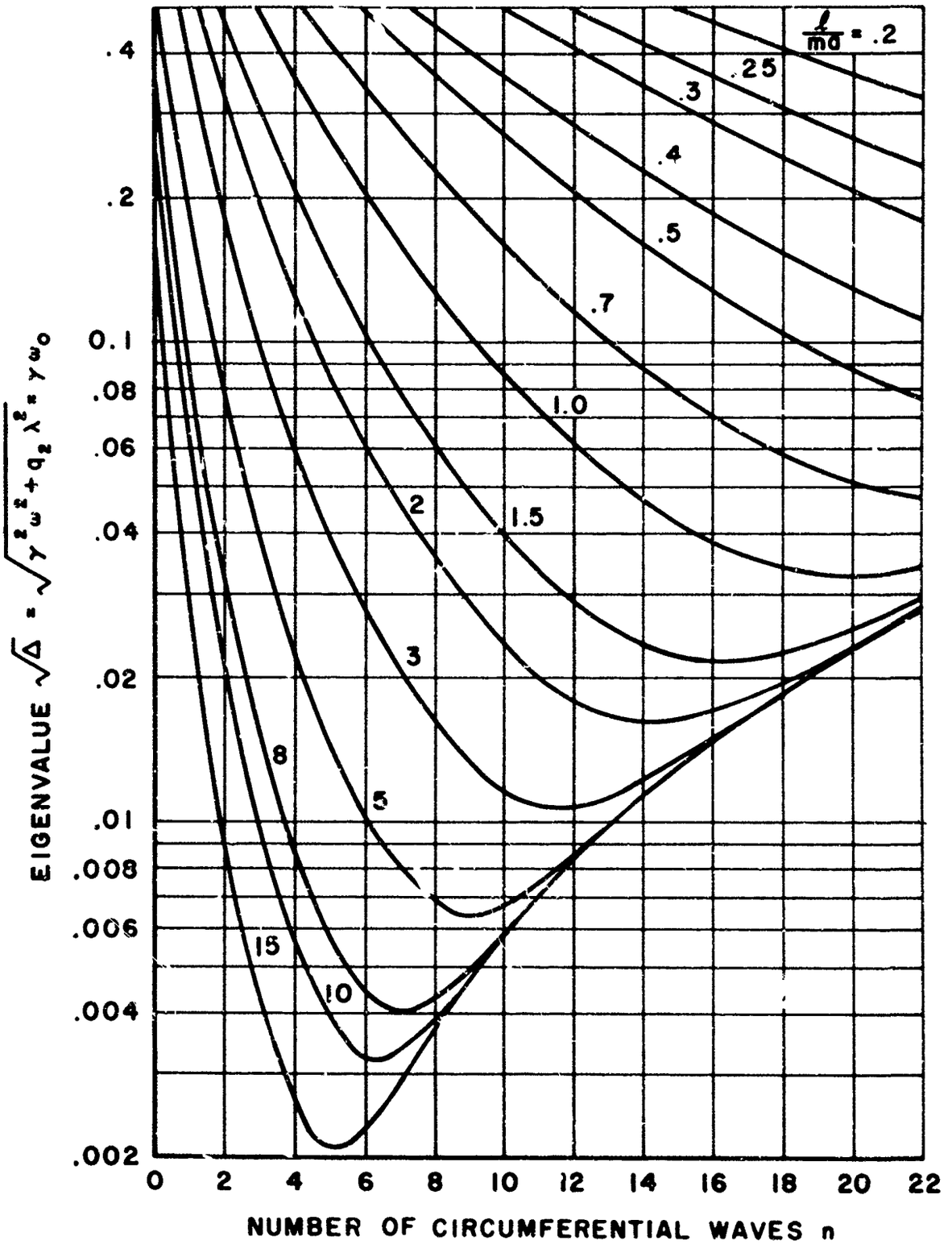

Figure 16. Radial Vibration Frequencies. $\frac{a}{h}$=5000. No External Pressure (q_1 = 0)

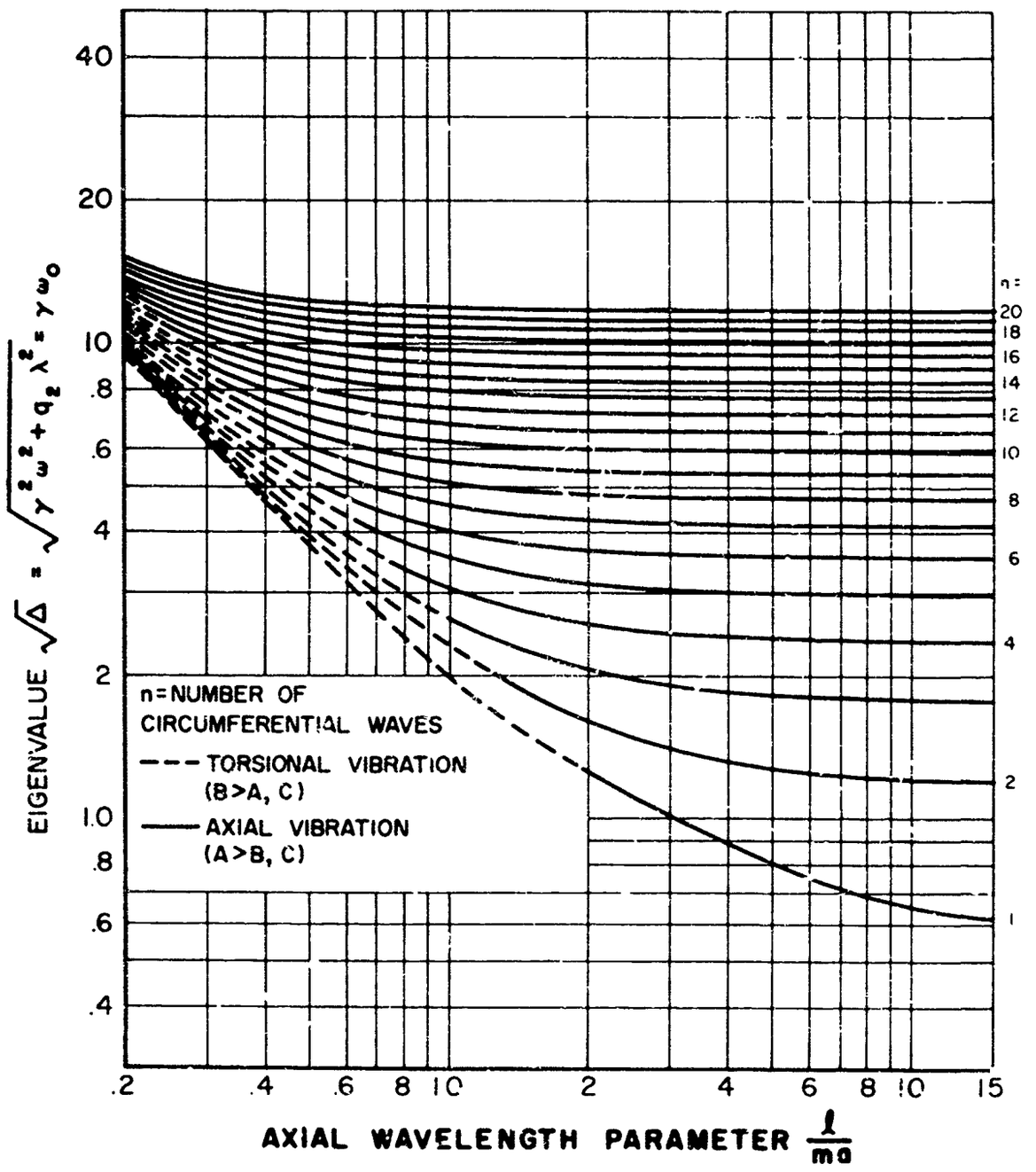

Figure 17. Second Vibration Frequencies, $\frac{a}{h} = 20\text{-}5000$, No External Pressure ($q_1 = 0$)

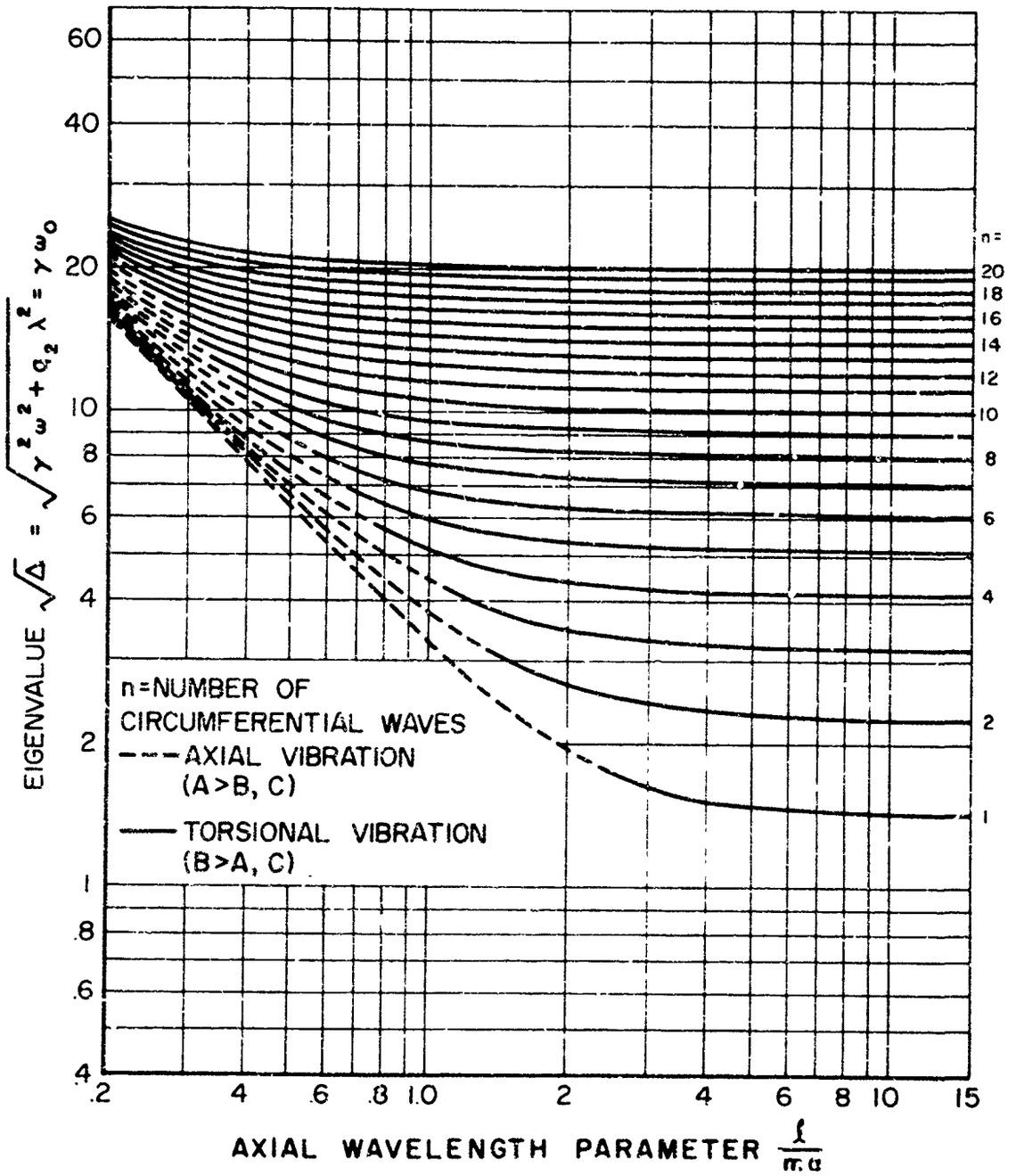

Figure 18. Third Vibration Frequencies, $\frac{a}{h}$ - 20-500, No External Pressure ($q_1 = 0$)

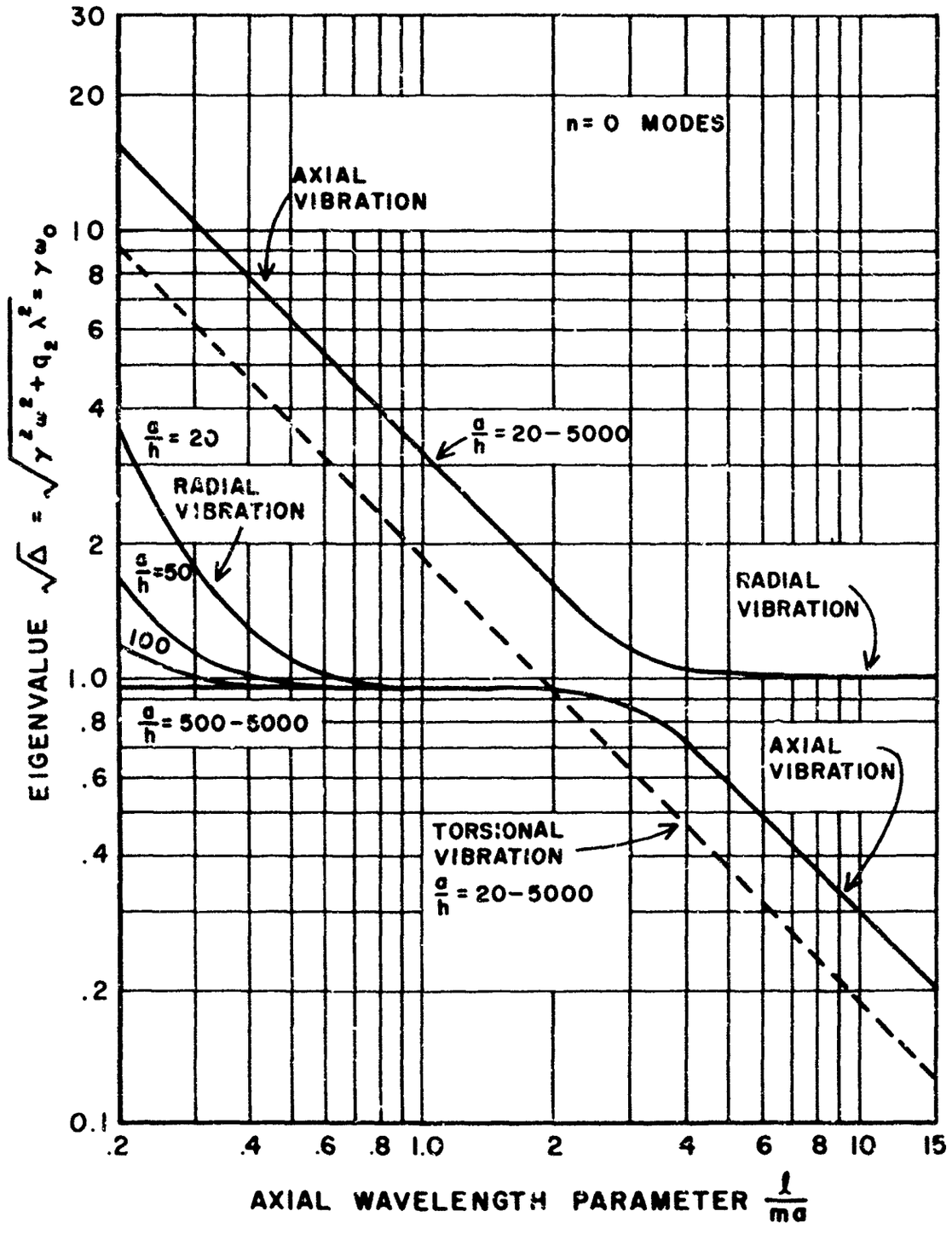

Figure 19. Axisymmetric Vibration Frequencies. $\frac{a}{h}$ = 20-5000. No External Pressure ($q_1 = 0$)

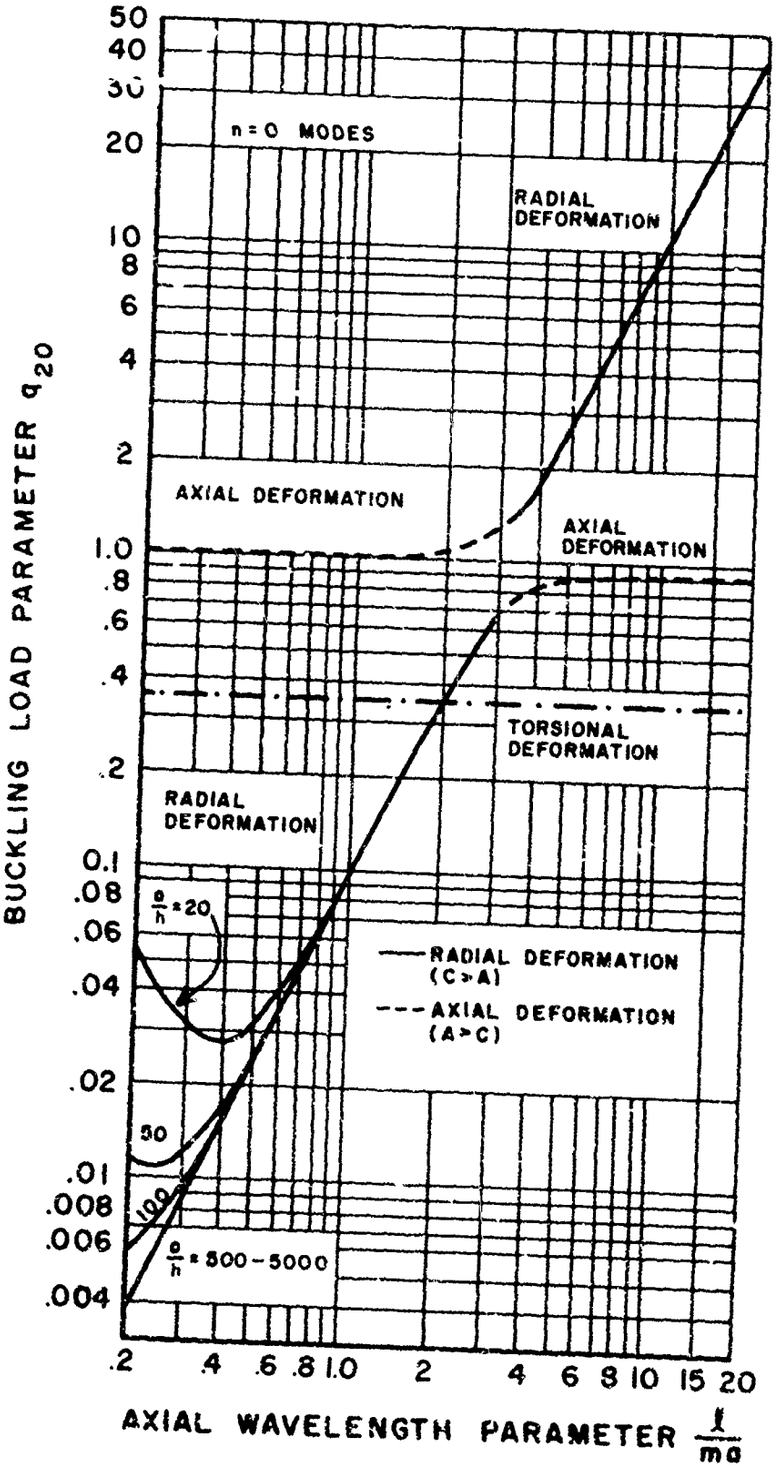

Figure 20. Axisymmetric Buckling, Axial Compressior $\frac{a}{h}$ = 20-5000. No External Pressure (q_1 = 0)

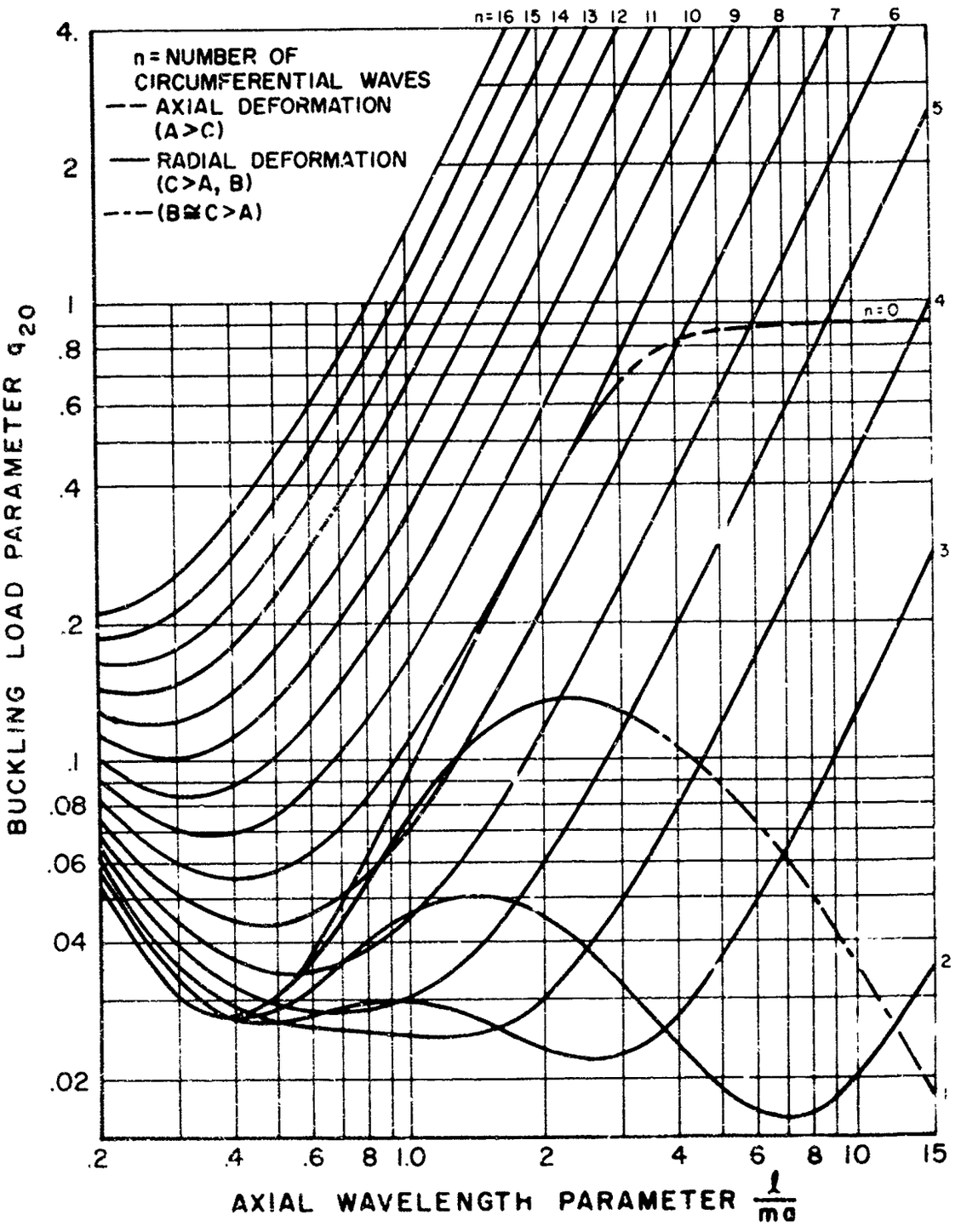

Figure 21. Buckling Values for Axial Compression, $\frac{a}{h}$=20, No External Pressure ($q_1 = 0$)

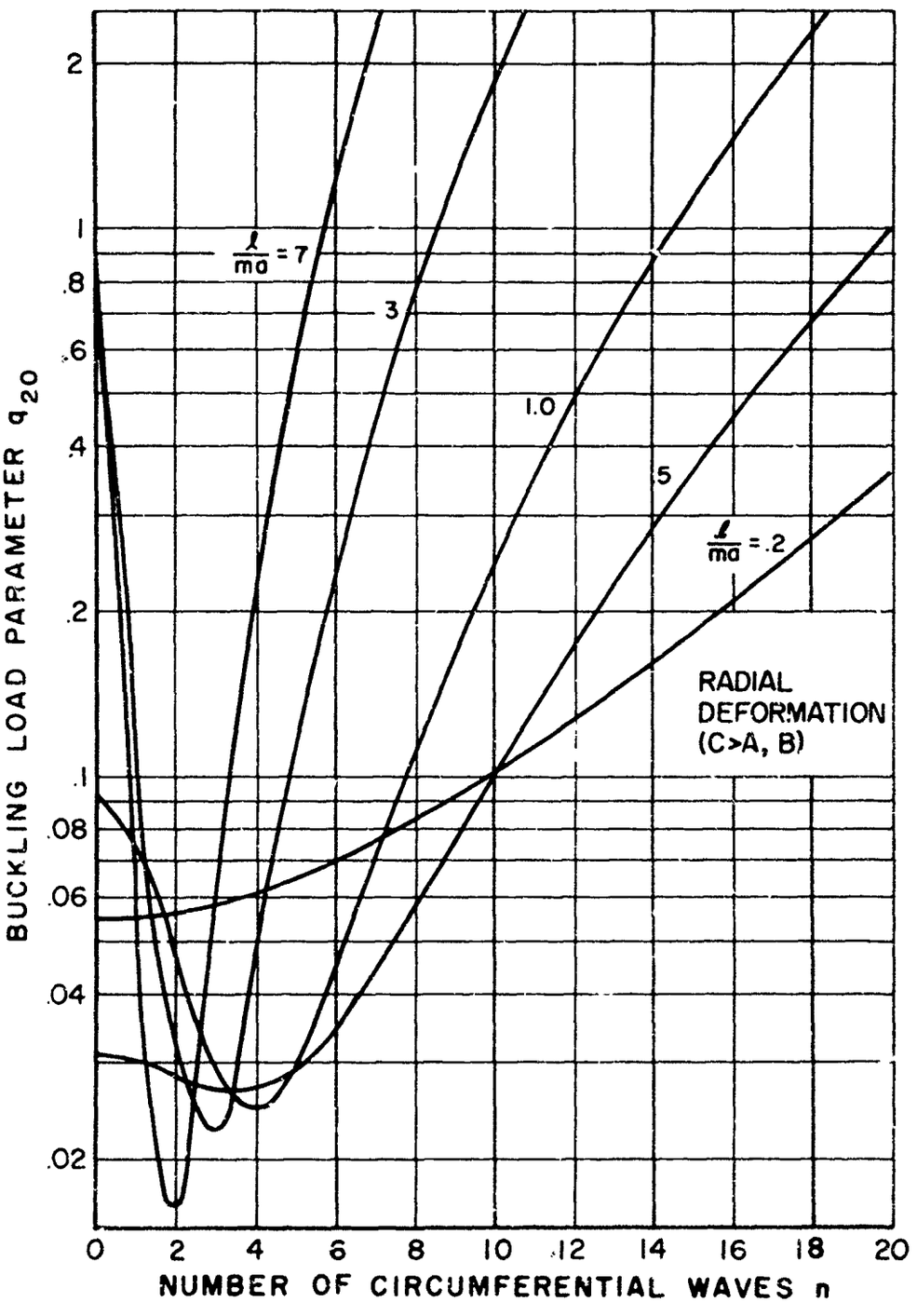

Figure 22. Buckling Values for Axial Compression. $\frac{a}{h} = 20$. No External Pressure ($q_1 = 0$)

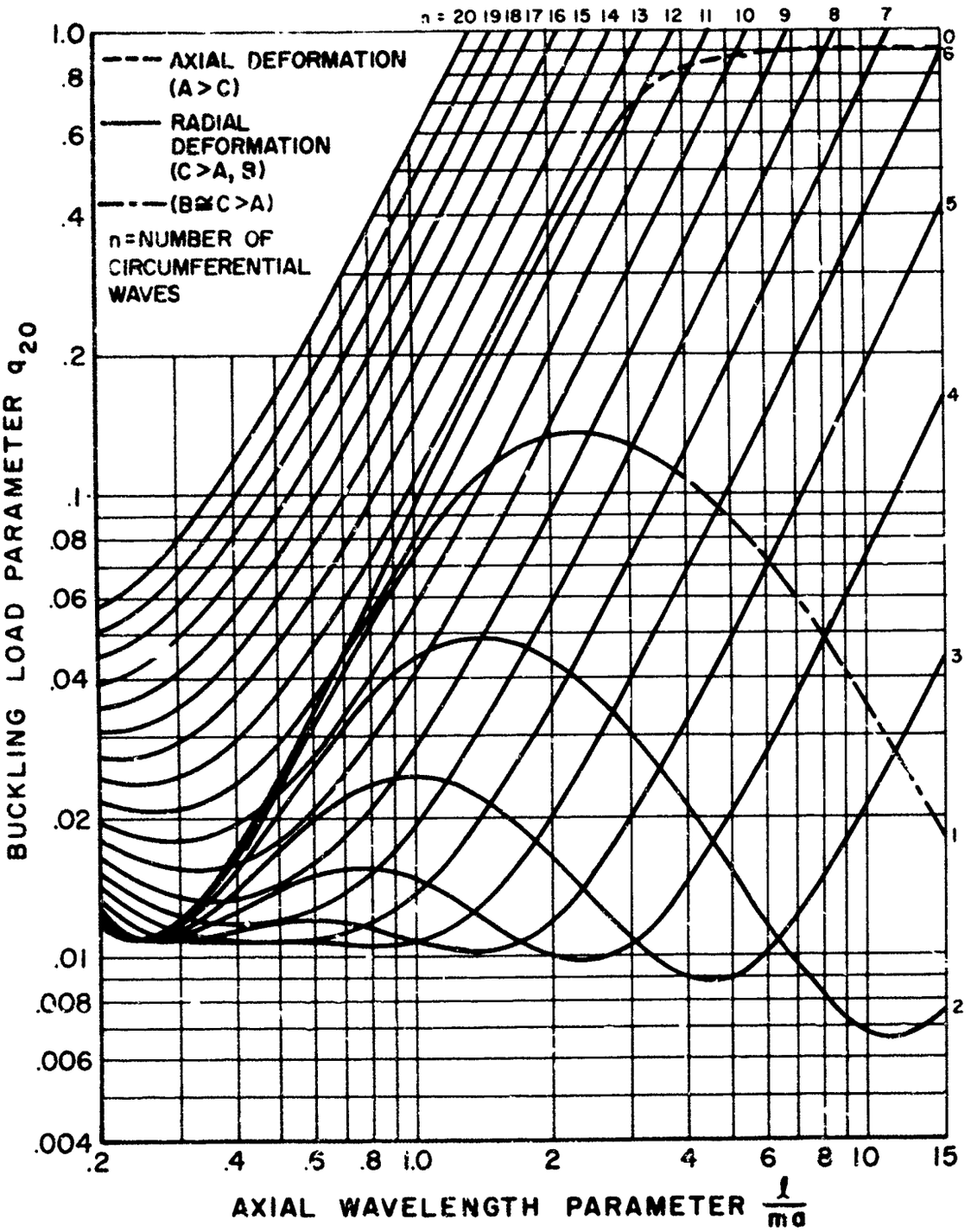

Figure 23 Buckling Values for Axial Compression. $\frac{a}{h} = 50$. No External Pressure ($q_1 = 0$)

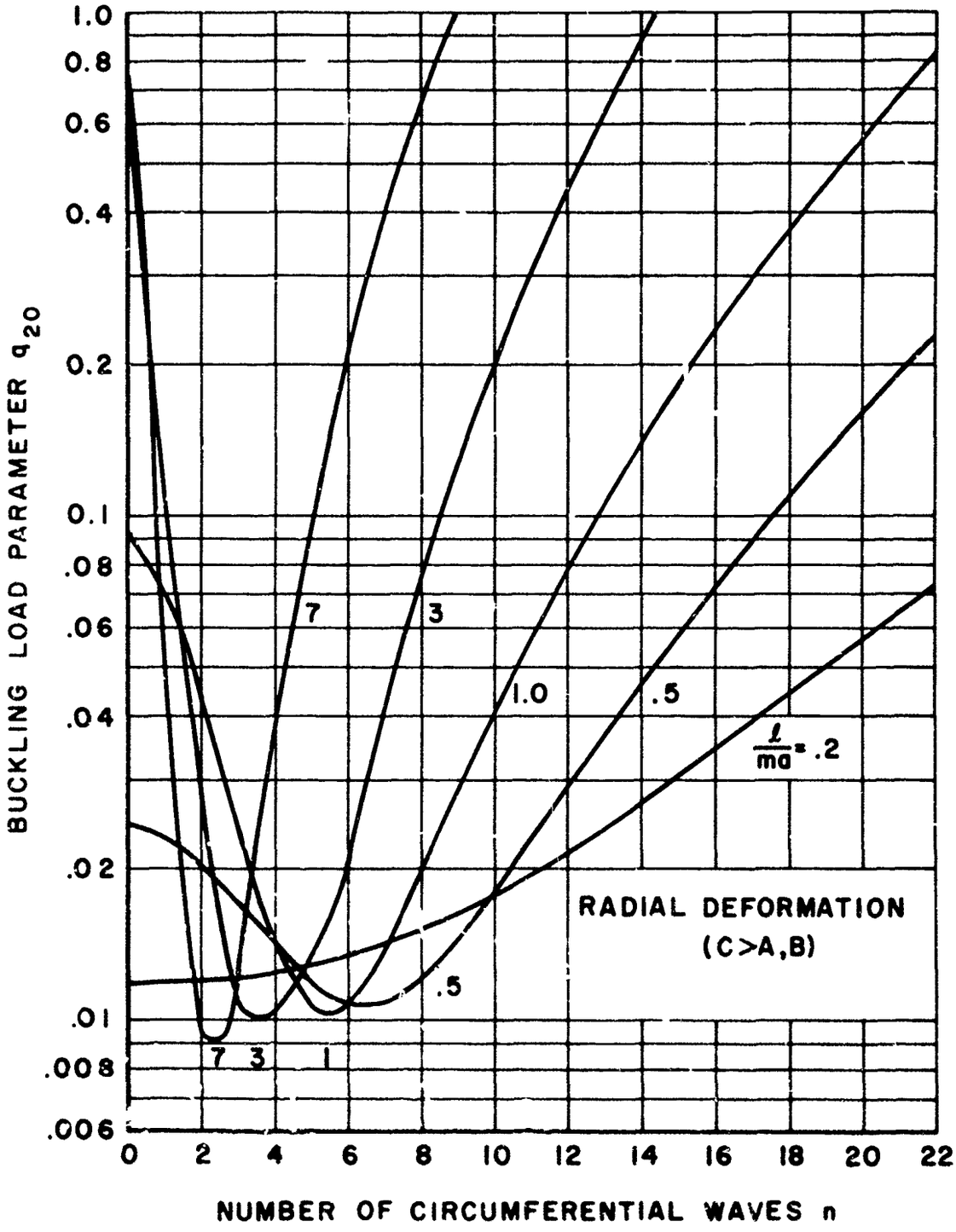

Figure 24. Buckling Values for Axial Compression. $\frac{a}{h}$=50. No External Pressure (q_1 = 0)

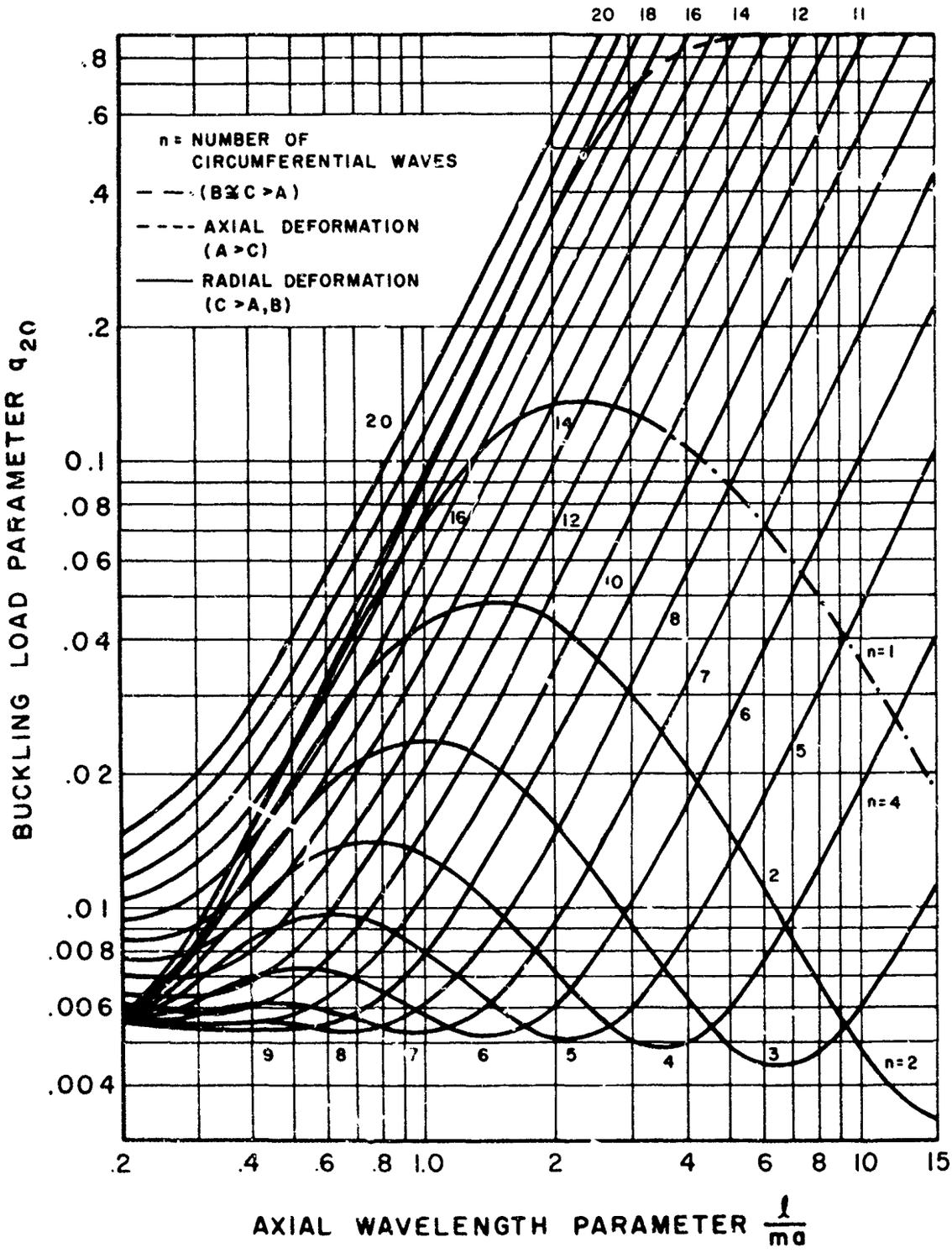

Figure 25. Buckling Values for Axial Compression, $\frac{a}{h}$ =100, No External Pressure (q_1 = 0)

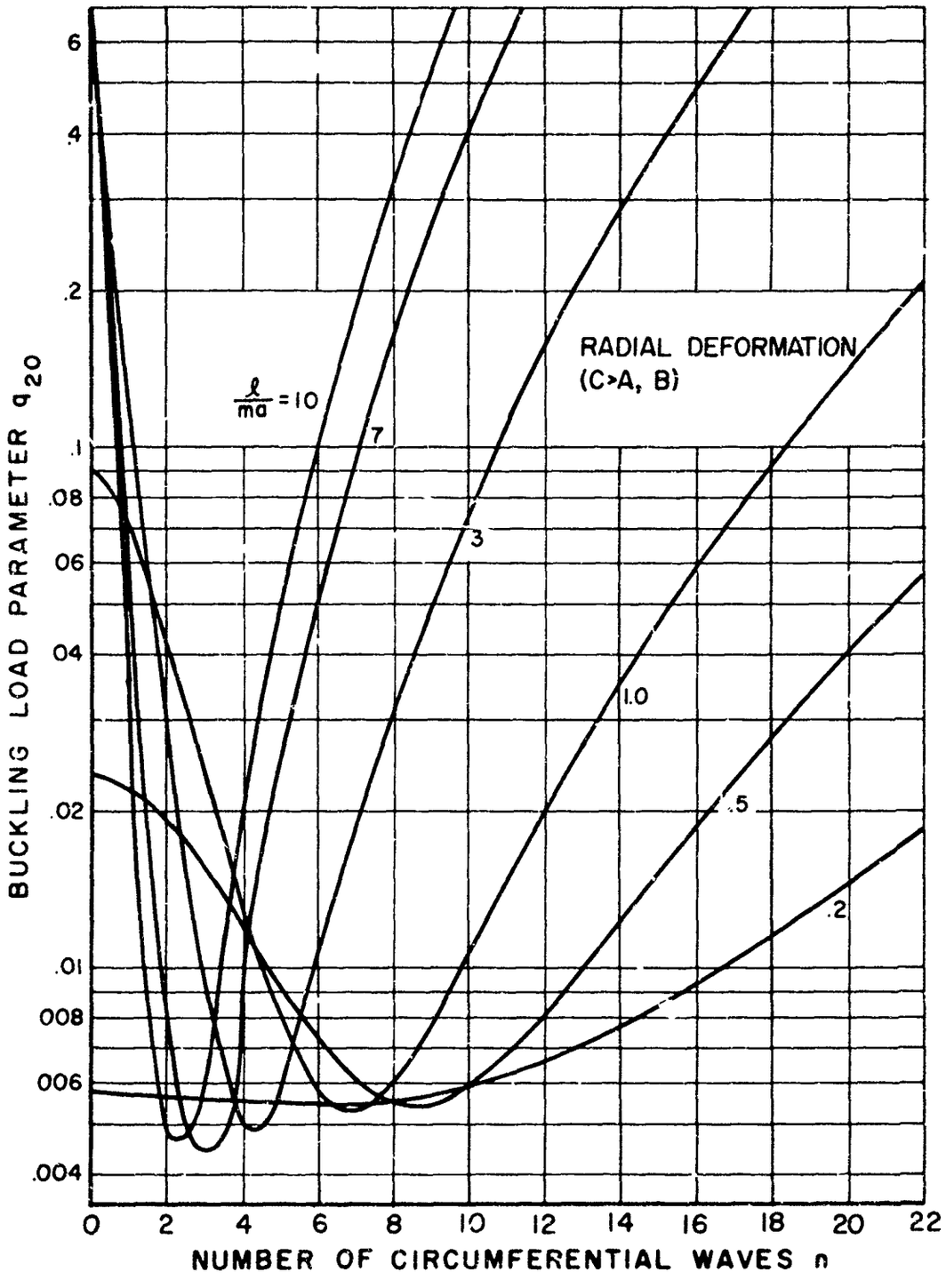

Figure 26. Buckling Values for Axial Compression. $\frac{a}{h}$=100. No External Pressure (q_1 = 0)

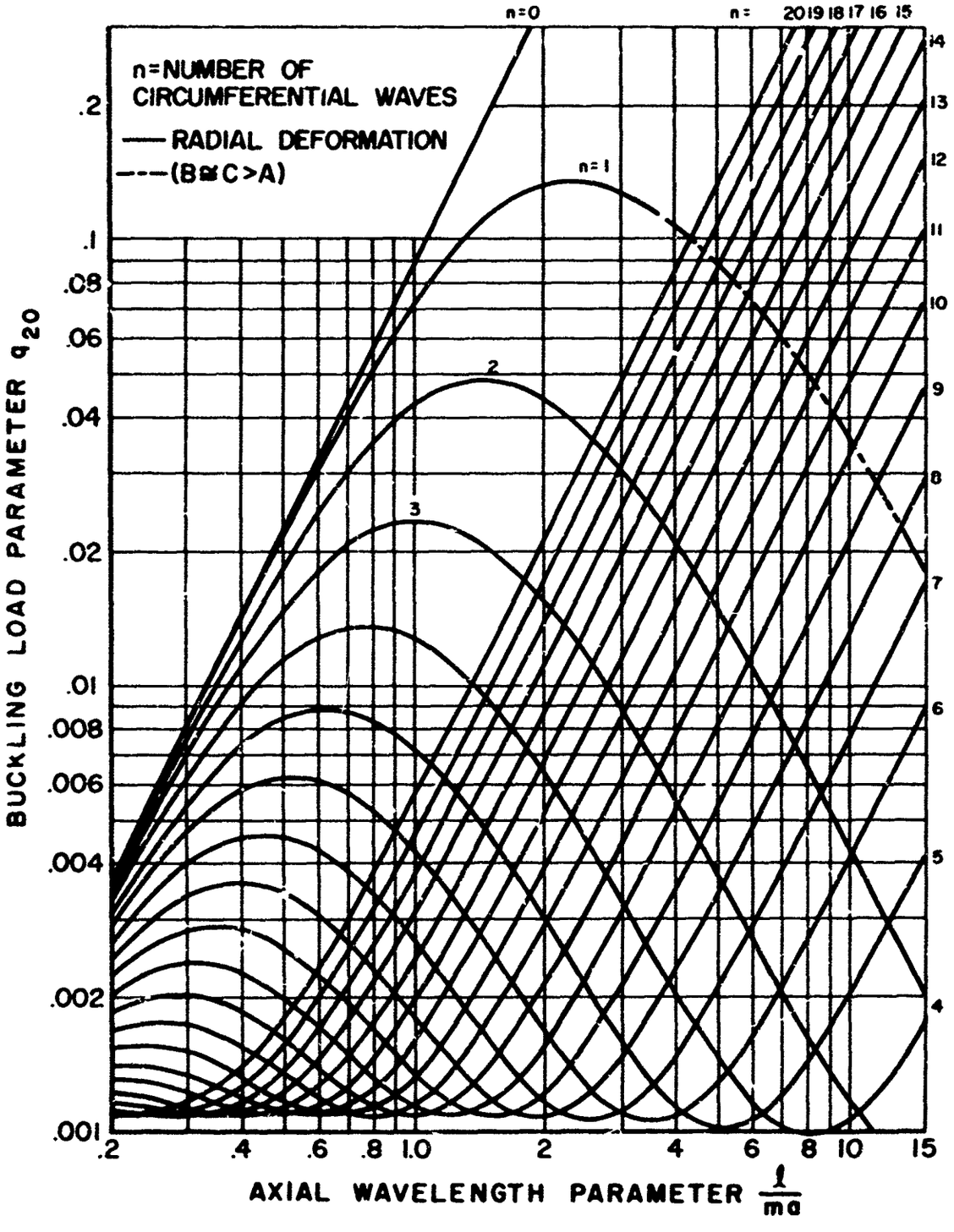

Figure 27. Buckling Values for Axial Compression. $\frac{a}{b}$=500. No External Pressure ($q_1 = 0$)

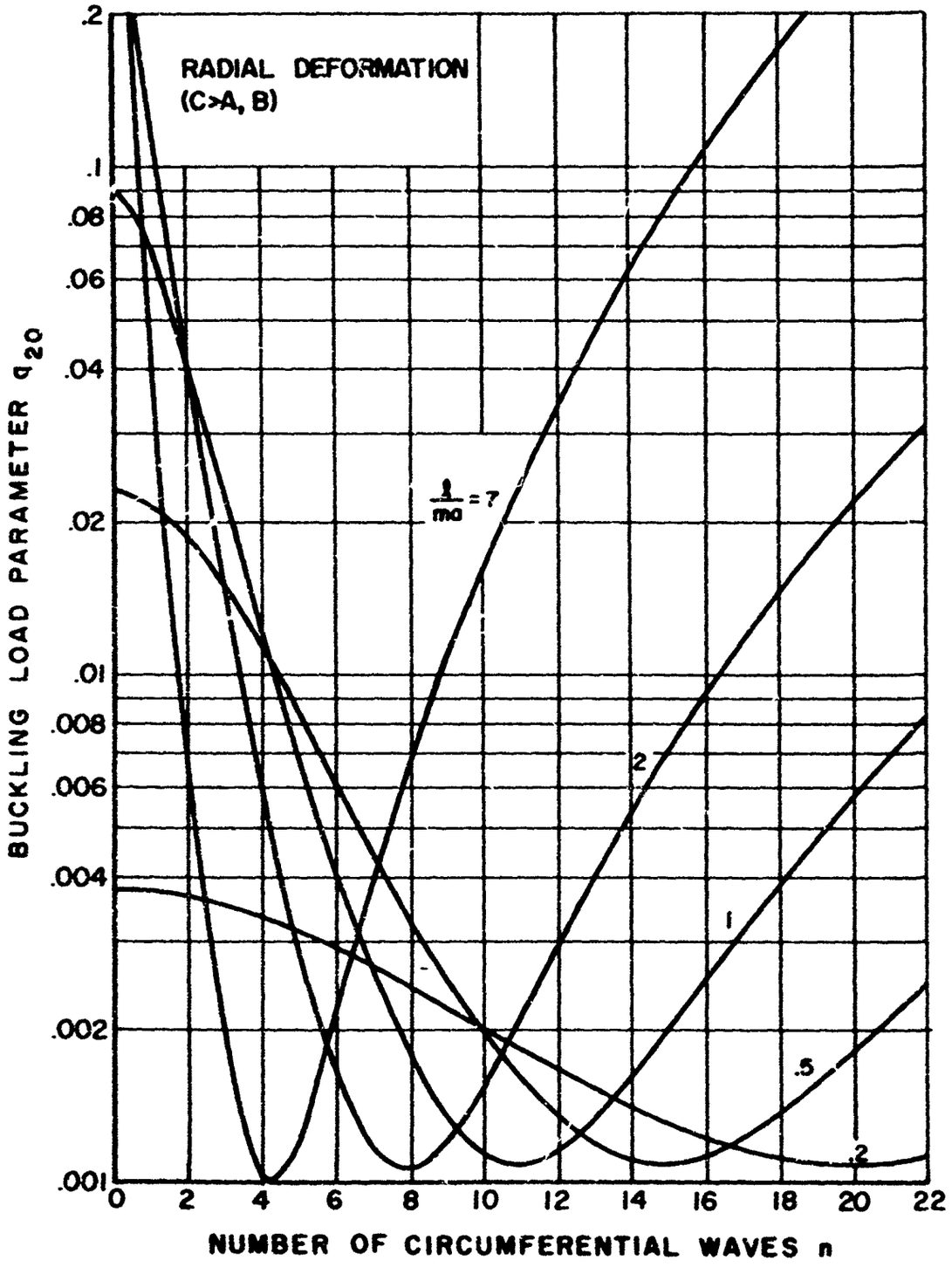

Figure 28. Buckling Values for Axial Compression. $\frac{a}{b}$=500. No External Pressure (q_1 = 0)

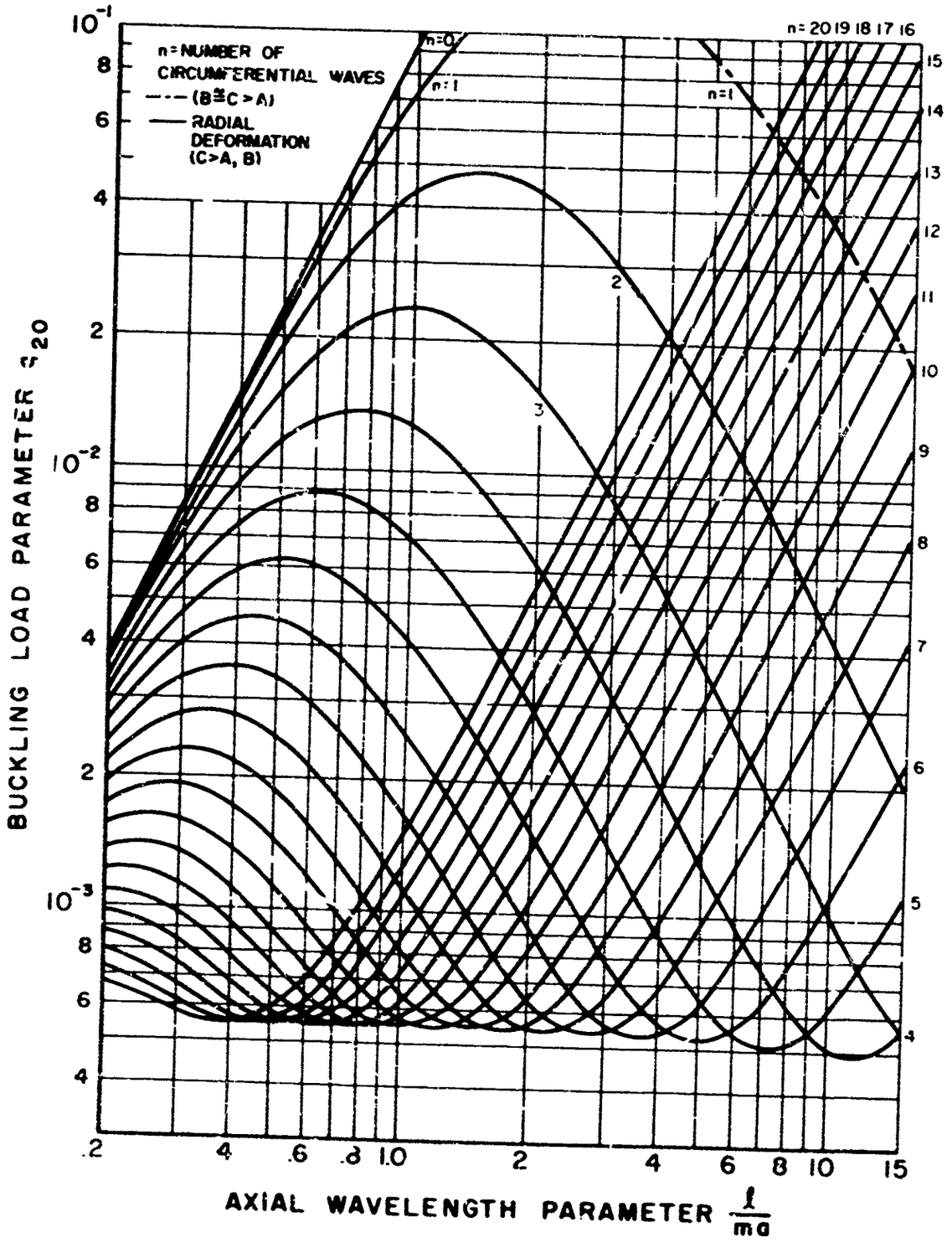

Figure 29. Buckling Values for Axial Compression, $\frac{a}{h}$=1000. No External Pressure (q_1 = 0)

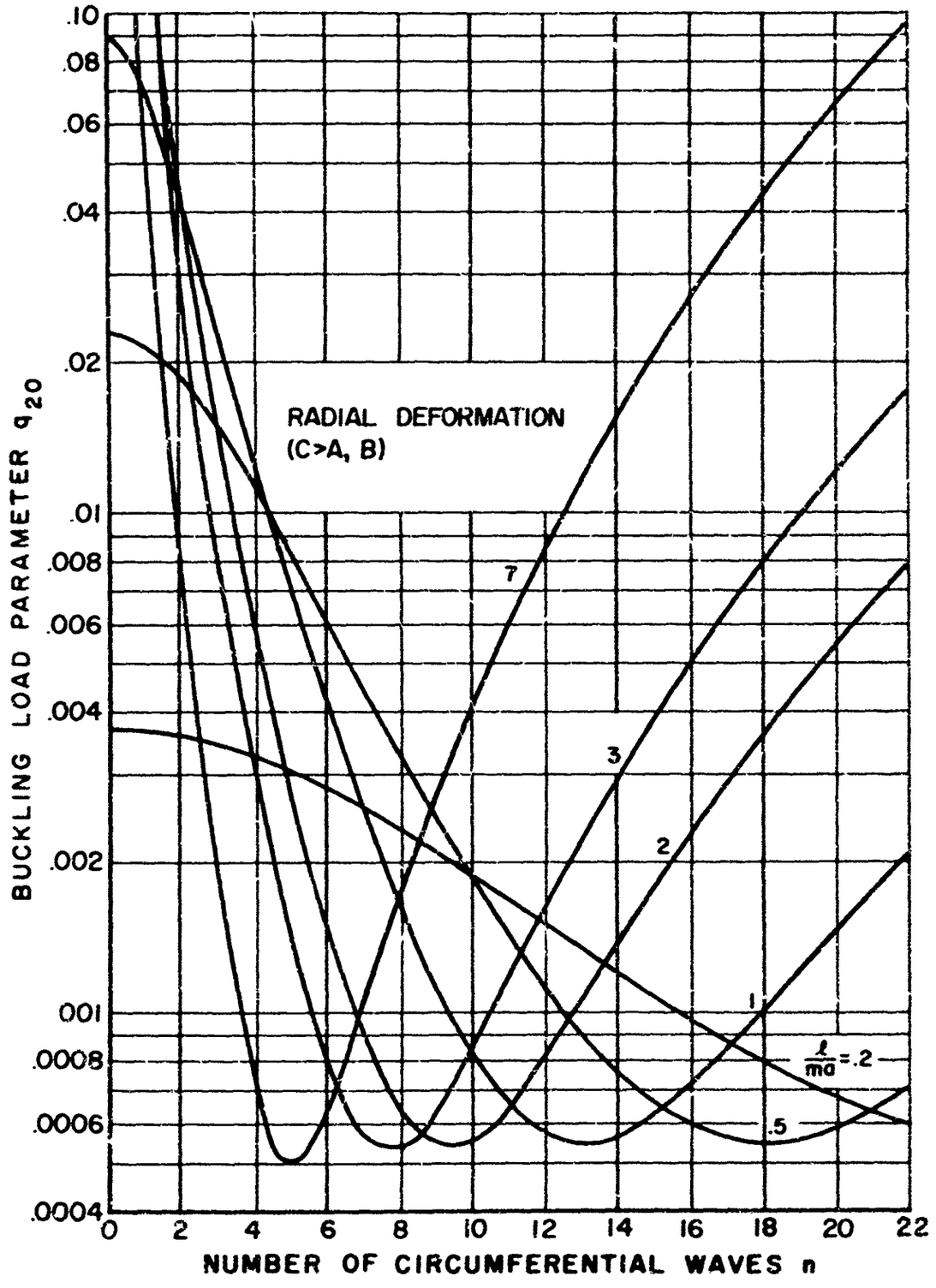

Figure 30. Buckling Values for Axial Compression. $\frac{a}{h}$=1000. No External Pressure ($q_1 = 0$)

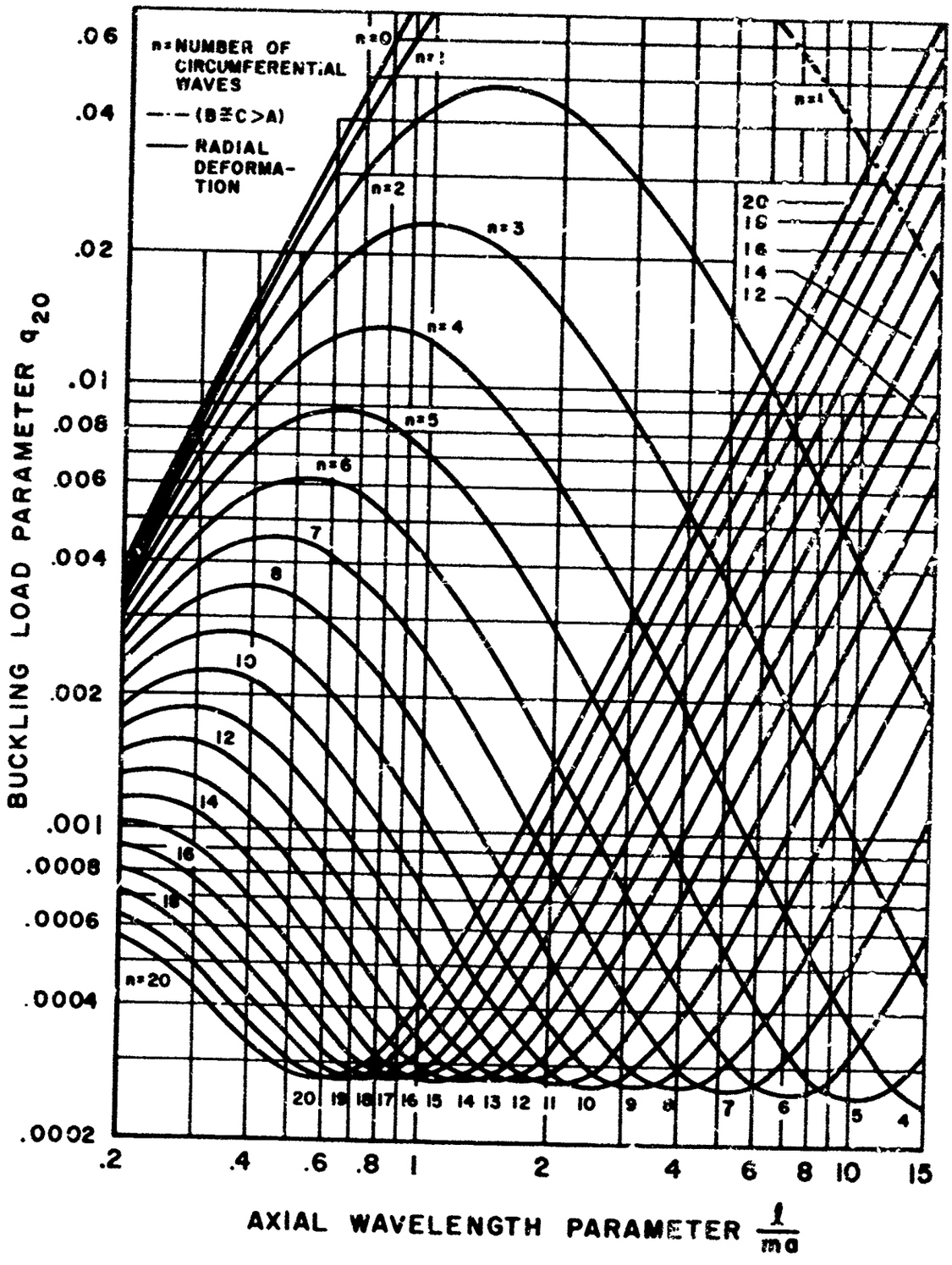

Figure 31. Buckling Values for Axial Compression. $\frac{a}{h}$=2000. No External Pressure (q_1 = 0)

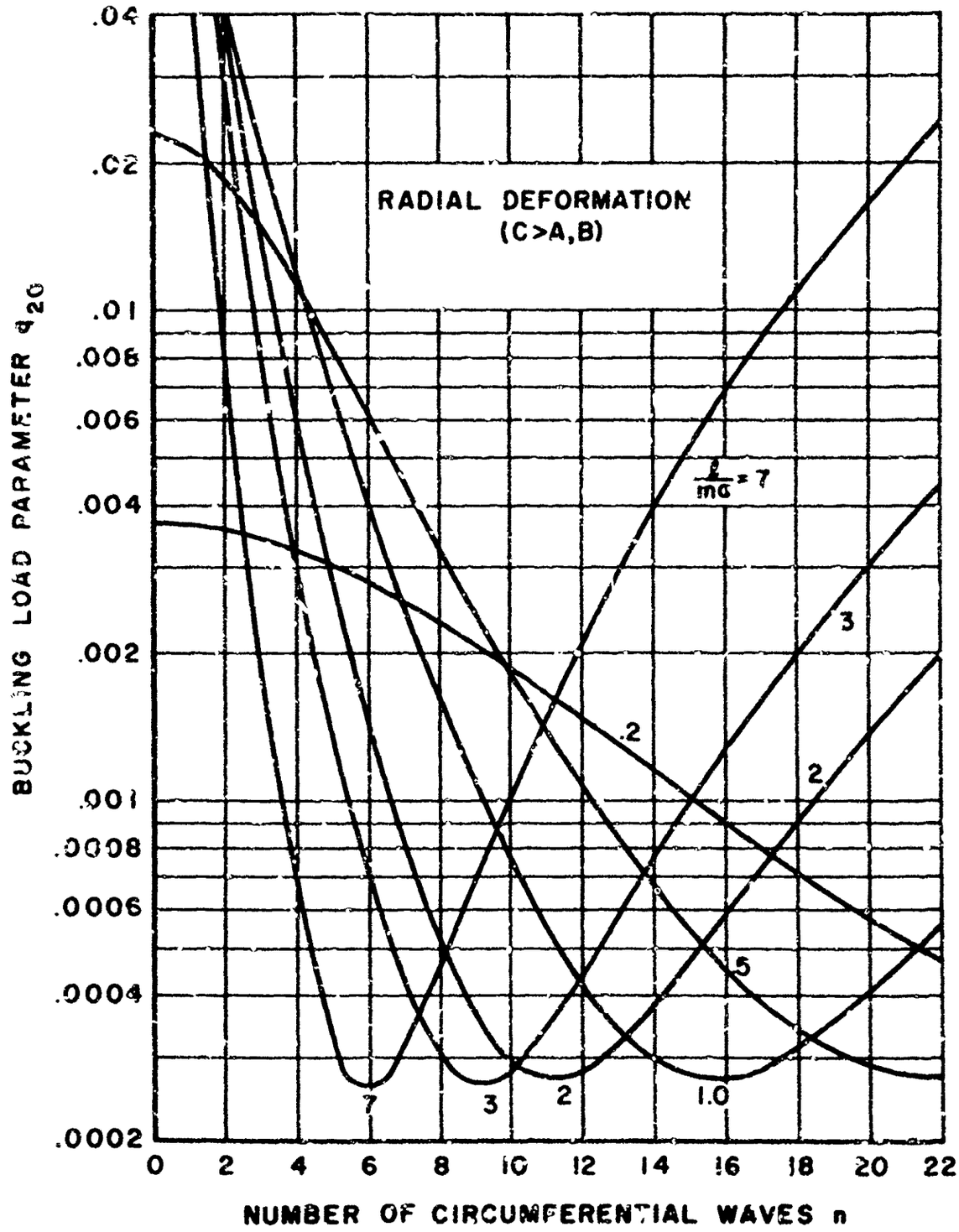

Figure 32. Buckling Values for Axial Compression. $\frac{a}{h} = 2000$. No External Pressure ($q_1 = 0$)

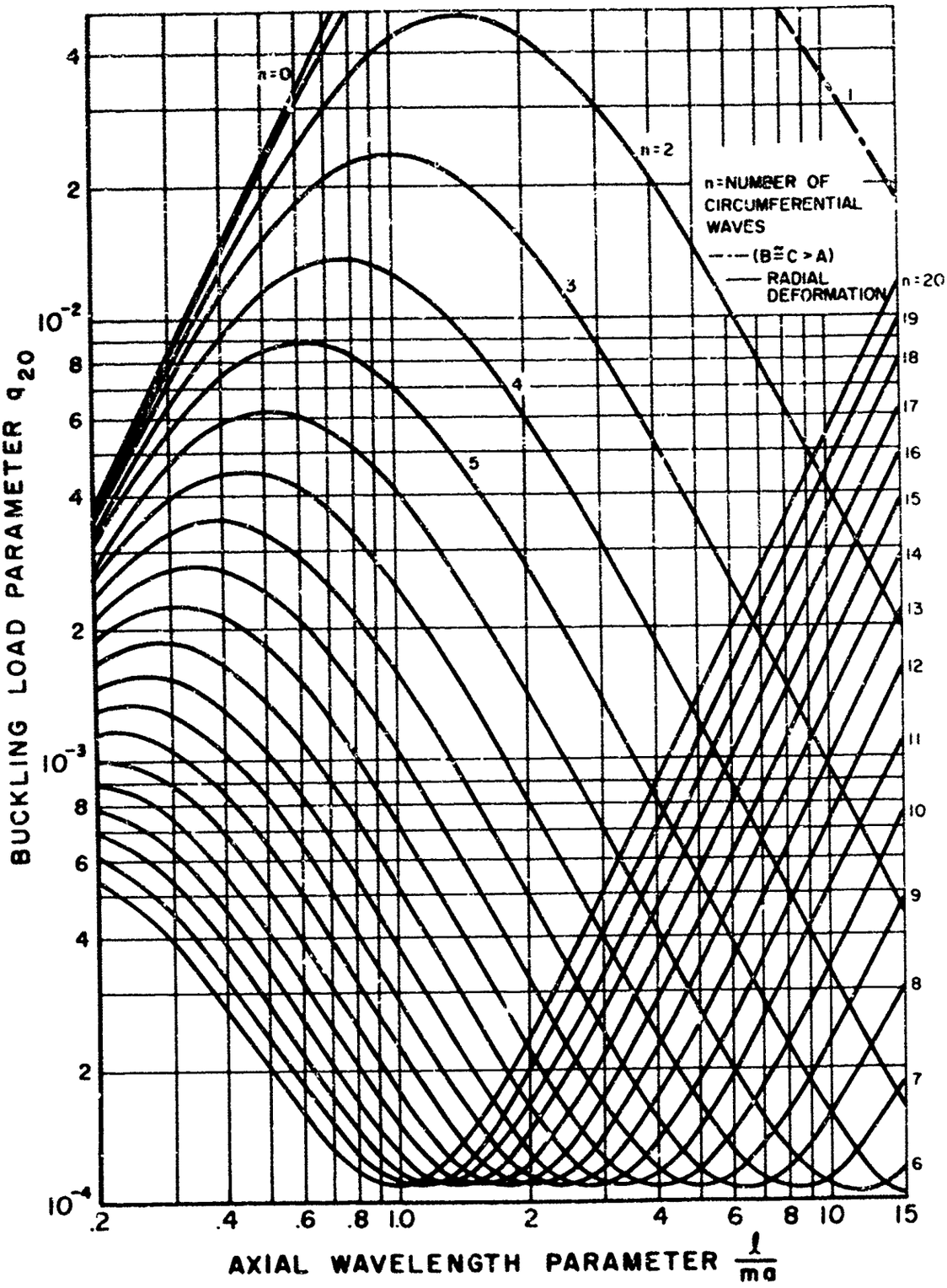

Figure 33. Buckling Values for Axial Compression, $\frac{a}{h}$=5000, No External Pressure (q_1 = 0)

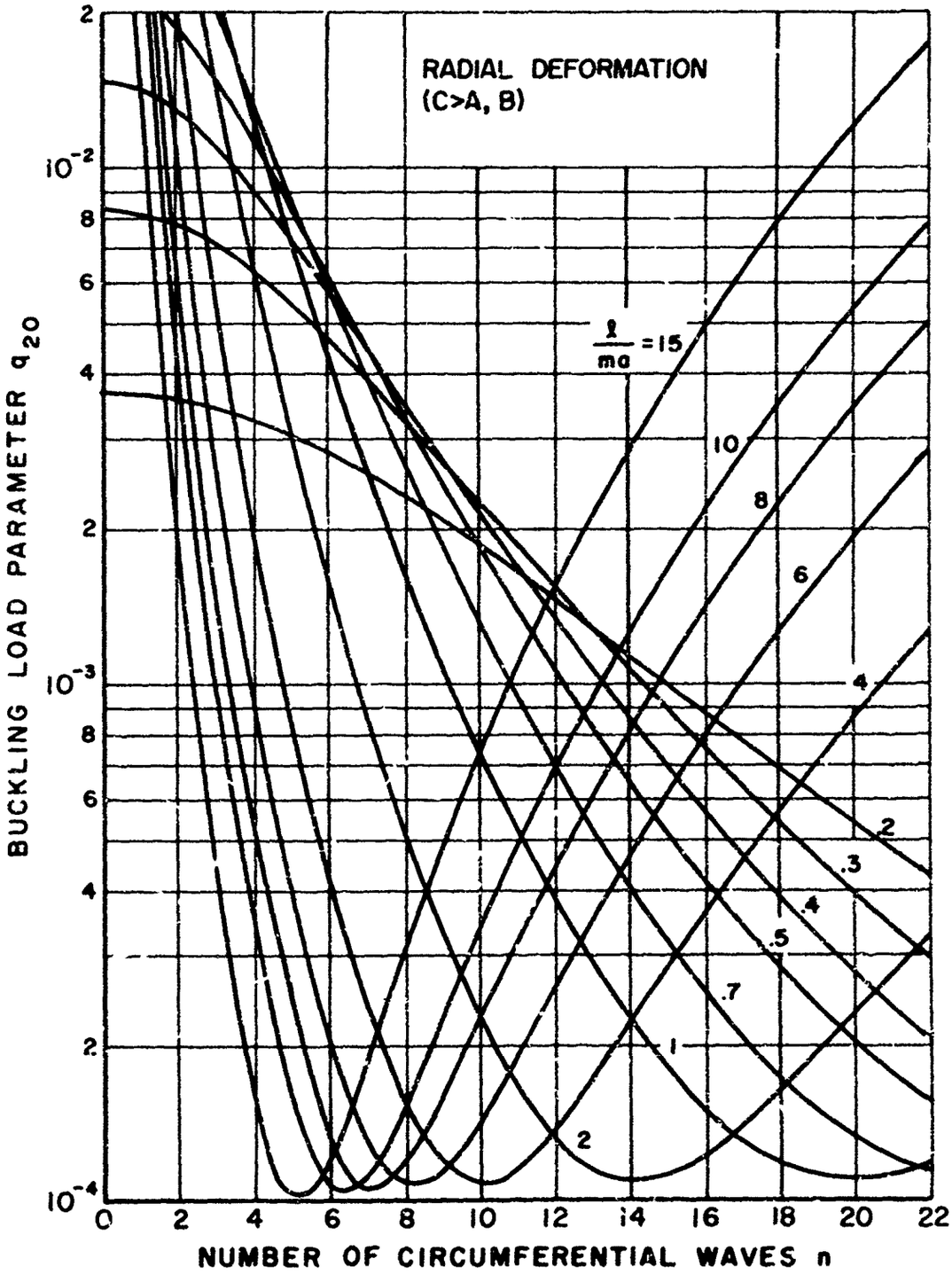

Figure 34. Buckling Values for Axial Compression. $\frac{a}{h}$ = 5000. No External Pressure (q_1 = 0)

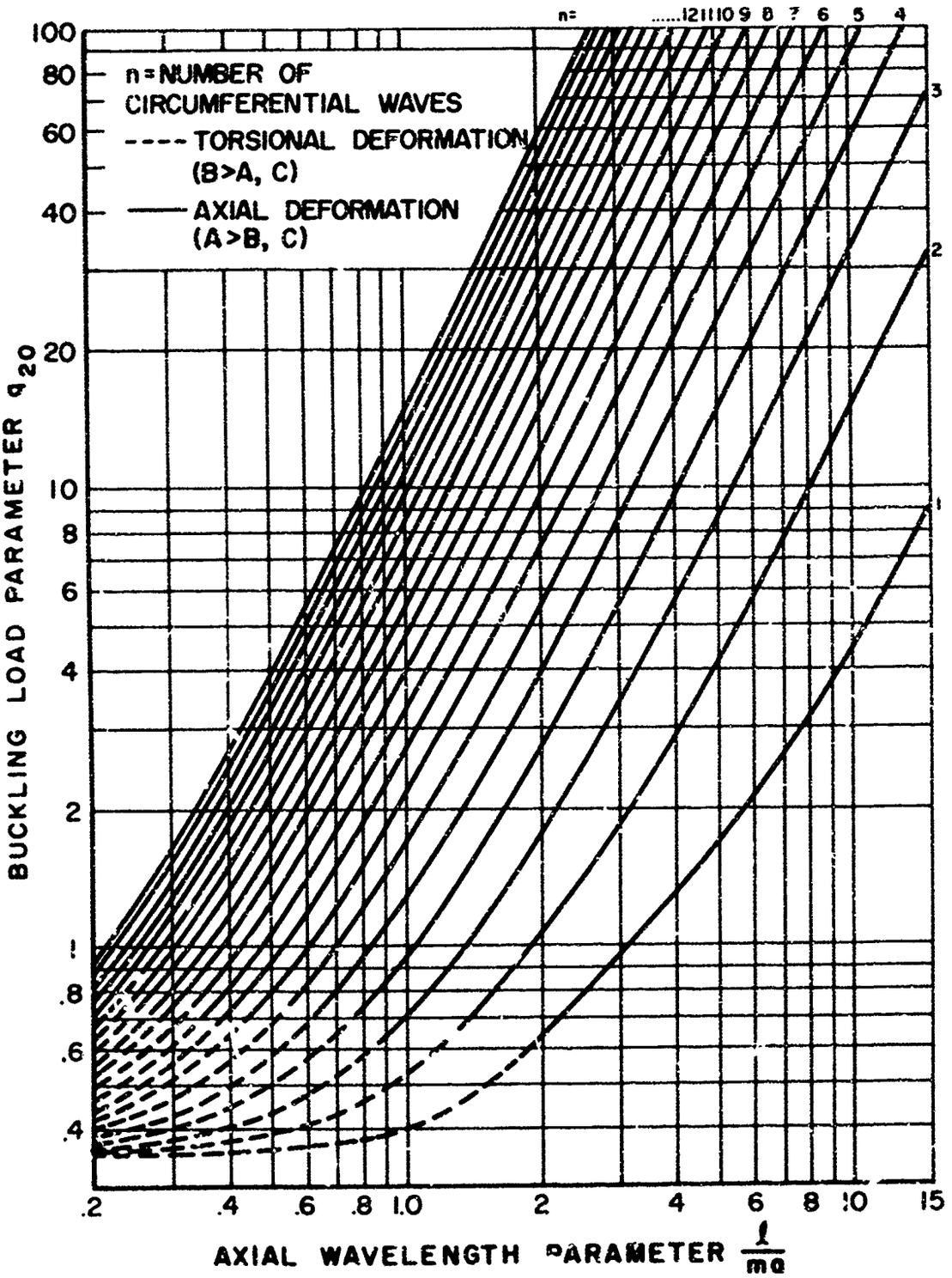

Figure 35. Second Buckling Value for Axial Compression. $\frac{a}{h}$ = 20-5000, No External Pressure (q_1 = 0)

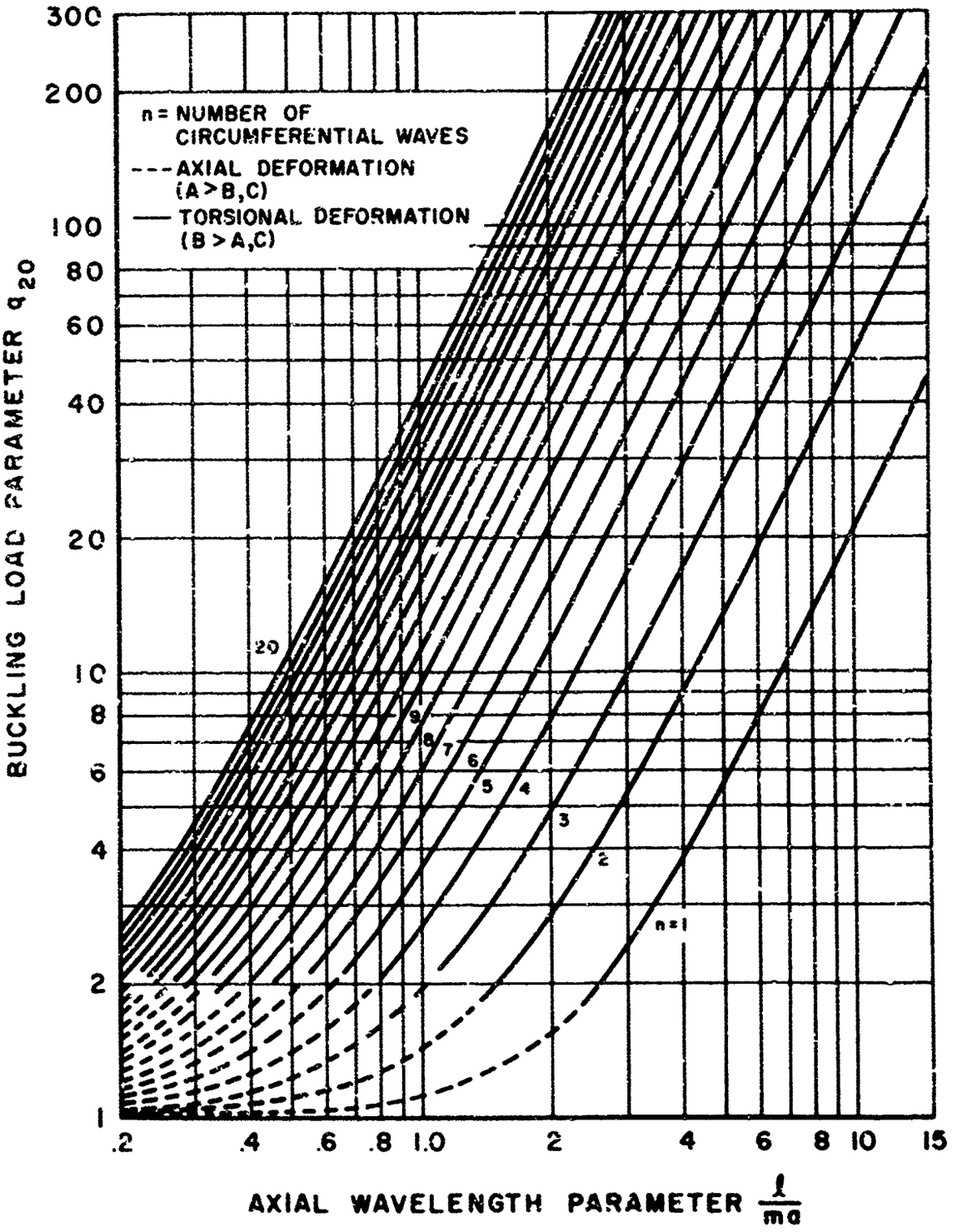

Figure 36. Third Buckling Value for Axial Compression. $\frac{a}{h}$=20-5000. No External Pressure (q_1 = 0)

SECTION V

BUCKLING RESULTS FOR EXTERNAL PRESSURE

The buckling values for a freely-supported cylinder subjected to only external pressure can be obtained by setting the parameters q_2 and ω equal to zero in the various terms of the characteristic determinant and separating the terms containing q_1 from the expressions D_{ij} in Equation 98. The external pressure parameter q_1 is given the symbol q_{10} to indicate that it is the buckling value.

$$\begin{bmatrix} (H_{11} - q_{10} n^2) & H_{12} & (H_{13} - q_{10} \lambda) \\ H_{12} & (H_{22} - q_{10} n^2) & (H_{23} - q_{10} n) \\ (H_{13} - q_{10} \lambda) & (H_{23} - q_{10} n) & (H_{33} - q_{10} n^2) \end{bmatrix} \begin{Bmatrix} A \\ B \\ C \end{Bmatrix} = 0 \qquad (131)$$

Expressions for the various terms H_{ij} can be obtained by subtracting the q_1 terms from the expressions for D_{ij} in Equations 100 through 105.

For a non-trivial solution, the determinant of the 3 x 3 matrix above must be zero. After expanding this determinant and collecting like powers of q_{10} the following third order characteristic equation for buckling due to external pressure is obtained:

$$\begin{aligned} & q_{10}^3 \left[-n^6 + \lambda^2 n^2 + n^4 \right] + q_{10}^2 \left[n^4 (H_{11} + H_{22} + H_{33}) + 2 H_{12} n\lambda - 2n^2 \lambda H_{13} - \lambda^2 H_{22} \right. \\ & \left. - 2n^3 H_{23} - n^2 H_{11} \right] + q_{10} \left[-n^2 (H_{11} H_{22} + H_{11} H_{33} + H_{22} H_{33}) + n^2 (H_{13}^2 + H_{12}^2 + H_{23}^2) \right. \\ & \left. - 2 H_{12} (n H_{13} + \lambda H_{23}) + 2\lambda H_{13} H_{22} + 2n H_{11} H_{23} \right] + H_{11} H_{22} H_{33} + 2 H_{12} H_{13} H_{23} \\ & - H_{13}^2 H_{22} - H_{12}^2 H_{33} - H_{23}^2 H_{11} = 0 \end{aligned} \qquad (132)$$

Equation 132 is valid only for non-axisymmetric modes (n>o). As in the case of vibration and buckling due to an axial load, the characteristic equation for buckling due to external pressure is a cubic equation, and three buckling values, q_{10}, can be obtained. The expressions for the amplitude ratios for the various buckling values are

$$\frac{A}{C} = \frac{\dfrac{(H_{22} - q_{10} n^2)(H_{13} - q_{10}\lambda)}{H_{12}} - (H_{23} - q_{10} n)}{H_{12} - \dfrac{(H_{22} - q_{10} n^2)(H_{11} - q_{10} n^2)}{H_{12}}} \qquad (133)$$

$$\frac{B}{C} = \frac{\dfrac{(H_{23} - q_{10} n)(H_{11} - q_{10} n^2)}{H_{12}} - (H_{13} - q_{10} \lambda)}{H_{12} - \dfrac{(H_{11} - q_{10} n^2)(H_{22} - q_{10} n^2)}{H_{12}}} \qquad (134)$$

As for both vibration and buckling due to axial load, the non-axisymmetric modes involve a a coupling between the three displacements u, v, and w.

For some modes, the solution of Equation 132 yields one negative and two positive buckling values. The negative value for q_{10} indicates buckling due to internal pressure, since a positive value for q_{10} corresponds to external pressure. In those cases where a negative buckling value was obtained for q_{10} there were two buckling values for the given mode which had primarily radial deformation. One of these was associated with the negative value of q_{10} and the other with the lowest positive value for q_{10}. The only exception is for modes having one circumferential wave, where for long shells the radial and tangential displacements were approximately equal and both were greater than the axial deformation (C≅B>A), which would represent "beam modes" for the cylinder. In the cases where three positive values were obtained for q_{10} one corresponded to radial deformation (C>A, B) one to tangential deformation (B>A, C) and one to axial deformation (A>B, C).

The lowest positive buckling values for q_{10} (external pressure) for various modes are plotted in Figures 37 to 50 for various values of radius to thickness from 20 to 5000. There are two figures for each radius to thickness ratio. In one figure q_{10} is plotted versus the axial wavelength parameter $\frac{\ell}{ma}$ for various values of n, and in the other q_{10} is plotted versus the number of circumferential waves, n, for various values of $\frac{\ell}{ma}$. A value of the lowest buckling load for the various modes was obtained from the cubic characteristic equation, Equation 132, and also the linear form of this equation, and the more accurate result plotted in the figures. This was determined by substituting each result back into Equation 132 and checking the residual. For small values of q_{10} associated with radius to thickness ratios from 2000 to 5000 and values of $\frac{\ell}{ma} > 5$, the linear equation generally gave greater accuracy for the lowest root. This is because of the numerical accuracy which was obtained from the digital computer program used to obtain the roots of the cubic equation. As for both vibration and buckling due to axial load, the lowest values of the character stic equation were generally associated with deformation which was primarily radial and the results were dependent on the radius to thickness ratio $\frac{a}{h}$ indicating that bending effects are important for these cases.

The modes having one circumferential wave do not appear in Figures 37 through 50 because the buckling values for external pressure for these modes are higher than for modes with two or more circumferential waves. The lowest buckling value for external pressure decreases as the parameter $\frac{\ell}{ma}$ increases, indicating that for a given cylinder the lowest buckling value, q_{10}, is associated with a mode having one axial half-wave, since this leads to the largest value of $\frac{\ell}{ma}$. For the large values of $\frac{\ell}{ma}$ the lowest buckling values for external pressure are associated with two circumferential waves (n = 2). As the value of the parameter $\frac{\ell}{ma}$ decreases the number of circumferential waves associated with the lowest buckling value increases. These results were obtained by Flugge (Reference 4), using only the linear terms of the characteristic equation. Flugge points out that the linear form of the characteristic equation n = 2 and $\lambda = 0$, where $\lambda = \frac{m\pi a}{\ell}$, gives a value of 3k for q_{10} where $k = \frac{h^2}{12a^2}$ indicating that the curve for n = 2 is asymptotic to 3k for large values of $\frac{\ell}{ma}$.

The buckling results for external pressure for modes having one circumferential wave are given in Figure 51 for values of $\frac{a}{h}$ from 20 to 5000. Two buckling values were obtained for external pressure and one negative buckling value for q_{10} which represents internal pressure. For values of $\frac{\ell}{ma} < \pi$ there are two buckling modes which involve radial deformation, with the value for external pressure lower than the value for internal pressure. There is also a higher buckling value for external pressure which involves torsional deformation. The buckling values appear to be a function of the ratio of radius to thickness for $\frac{\ell}{ma} < 1$, and are essentially the same for values of $\frac{a}{h}$ from 20 to 5000 for $\frac{\ell}{ma} > 1$.

Flugge (Reference 4), in working with the linear form of the characteristic equation, points out that the buckling load q_{10} for this case changes from positive to negative at $\frac{\ell}{ma} = \pi$, with the negative values associated with $\frac{\ell}{ma} > \pi$. In Figure 51, where all three buckling values are shown, it can be seen that the buckling curve for internal pressure crosses the buckling curve for external pressure at $\frac{\ell}{ma} = \pi$. Thus the lowest buckling load, q_{10}, occurs for external pressure for $\frac{\ell}{ma} < \pi$ and internal pressure for $\frac{\ell}{ma} > \pi$. For values of $\frac{\ell}{ma} > \pi$ the buckling results for internal pressure have an amplitude ratio B/C which is approximately -1, indicating that the amplitude of the radial and tangential displacements are approximately equal and both are larger than the axial deformation. This represents deflection with little distortion of the cylinder cross section and would represent "beam modes" for the cylinder.

For values of $\frac{\ell}{ma} > 4$ the lowest buckling value for external pressure represents axial deformation. Thus, for values of $\frac{\ell}{ma} > 4$ the buckling value for internal pressure was a "beam mode", while the lowest buckling value for external pressure involved axial deformation, and the second buckling value for external pressure, torsional deformation.

For the case of axisymmetric buckling (n = 0 modes) due to external pressure, the terms H_{12} and H_{23} in Equation 131 are zero, and the tangential displacement v can be uncoupled from the axial and radial displacements as for both vibration and buckling due to axial load. Equation 98 can be written as two equations for these modes.

$$\begin{bmatrix} H_{11} & H_{13} - \lambda q_{10} \\ H_{13} - \lambda q_{10} & H_{33} \end{bmatrix} \begin{Bmatrix} A \\ C \end{Bmatrix} \tag{135}$$

$$H_{22} B = 0 \tag{136}$$

The uncoupled equation for torsional deformation, Equation 136 has only the trivial solution B = 0, indicating that axisymmetric torsional buckling does not exist for a freely-supported cylinder subjected to external pressure.

The determinant of the 2 x 2 matrix in Equation 135 is expanded to form the quadratic characteristic equation for the axisymmetric case.

$$q_{10}^2 (\lambda^2) - q_{10} (2 \lambda H_{13}) + H_{13}^2 - H_{11} H_{33} = 0 \tag{137}$$

The amplitude ratio involves only coupled radial and axial displacement for this case,

$$\frac{A}{C} = - \frac{(H_{13} - q_{10}\lambda)}{H_{11}} \tag{138}$$

The buckling values for external pressure obtained from Equation 137 are plotted in Figure 52. One positive value for q_{10} and one negative value for q_{10} were obtained for range of radius to thickness ratios from 20 to 5000 and the range of the axial wavelength parameter, $\frac{\ell}{ma}$ from .2 to 15. The lower buckling value is for external pressure. For small values of k, (k<<1), where $k = \frac{h^2}{12a^2}$, and for $\lambda = 0$, where $\lambda = \frac{m\pi a}{\ell}$ Equation 137 yields the following values for q_{10}:

$$q_{10} = -\nu \pm 1 \tag{139}$$

This gives a buckling value for external pressure of $q_{10} = 1-\nu$, and a buckling value of $q_{10} = -1-\nu$, which represents internal pressure, for long thin shells. If Poisson's ratio, ν, were zero, the buckling value for internal and external pressure would be 1. In Figure 52 it is shown that these simple buckling values appear to be valid for values of $\frac{a}{h}$ from 500 to 5000 for the full range of $\frac{\ell}{ma}$ examined ($.2 \leq \frac{\ell}{ma} \leq 15$), and for values of $\frac{a}{h}$ from 20 to 100 for $\frac{\ell}{ma} > 1$.

The buckling values for internal pressure for all modes are shown in Figure 53. These buckling values are associated with radial deformation, except for n = 1 with $\frac{\ell}{ma} > \pi$, which represents the "beam mode" as previously discussed. The modes with two circumferential waves yield a negative value for q_{10} for $\frac{\ell}{ma} < 1$, which appears to get very large as $\frac{\ell}{ma}$ approaches 1. For a value of $\frac{\ell}{ma} \geq 1$, Equation 132 gave only positive buckling values for q_{10}. Similarly for three circumferential waves, a negative buckling value could be obtained for $\frac{\ell}{ma} < .4$ and all values of $\frac{a}{h}$ examined, but at $\frac{\ell}{ma} \geq .4$ only positive values are obtained for q_{10}. Although it is not shown on the figure, a large negative value for q_{10} was obtained for four circumferential waves for $\frac{\ell}{ma} = .2$, while for all values of $\frac{\ell}{ma} \geq .25$ only positive buckling values q_{10} were obtained.

The second positive buckling value for external pressure is plotted in Figure 54, and the third positive buckling value is plotted in Figure 55. As for both vibration and buckling due to axial load, the second buckling value for external pressure involves torsional deformation for some modes and axial deformation for the rest. A similar result is obtained for the third buckling value for external pressure. The second and third positive buckling values were essentially the same for all radius thickness ratios from 20 to 5000, indicating the predominance of membrane effects. In Figure 55, which gives the third buckling value, the curves for n = 2, 3, and 4 were stopped at $\frac{\ell}{ma} = 1$, .4, and .25 respectively, since a third positive value for q_{10} did not exist for the next increment $\frac{\ell}{ma}$ below these values.

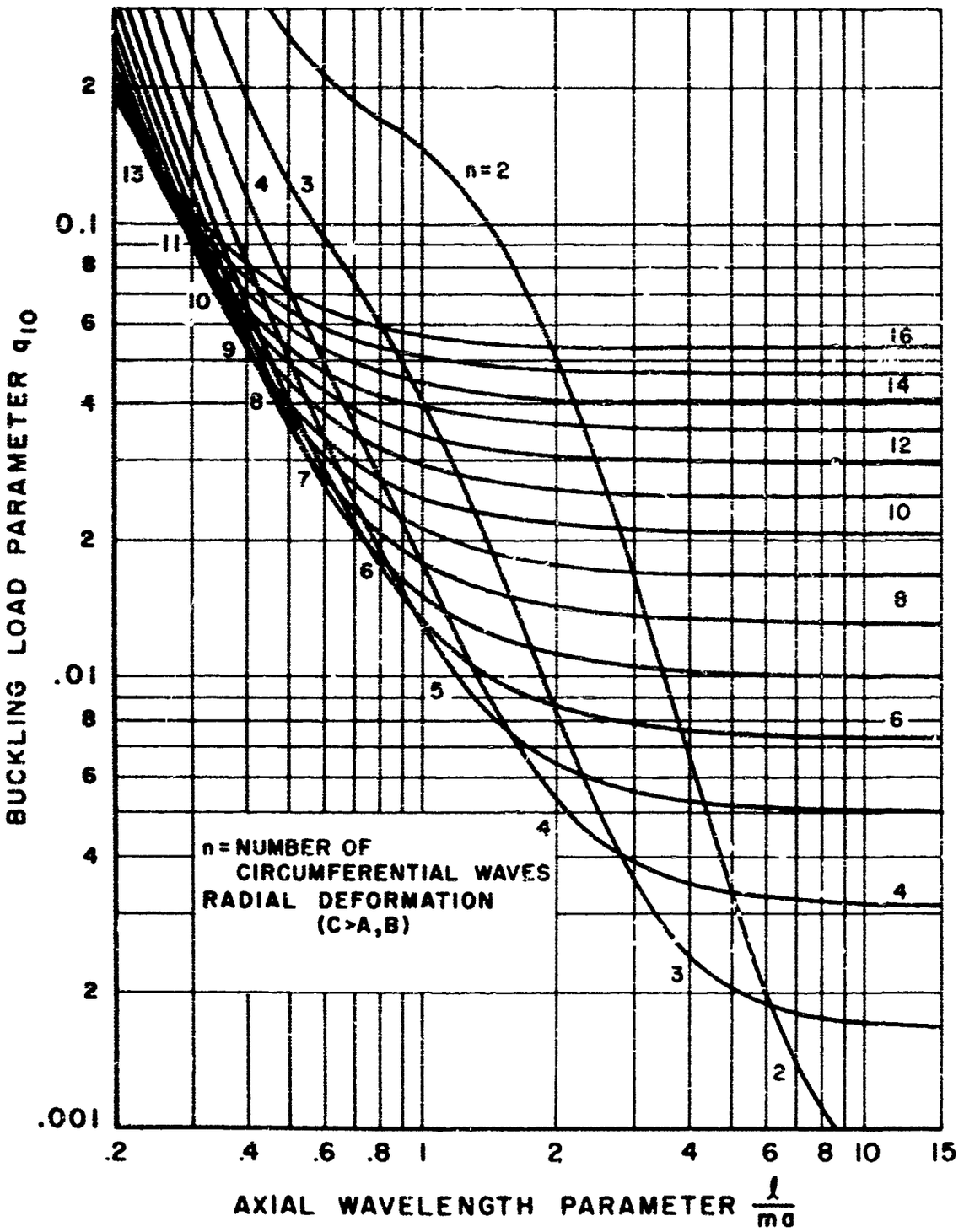

Figure 37. Buckling Values for External Pressure, $\frac{a}{h} = 20$, No Axial Load ($q_2 = 0$)

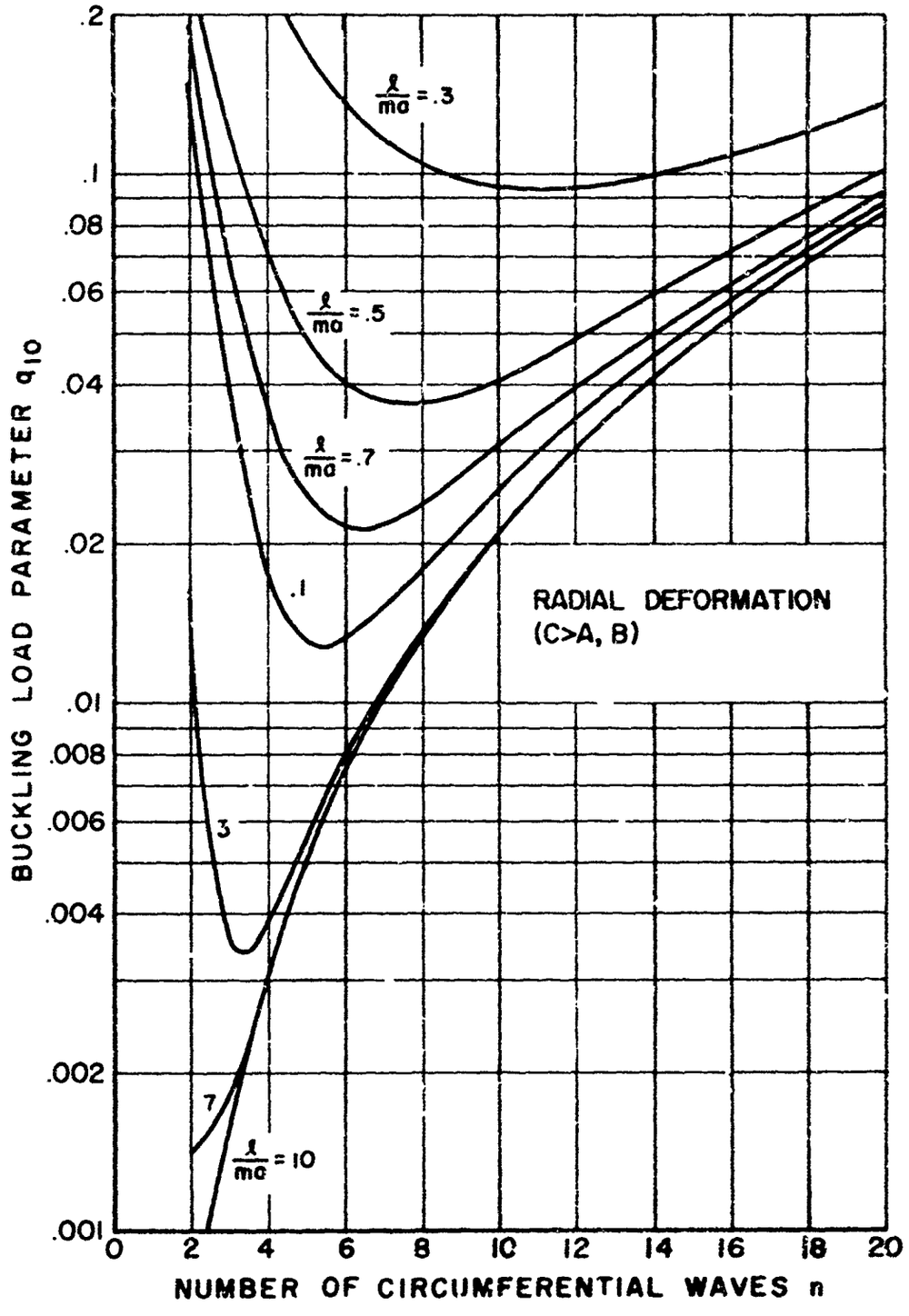

Figure 38. Buckling Values for External Pressure. $\frac{a}{h} = 20$. No Axial Load ($q_2 = 0$)

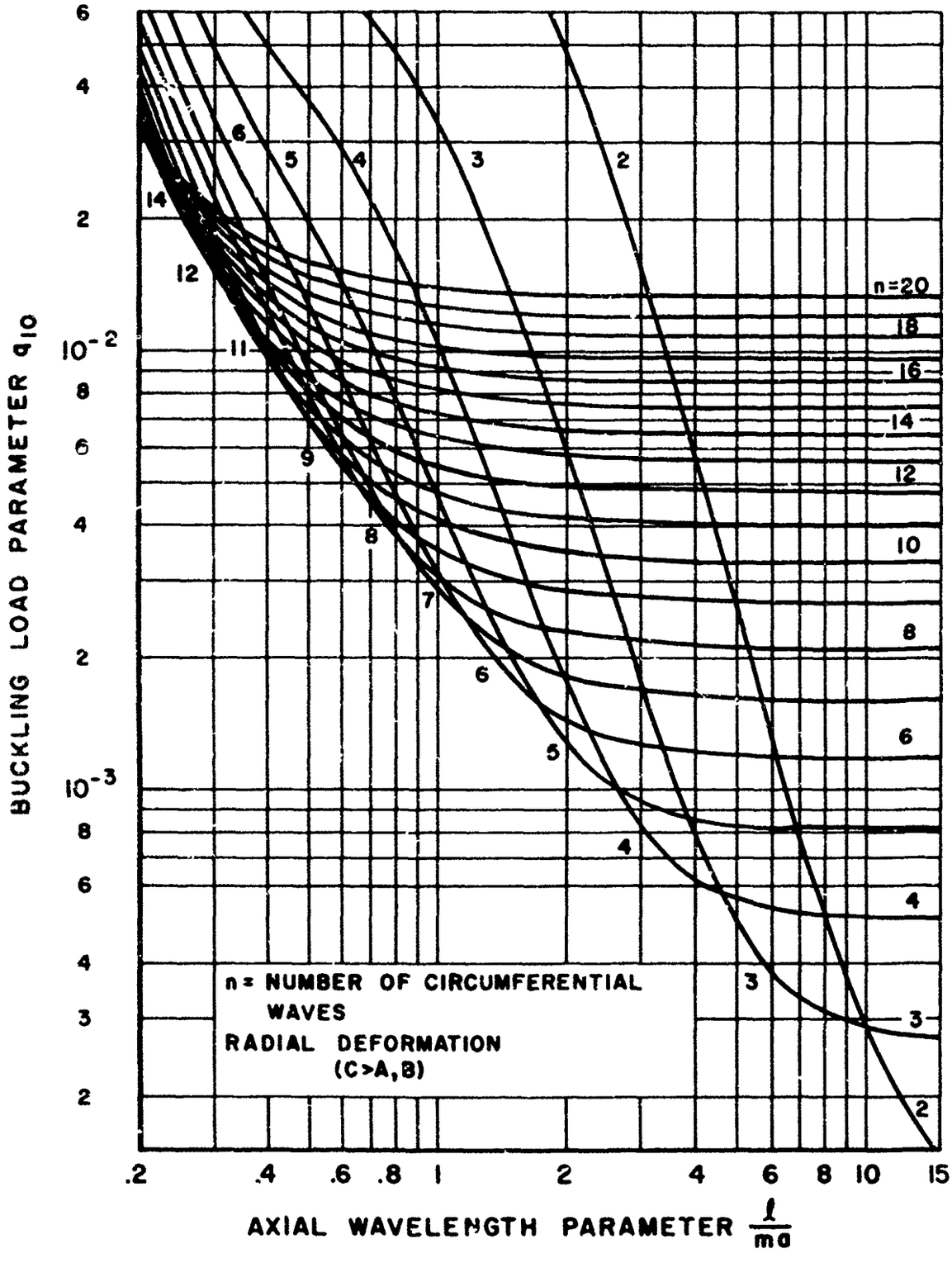

Figure 39. Buckling Values for External Pressure. $\frac{a}{h}$=50. No Axial Load (q_2 = 0)

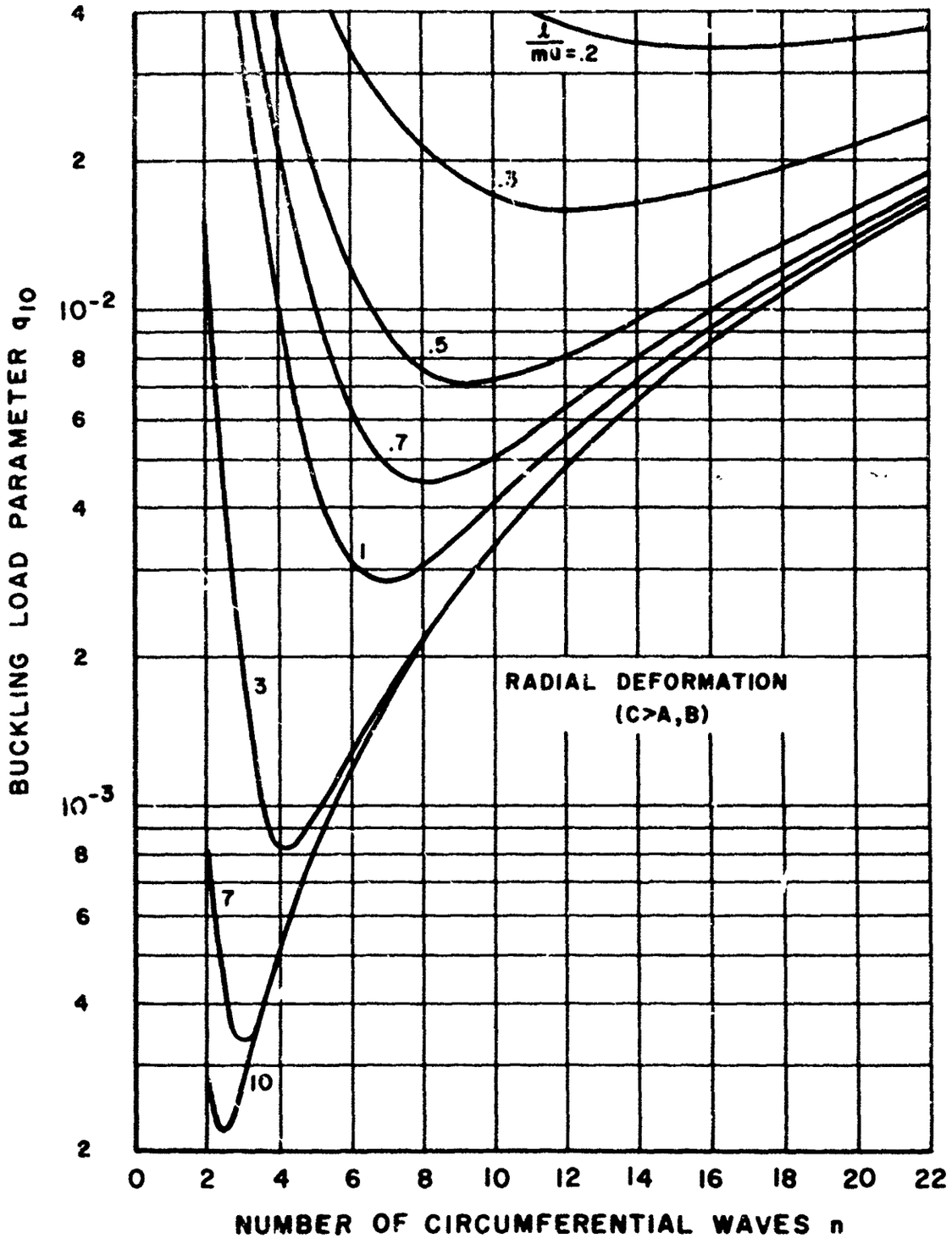

Figure 40. Buckling Values for External Pressure, $\frac{a}{h}$= 50. No Axial Load (q_2 = 0)

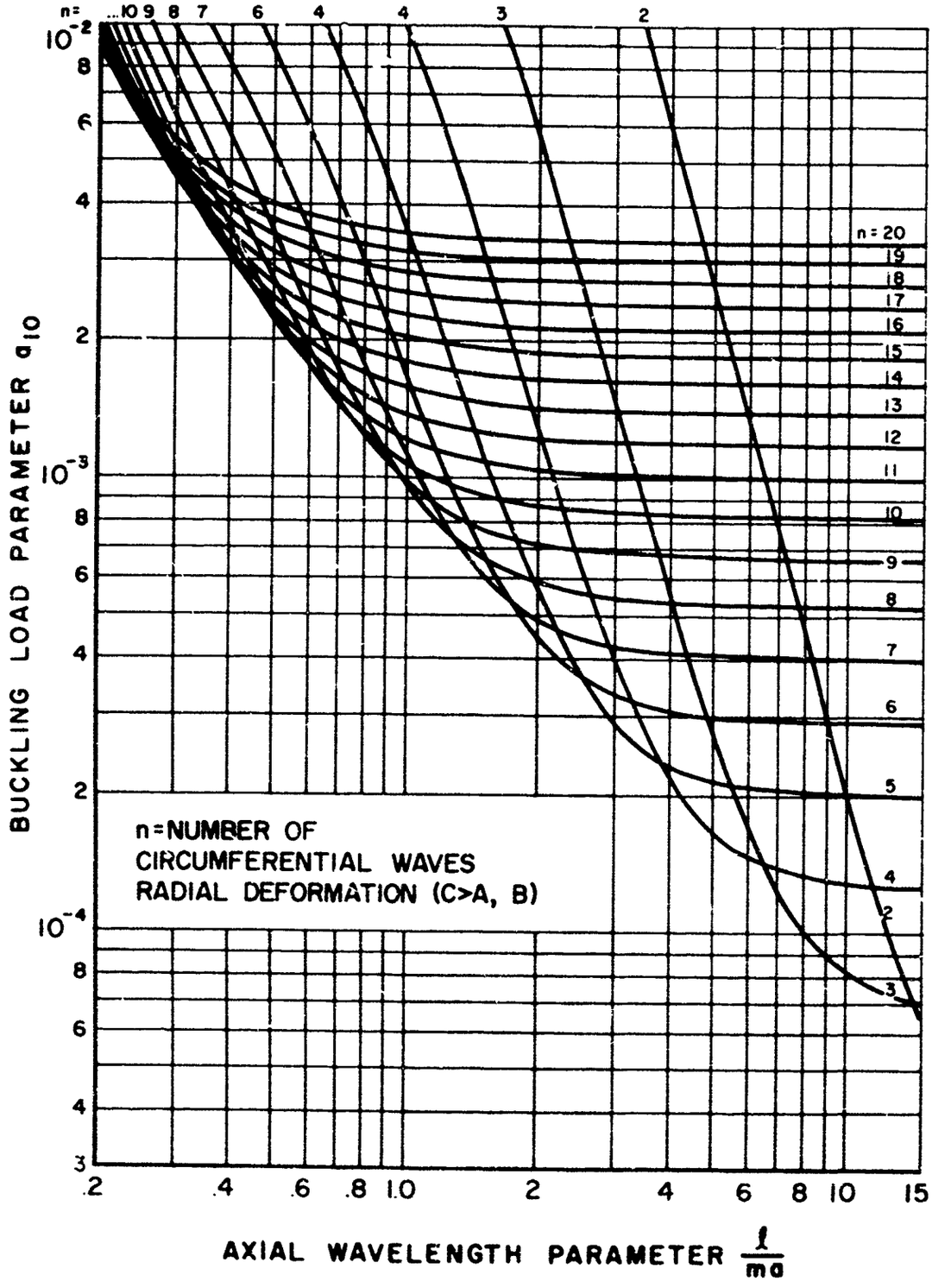

Figure 41. Buckling Values for External Pressure. $\frac{a}{h} = 100$. No Axial Load ($q_2 = 0$)

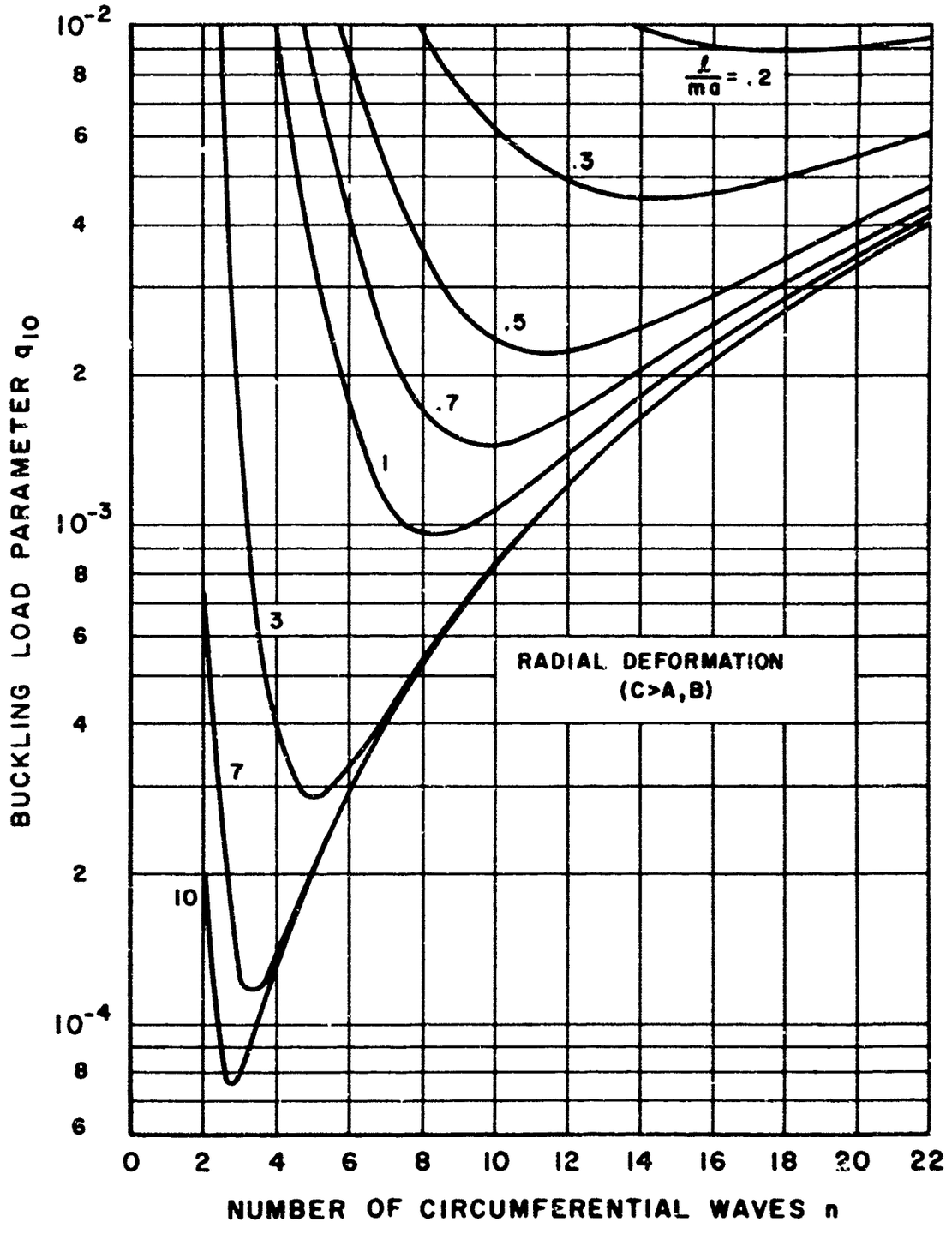

Figure 42. Buckling Values for External Pressure. $\frac{a}{h}$=100. No Axial Load (q_2 = 0)

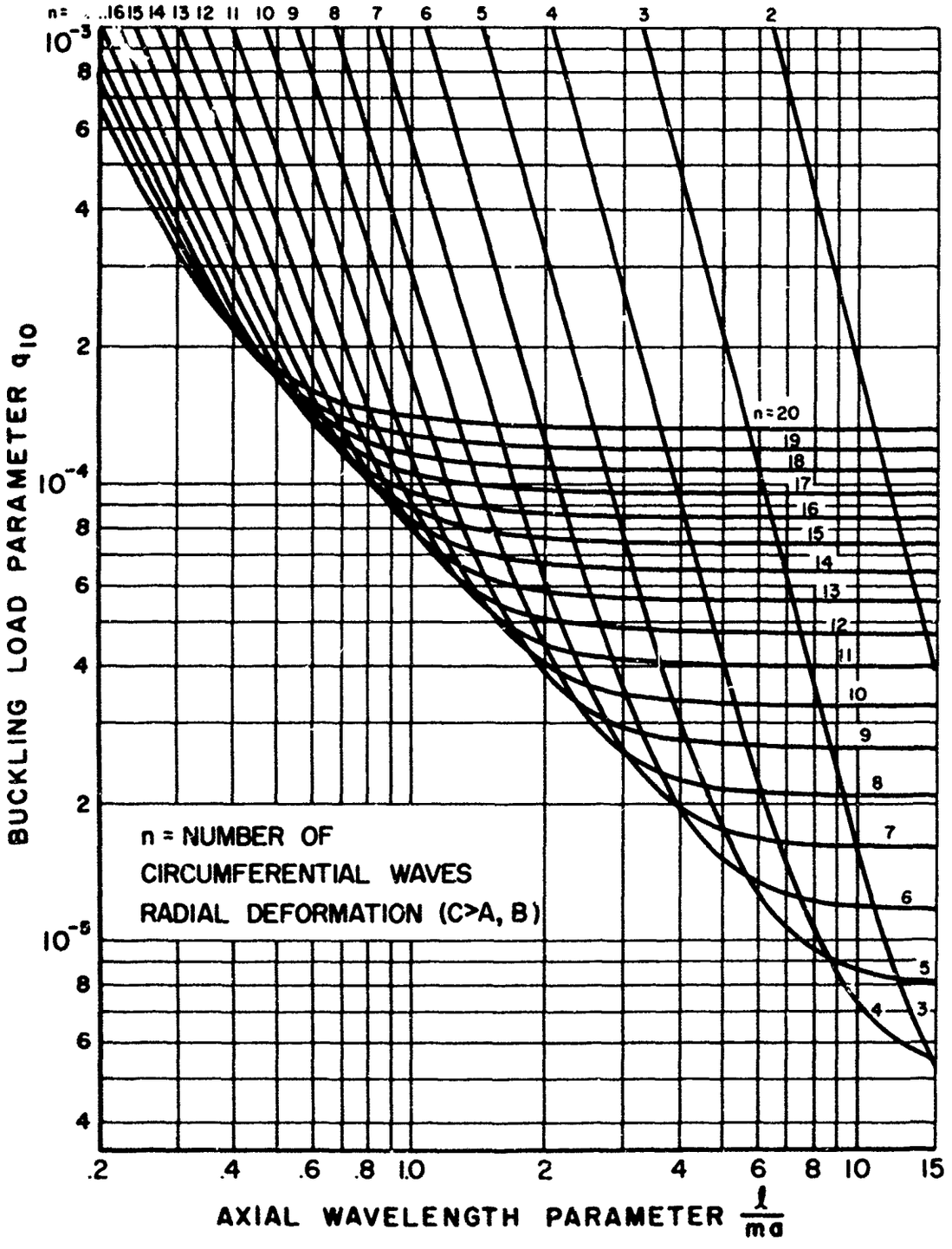

Figure 43. Buckling Values for External Pressure. $\frac{a}{h}$=500. No Axial Load (q_2= 0)

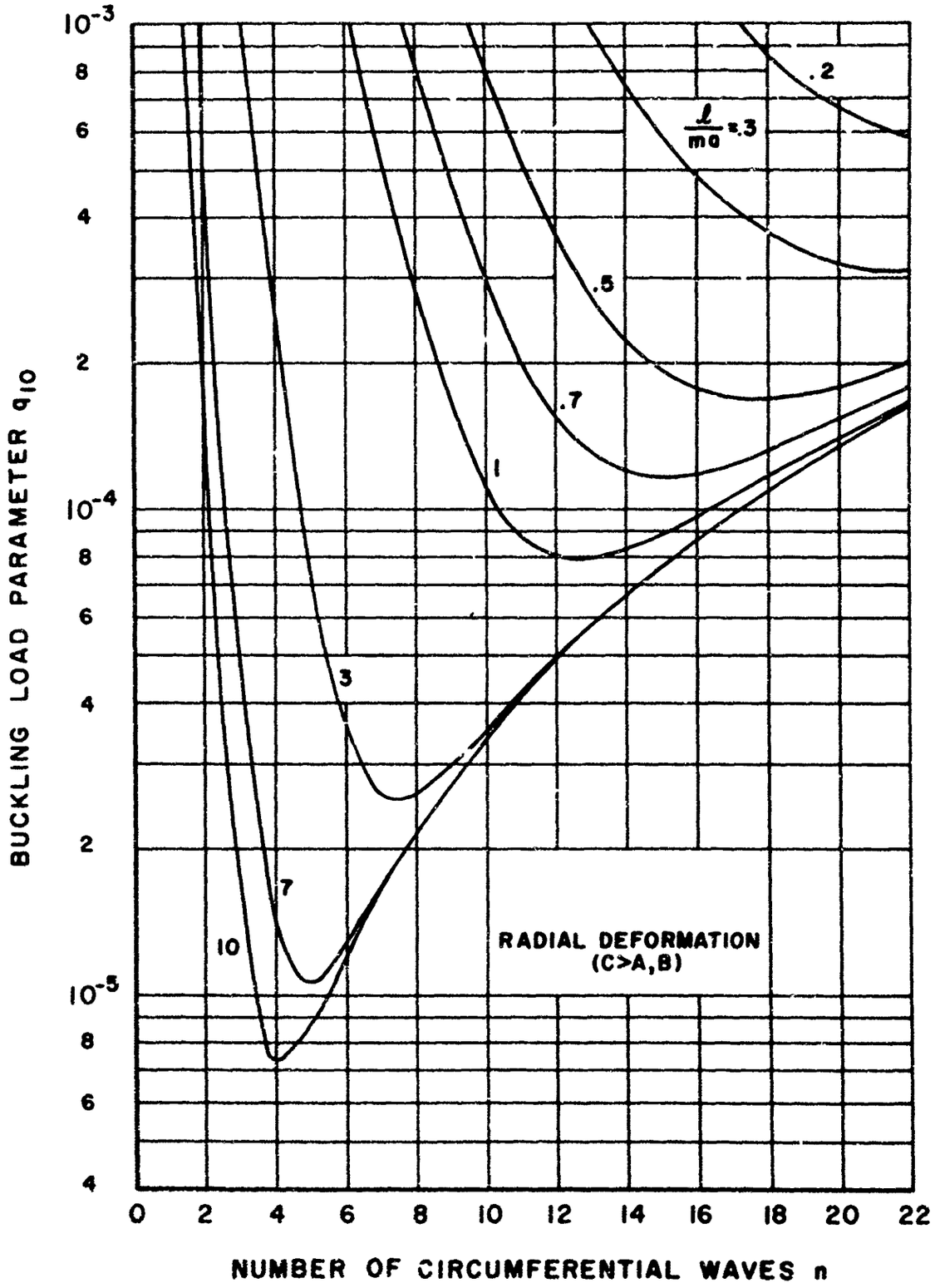

Figure 44. Buckling Values for External Pressure. $\frac{a}{h}$=500. No Axial Load (q_2 = 0)

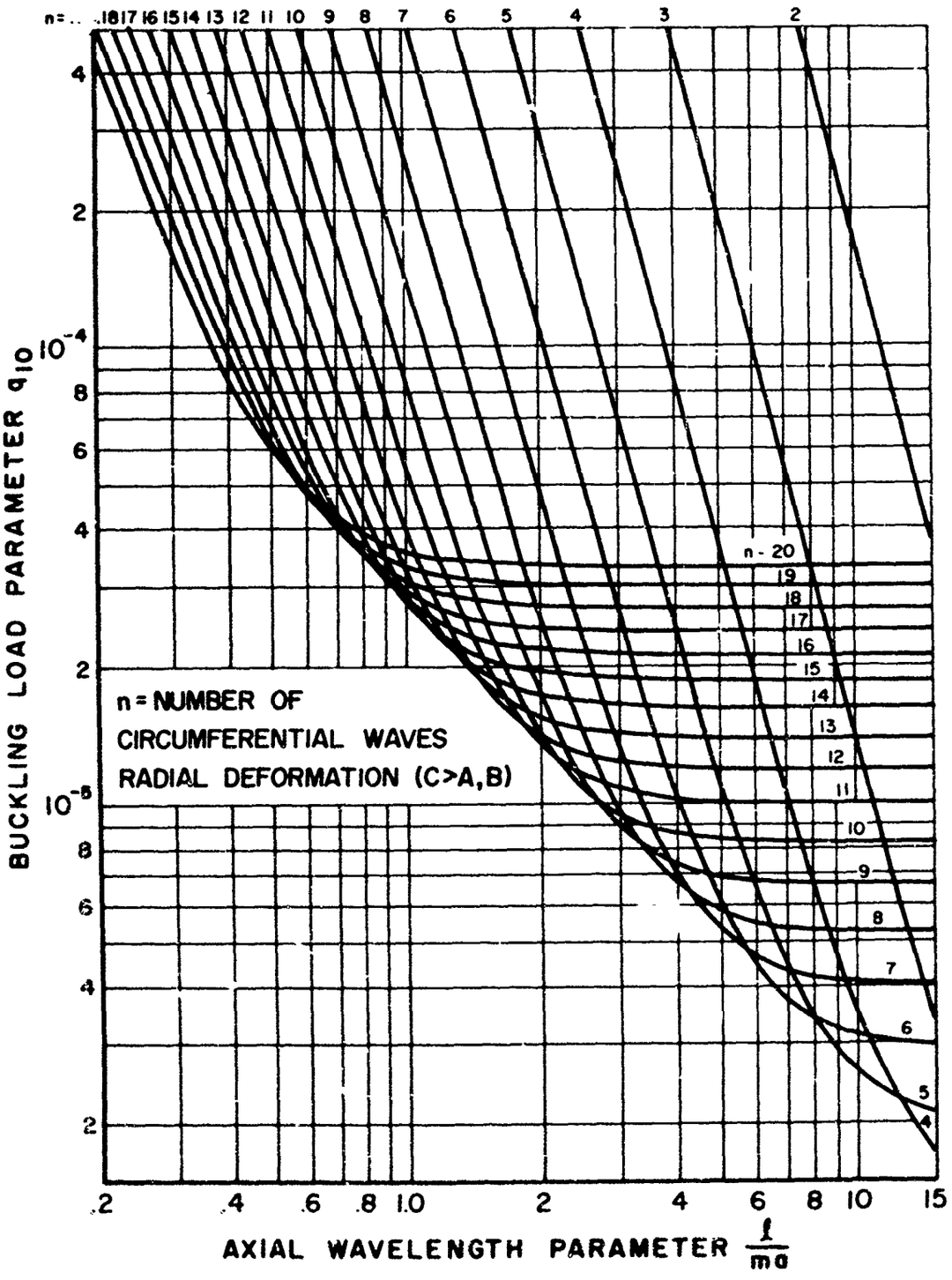

Figure 45. Buckling Values for External Pressure. $\frac{a}{h} = 1000$, No Axial Load ($q_{..} = 0$)

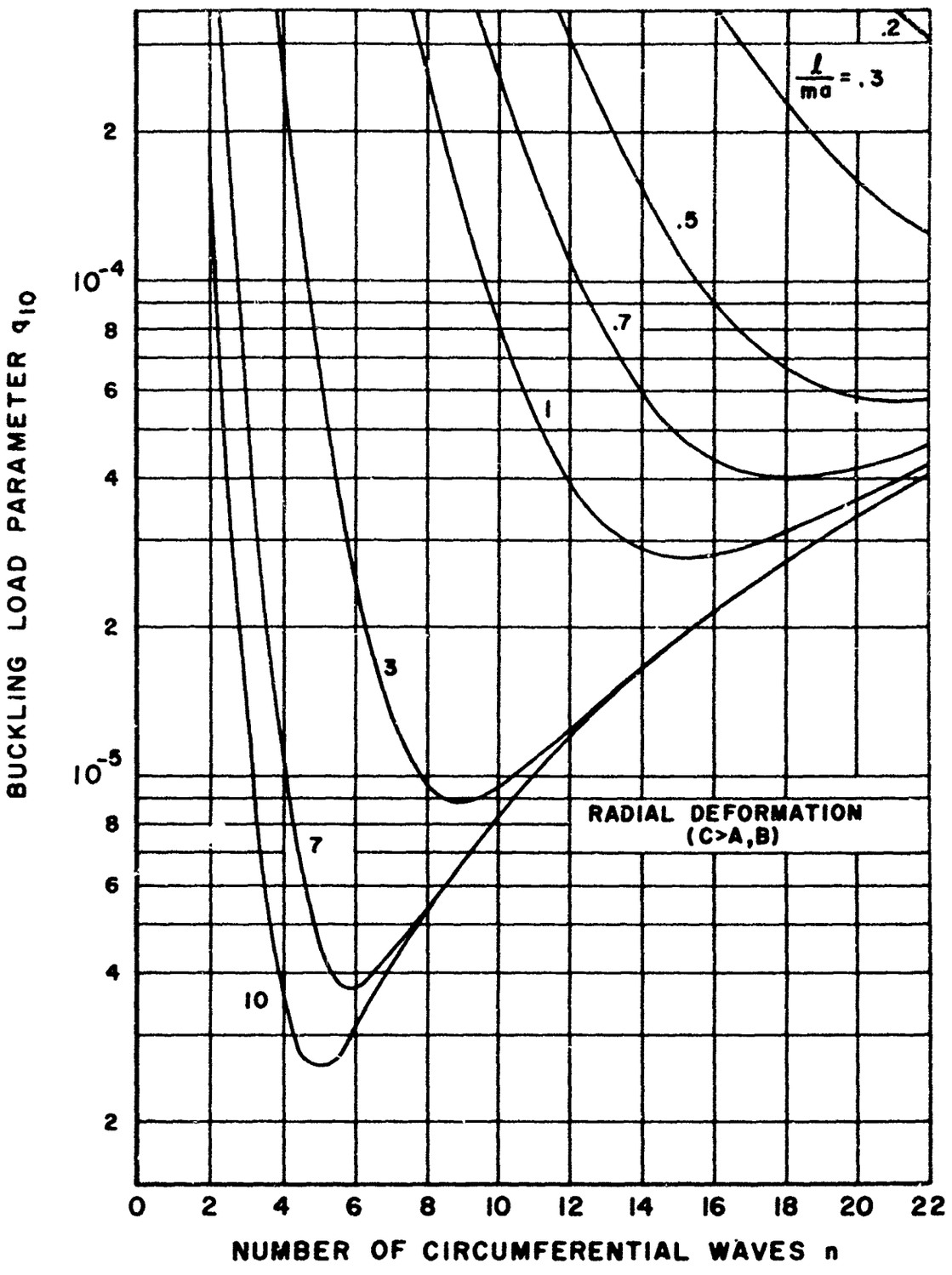

Figure 46. Buckling Values for External Pressure. $\frac{a}{h} = 1000$. No Axial Load ($q_2 = 0$)

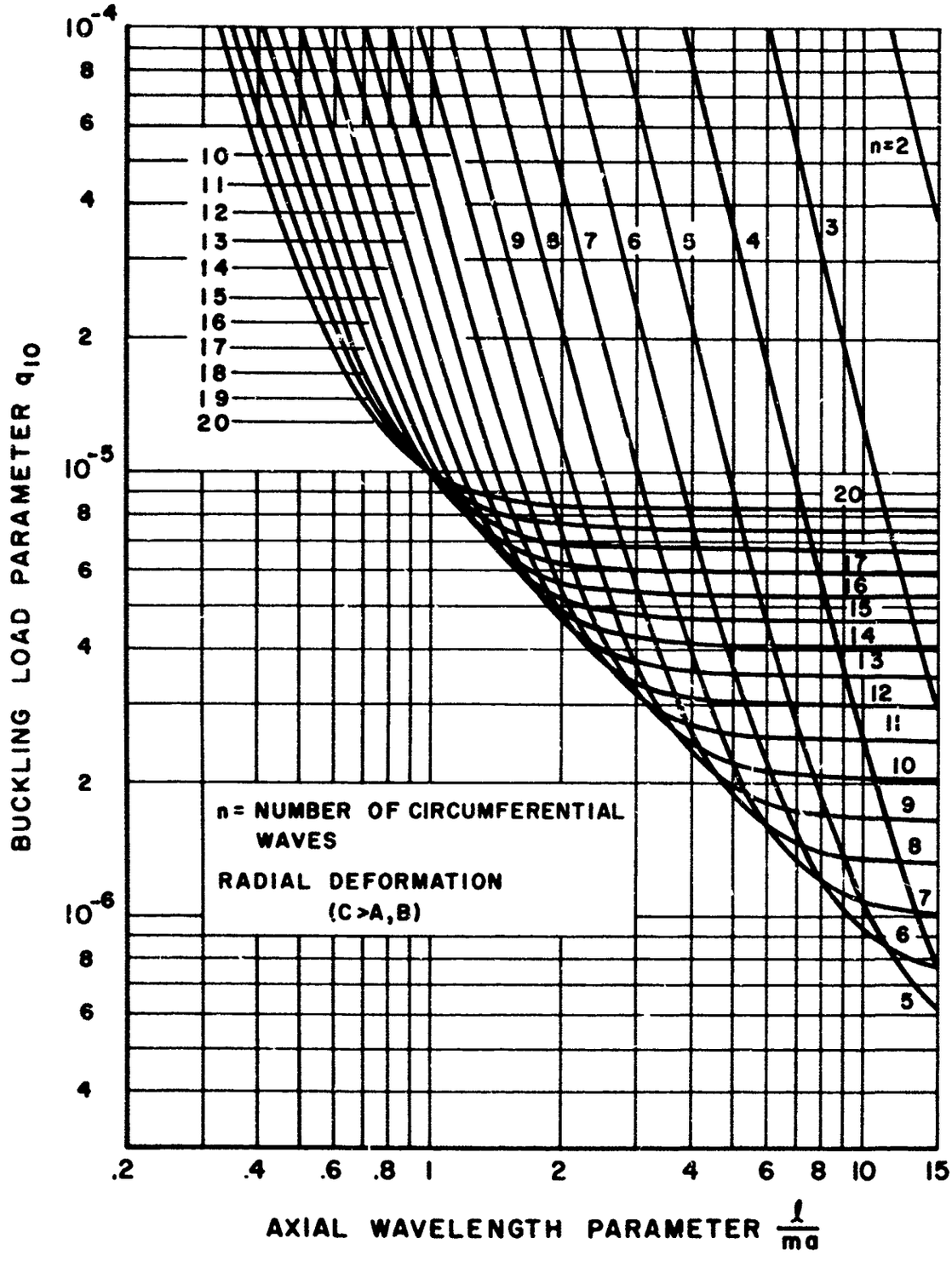

Figure 47. Buckling Values for External Pressure. $\frac{a}{h} = 2000$. No Axial Load ($q_2 = 0$)

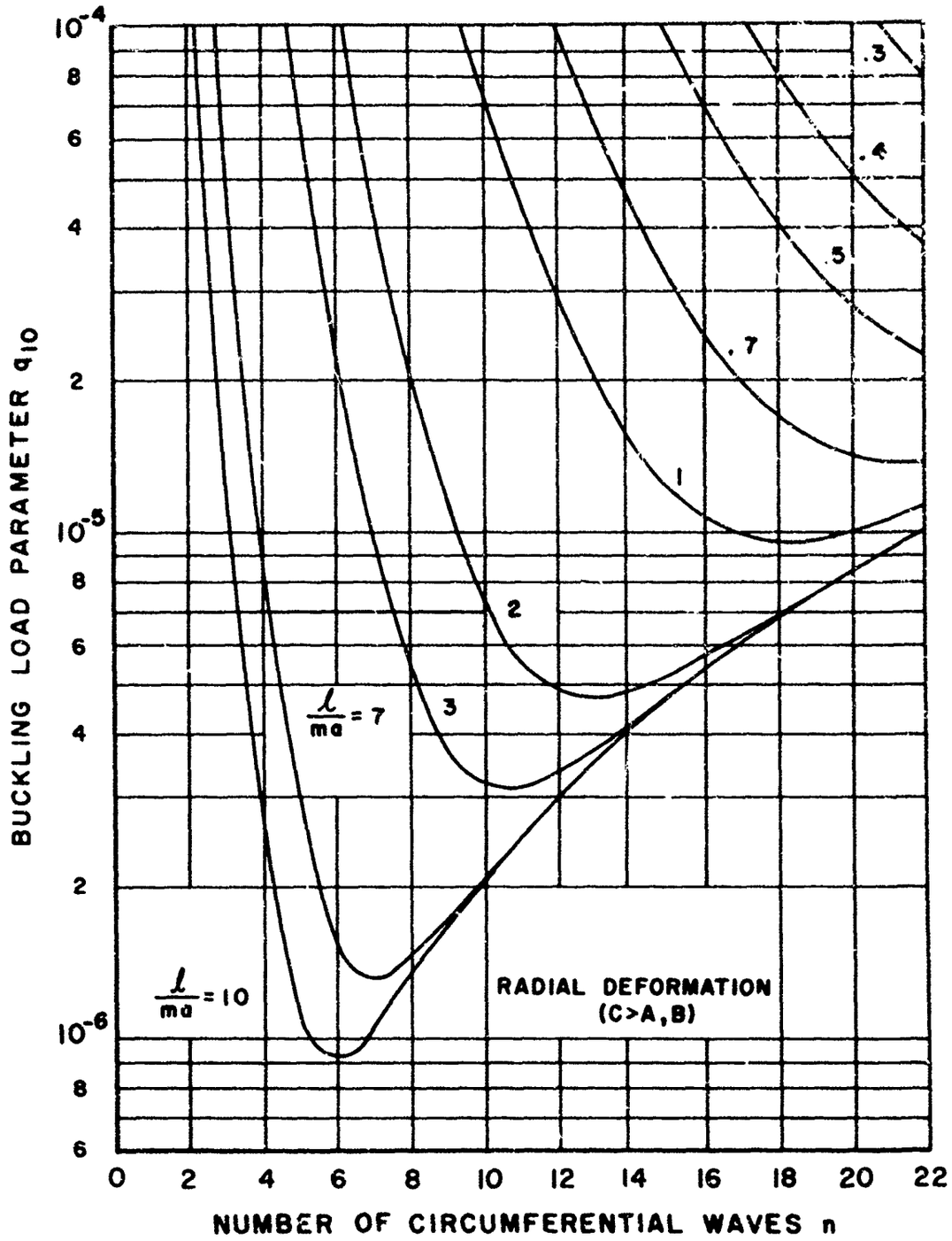

Figure 48. Buckling Values for External Pressure. $\frac{a}{h} = 2000$. No Axial Load ($q_2 = 0$)

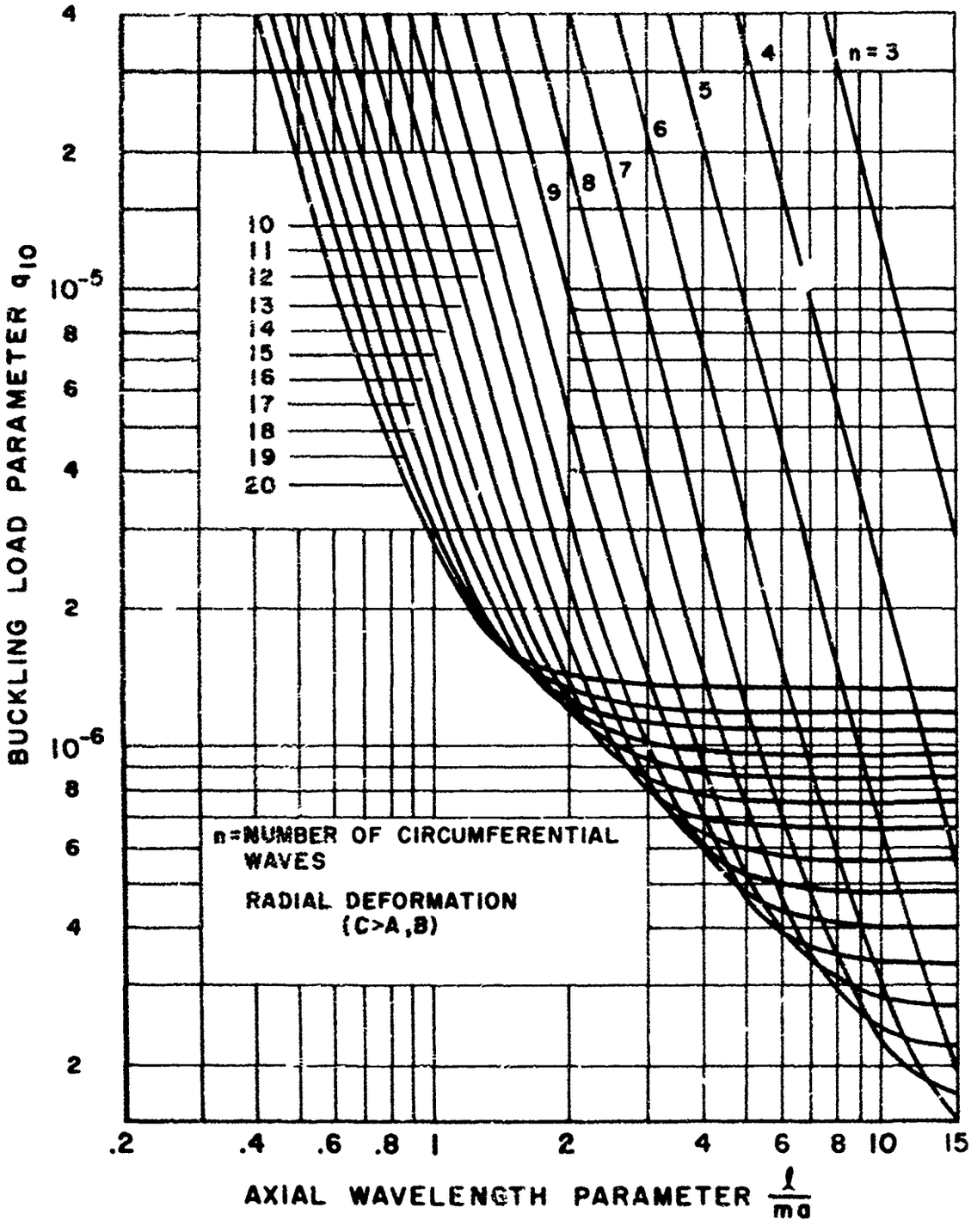

Figure 49. Buckling Values for External Pressure, $\frac{a}{h}$ =5000. No Axial Load (q_2 = 0)

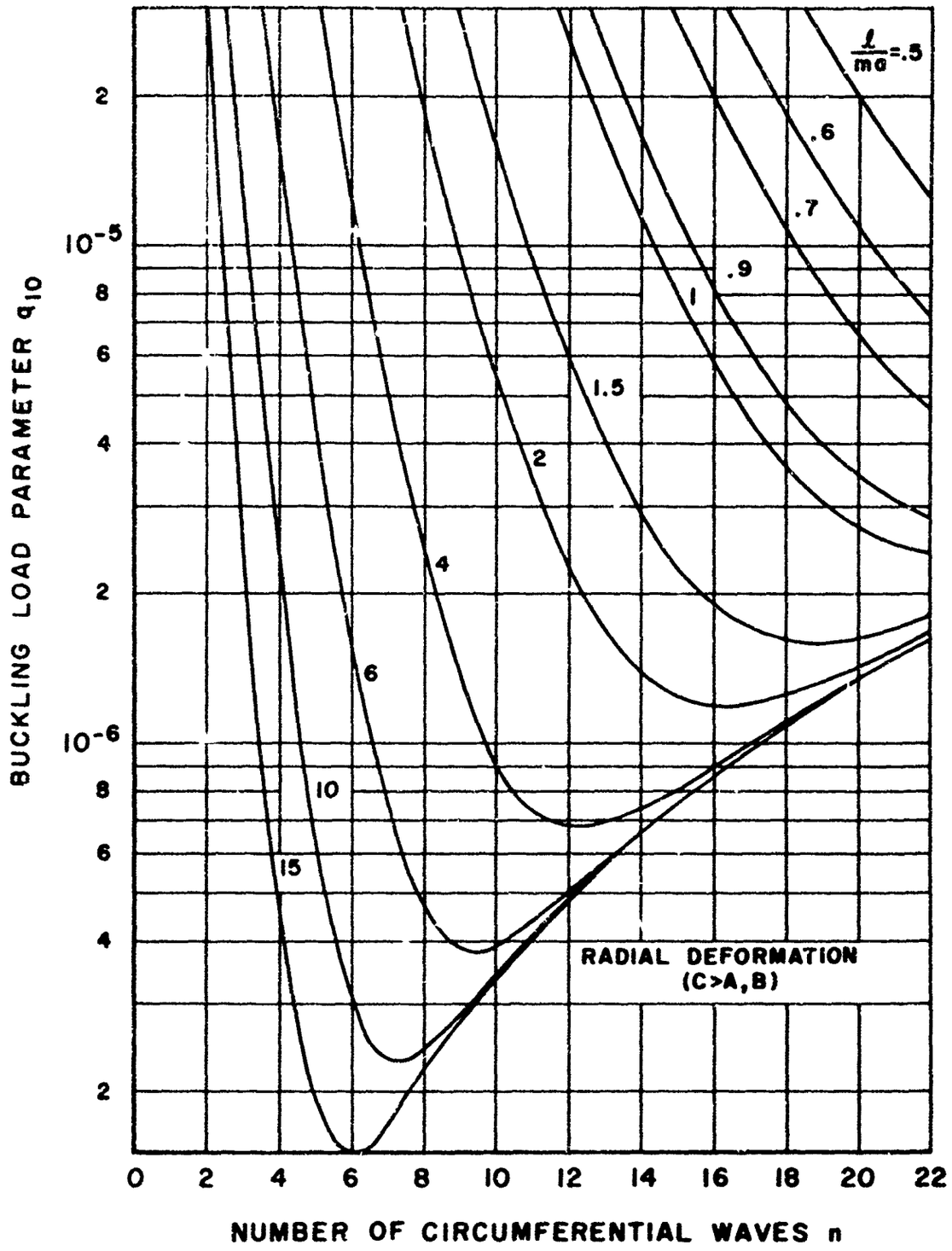

Figure 50. Buckling Values for External Pressure. $\frac{a}{h}$ = 5000. No Axial Load (q_2 = 0)

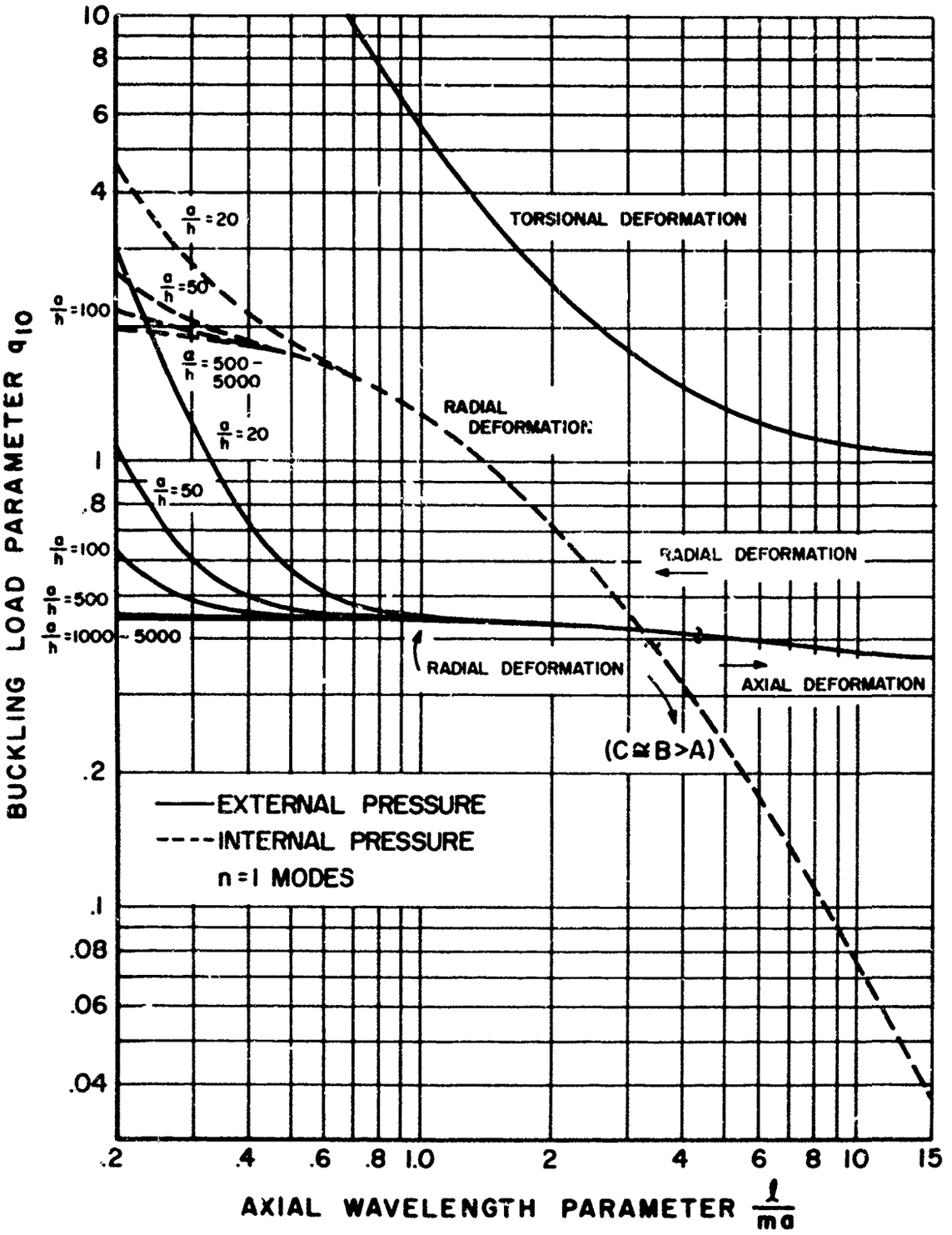

Figure 51. Buckling Values for One Circumferential Wave, Internal and External Pressure. $\frac{a}{h}$ = 20-5000. No Axial Load (q_2 = 0)

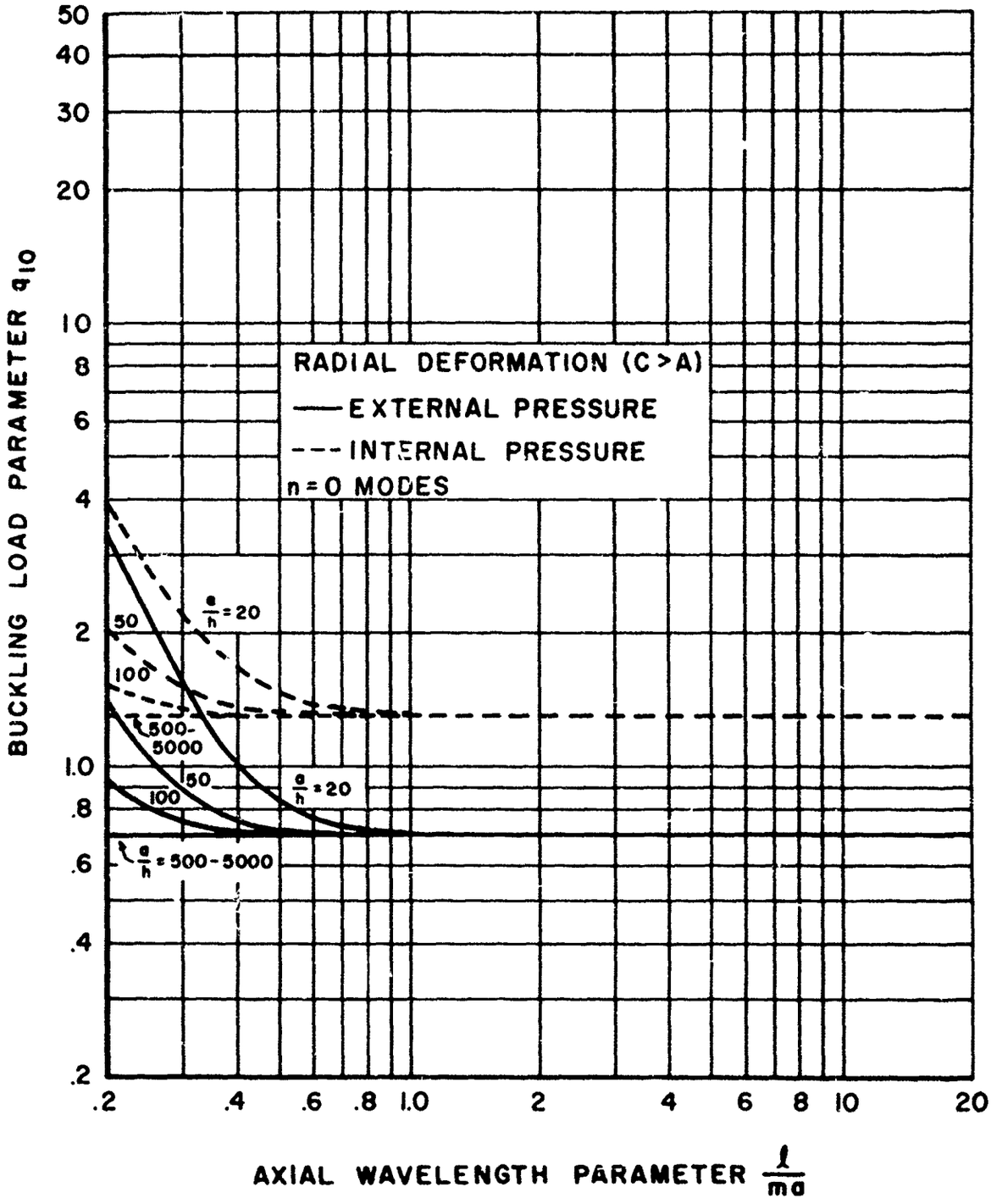

Figure 52. Axisymmetric Buckling, Internal, and External Pressure. $\frac{a}{h}$= 20-5000. No Axial Load (q_2 = 0)

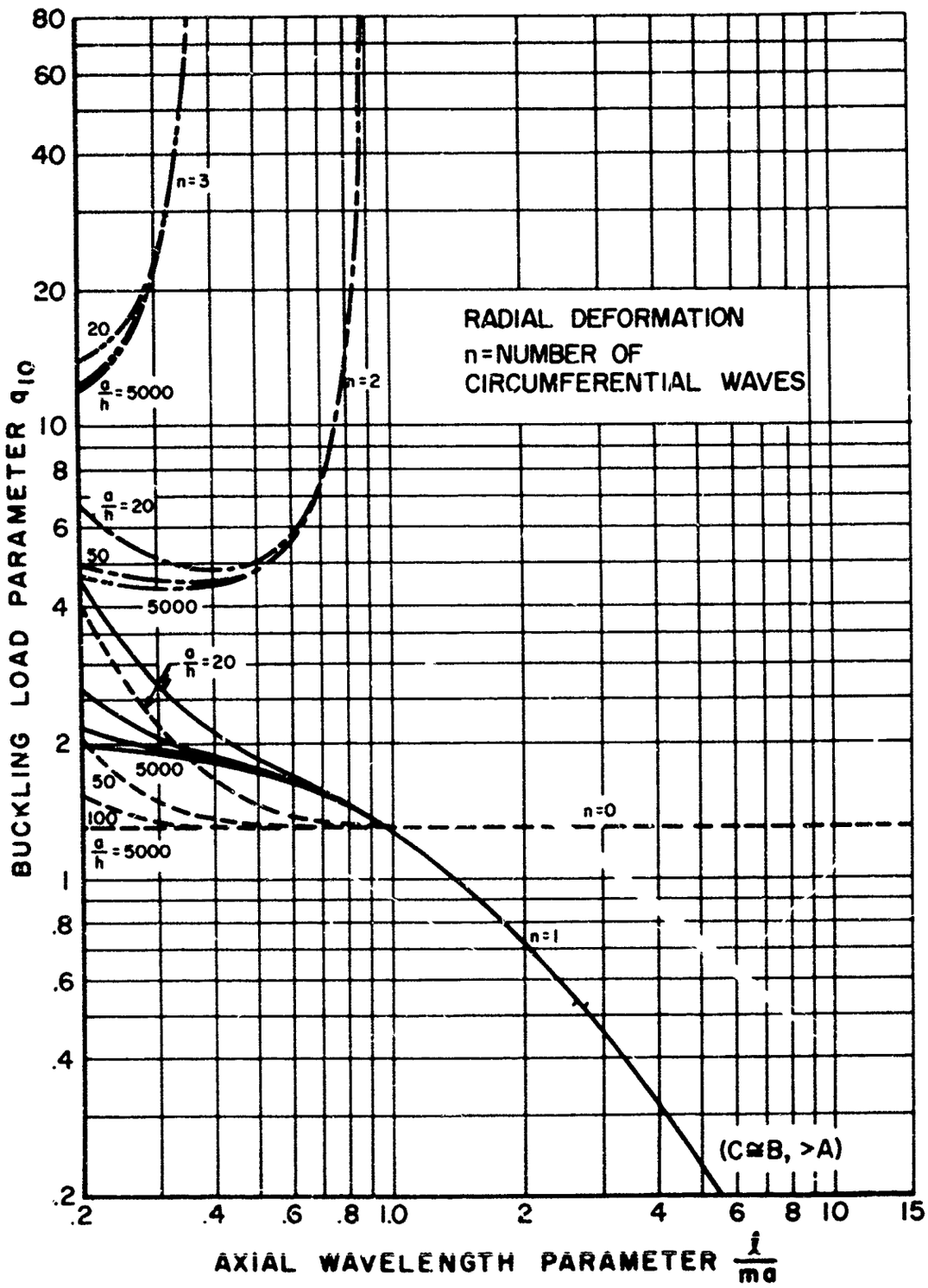

Figure 53. Buckling Values for Internal Pressure, $\frac{a}{h}$=20-5000, No Axial Load (q_2 = 0)

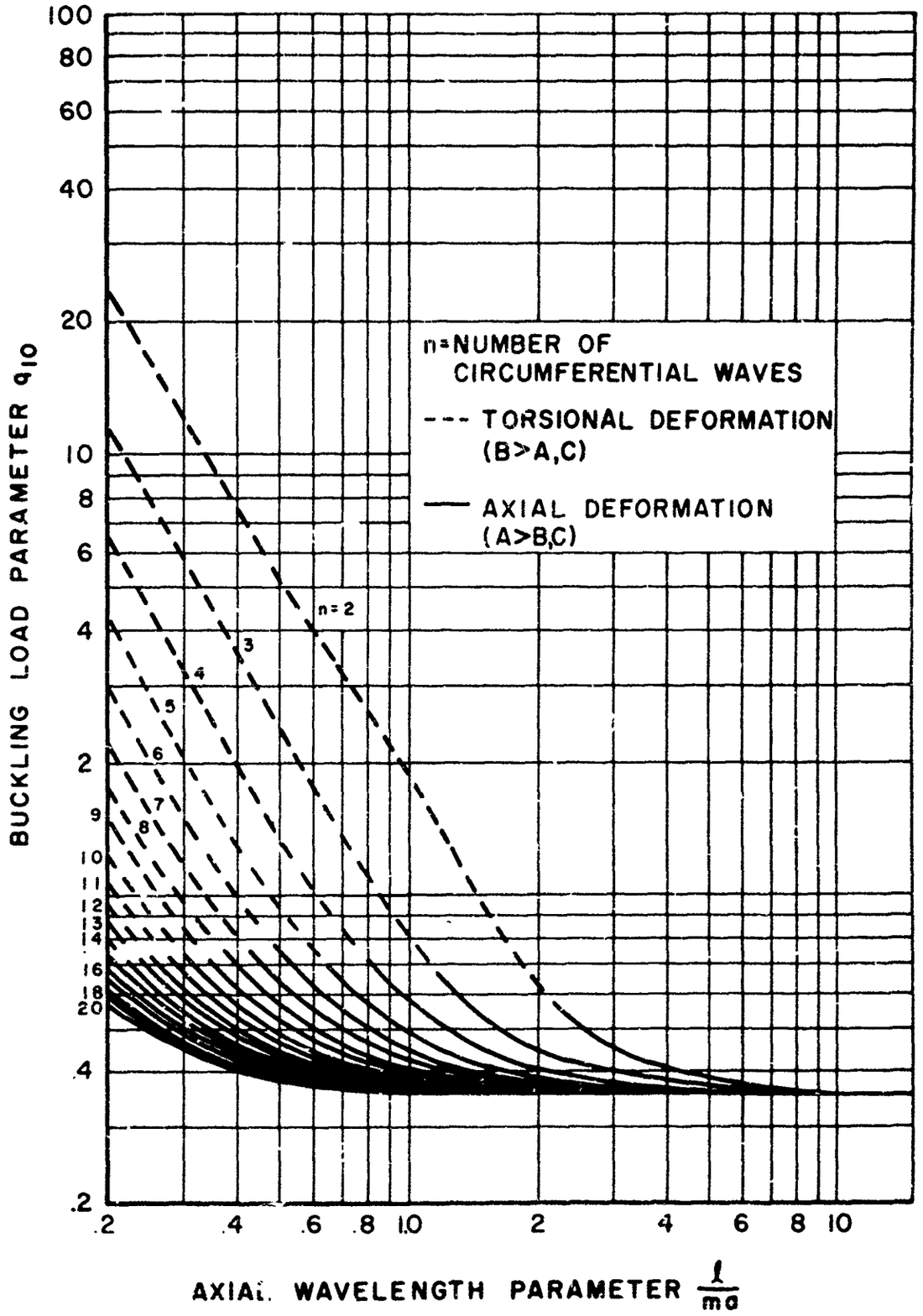

Figure 54. Second Buckling Value for External Pressure, $\frac{a}{h}$ = 20-5000, No Axial Load ($q_2 = 0$)

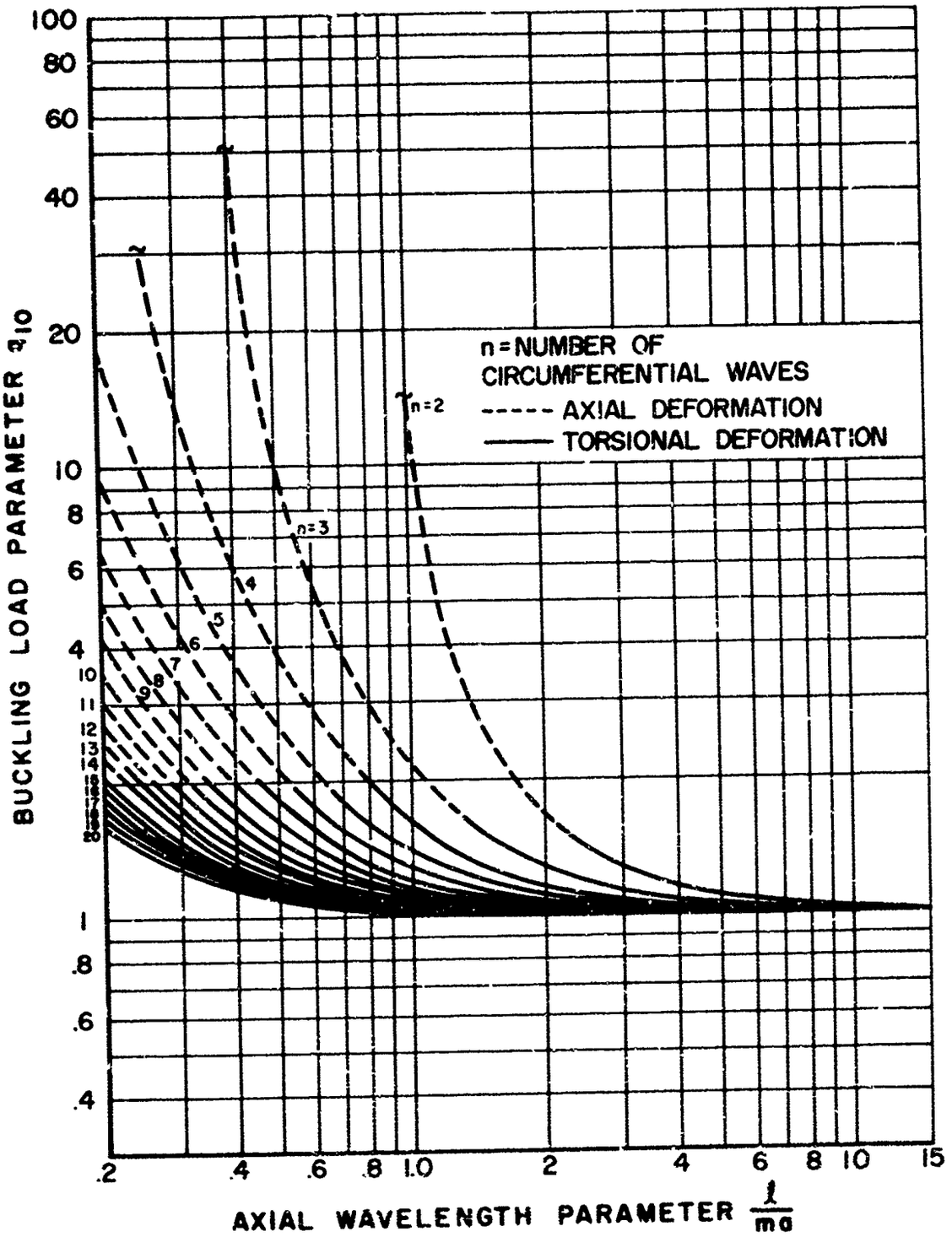

Figure 55. Third Buckling Value for External Pressure, $\frac{a}{h}$=20-5000, No Axial Load ($q_2 = 0$)

SECTION VI

THE VIBRATION OF FREELY-SUPPORTED CYLINDERS SUBJECTED TO AXIAL LOAD AND EXTERNAL PRESSURE

It was shown in Section IV that the axial load parameter, q_2 can be combined with the frequency parameter, ω, to form a single eigenvalue expression, while the internal pressure parameter q_1 appears in the coefficients of the resulting characteristic equation. An examination of the expressions D_{ij}, given in Equations 100 through 105, which appear in Equation 98, reveals that the term $-q_1 n^2$ appears on the main diagonal of that equation. These terms can be moved to the right-hand side of Equation 98 and combined with the eigenvalue expression as was done with the parameter q_2. The factor q_1 also appears in the terms D_{13} and D_{23}, indicating that the coefficients of the resulting characteristic equation would still be a function of the external pressure parameter q_1. With these changes, Equation 98 can be written

$$\begin{bmatrix} H_{11}^m & H_{12}^m & (H_{13}^m - q_1 \lambda) \\ H_{12}^m & H_{22}^m & (H_{23}^m - q_1 n) \\ (H_{13}^m - q_1 \lambda) & (H_{23}^m - q_1 n) & H_{33} \end{bmatrix} \begin{Bmatrix} A_m \\ B_m \\ C_m \end{Bmatrix} = (\gamma^2 \omega^2 + q_2 \lambda^2 + q_1 n^2) \begin{Bmatrix} A_m \\ B_m \\ C_m \end{Bmatrix} \tag{140}$$

where the terms H_{ij} are given by subtracting the q_1 terms from the expressions for D_{ij} (Equations 100 to 105).

If the value of q_1 is small in the expressions for H_{13} and H_{23}, the parameter q_1 can be dropped from the left-hand side of Equation 140 without affecting results significantly. With this simplification, a new eigenvalue expression $\overline{\Delta}(\lambda, n)$ would result

$$\overline{\Delta}\ (\lambda, n) = (\gamma^2\ \omega^2 + q_2\ \lambda^2 + q_1\ n^2) \tag{141}$$

The eigenvalues $\overline{\Delta}(\lambda, n)$ would be the same as $\Delta(\lambda, n)$ of Section IV because the coefficients H_{ij} in Equation 140 are the same as the D_{ij} with $q_1 = 0$.

A buckling value, q_{10}, can be obtained from Equation 141 by setting ω and q_2 equal to zero.

$$\overline{\Delta}\ (\lambda, n) = \Delta(\lambda, n) = q_{10}\ n^2 \tag{142}$$

$$q_{10} = \frac{\Delta(\lambda, n)}{n^2} \tag{143}$$

If the approximation discussed in Section IV is assumed to be valid, an expression similar to Equations 124 and 125 which include the effects of both axial load and internal pressurization can be obtained.

$$\left(\frac{\omega}{\omega_0}\right)^2 = 1 - \frac{q_2}{q_{20}} - \frac{q_1}{q_{10}} \tag{144}$$

or

$$\omega^2 = \omega_0^2 \left(1 - \frac{q_2}{q_{20}} - \frac{q_1}{q_{10}}\right) \tag{145}$$

Equations 144 and 145 indicate that the square of the vibration frequency for a freely-supported cylinder varies linearly with both axial load and internal pressure for a given deformation mode. For buckling due to combined loads, Equation 145 can be written

$$1 = \frac{q_1}{q_{10}} + \frac{q_2}{q_{20}} \tag{146}$$

These results are shown in Figure 56. The line $\left(\frac{\omega}{\omega_0}\right)^2 = 0$ represents buckling of the cylinder. Thus the coordinates of any point on this line represent combinations of axial loading and external pressure necessary to buckle the cylinder in a given mode. Similarly the line $\left(\frac{\omega}{\omega_0}\right)^2 = 0.5$ would represent the combinations of axial load and external pressure which reduce the square of the vibration frequency to a value of one half that for the unloaded cylinder. The line $\left(\frac{\omega}{\omega_0}\right)^2 = 1$ represents combinations of axial load and external pressure for which the vibration frequency remains unchanged.

The results obtained for buckling due to external pressure in Section V indicate that for some modes negative buckling values are obtained, which correspond to buckling due to internal pressure. With Equation 143, however, only positive buckling values could be obtained since all the eigenvalues $\Delta(\lambda, n)$ are positive. Thus, buckling values obtained using Equation 143 could lead to significant errors for some modes If the actual results for q_{10} obtained from the buckling equations of Section V are used in Equations 144 or 145 rather than the values given by Equation 143, the problems arising from the negative buckling values would be alleviated. The use of the true values for q_{10} obtained from the buckling equations, essentially forces Equations 144 and 145 to be correct at $\frac{q_1}{q_{10}} = 1$. In addition, use of the actual buckling results for q_{10} was found to extend the range of validity of Equations 144 and 145 considerably, that is, the equations were found to be valid where the buckling value was of the same order of magnitude as ν.

It is proposed that Equations 144, 145 or Figure 56 be used together with Figures 3 through 55 to obtain values for the vibration frequencies or buckling values for freely-supported cylinders subjected to axial loading and external pressure. For a given freely-supported cylinder, the ratio of length to radius, $\frac{\ell}{a}$ and radius to thickness, $\frac{a}{h}$ would be fixed. A particular mode of interest could be selected by assigning integer values to the number of circumferential waves, n, and the number of axial half-waves, m, in the parameter $\frac{\ell}{ma}$. It would then be necessary to establish which of the eigenvalues associated with the particular mode shape is to be examined; that is, whether radial, torsional, axial, or in some cases, the "beam" modes are of interest. The values of ω_0, q_{10}, and q_{20} for the particular mode of interest can be obtained from the appropriate figure. If a given axial loading or external pressure is specified, a value for the

parameter q_2 or q_1 can be calculated. With this information the vibration frequency or reduction in frequency can be obtained from Equation 144, 145, or Figure 56. For combined buckling results either q_1 or q_2 could be taken as the unknown to be determined. The greatest change in vibration frequency occurs for those modes having the lowest buckling values q_{10} and q_{20} which are usually those involving primarily radial deformation.

No simplification or approximations, other than those inherent in the original differential equations or in the assumption of the form of the solution, are associated with the axial load effects, discussed in Section IV. The simplifications made in arriving at Equations 144 to 146 or Figure 56 involve only the external pressure effects. The range of validity, or errors resulting from use of the procedures previously outlined, were determined by comparing these results with those obtained by using Equation 98 or 108 with all of the q_1 terms retained. To avoid errors arising from reading the figures, the digital results, used in plotting the figures, were used in this error analysis. Calculations were made for the full range of the various parameters involved.

Buckling calculations were made for values of pressurization equal to $-.3q_{10}$, $.3q_{10}$, $.6q_{10}$ and $1.4q_{10}$ for various modes. The value of q_{10} used in the calculations was that which was smallest in absolute value for that mode. In some cases this was a negative value, associated with internal pressure. The values of $\frac{q_2}{q_{20}}$ for buckling associated with the above pressurization values were determined by the two methods. A comparison of these results was made for 0, 1, 2, 5, 10, and 20 circumferential waves, values of $\frac{\ell}{ma}$ equal to .2, .5, 1, 5, and 10, and for radius to thickness ratios from 20 to 5000. Since the linear relationship between the square of the vibration frequency and axial load was established without any approximations, the relative error in $\frac{q_2}{q_{20}}$ for combined buckling would be the same as for the square of the vibration frequency ω^2 for loadings less than the buckling values.

In general a comparison of the results indicates that for the bulk of the cases examined the difference in the values obtained for $\frac{q_2}{q_{20}}$ were less than 1% of q_{20}. The largest discrepancy occurred for the axisymmetric modes (n = 0), and for modes with one circumferential wave.

The results for the axisymmetric modes are shown in Figure 57. The plotted points represent the correct results. The two methods produce the same results at $\frac{q_1}{q_{10}} = 0$ and $\frac{q_1}{q_{10}} = 1$. The greatest discrepancy occurred for $\frac{a}{h} = 20$ and $\frac{\ell}{ma} = .2$, which would represent a relatively thick short cylinder. The results for $\frac{\ell}{ma} = 5$ were essentially the same for all values of the radius to thickness ratio examined and produced the smallest discrepancy.

The error is generally less as n increases. Figure 58 shows a comparison of the results for modes with one circumferential wave. Again the largest discrepancy occurs for $\frac{a}{h} = 20$ and $\frac{\ell}{ma} = .2$. For values of $\frac{\ell}{ma} \geq 5$ the error was less than 2.3% of q_{20} for all values of radius to thickness.

The results for two circumferential waves are shown in Figure 59. For values of $\frac{\ell}{ma}$ equal to .5 and 1, the errors ranged from .59 to 6.8% of q_{20} for all values of the radius to thickness ratio. For values of $\frac{\ell}{ma} \geq 5$ the errors were much less than 1% for all values of the radius to thickness ratio.

For five circumferential waves the error for $\frac{a}{h} = 20$ and $\frac{\ell}{ma} = .2$ was 1.7% of q_{20} at $\frac{q_1}{q_{10}} = -.3$, .92% of q_{20} at $\frac{q_1}{q_{10}} = .3$, 1.05% of q_{20} at $\frac{q_1}{q_{10}} = .6$, and 2.39% of q_{20} at $\frac{q_1}{q_{10}} = 1.4$, and were less less than 1% for all other values of $\frac{\ell}{ma}$ and $\frac{a}{h}$, and in most cases substantially less than 1%.

For modes having 10 and 20 circumferential waves the results were found to agree to well within 1% for the entire range of $\frac{\ell}{ma}$ and $\frac{a}{h}$.

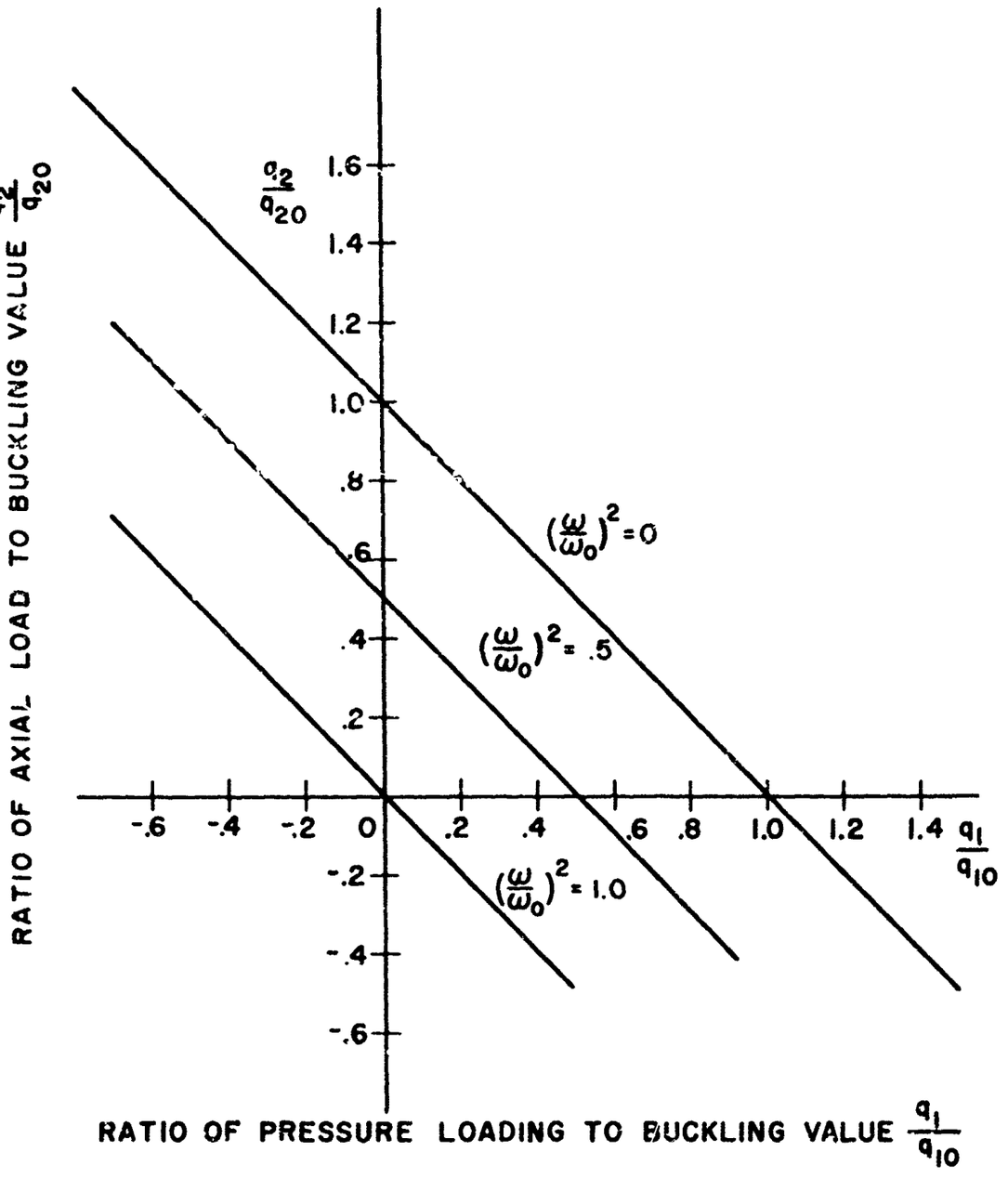

Figure 56. Reduction in Vibration Frequencies for Combined Effects of Axial Load and Pressurization

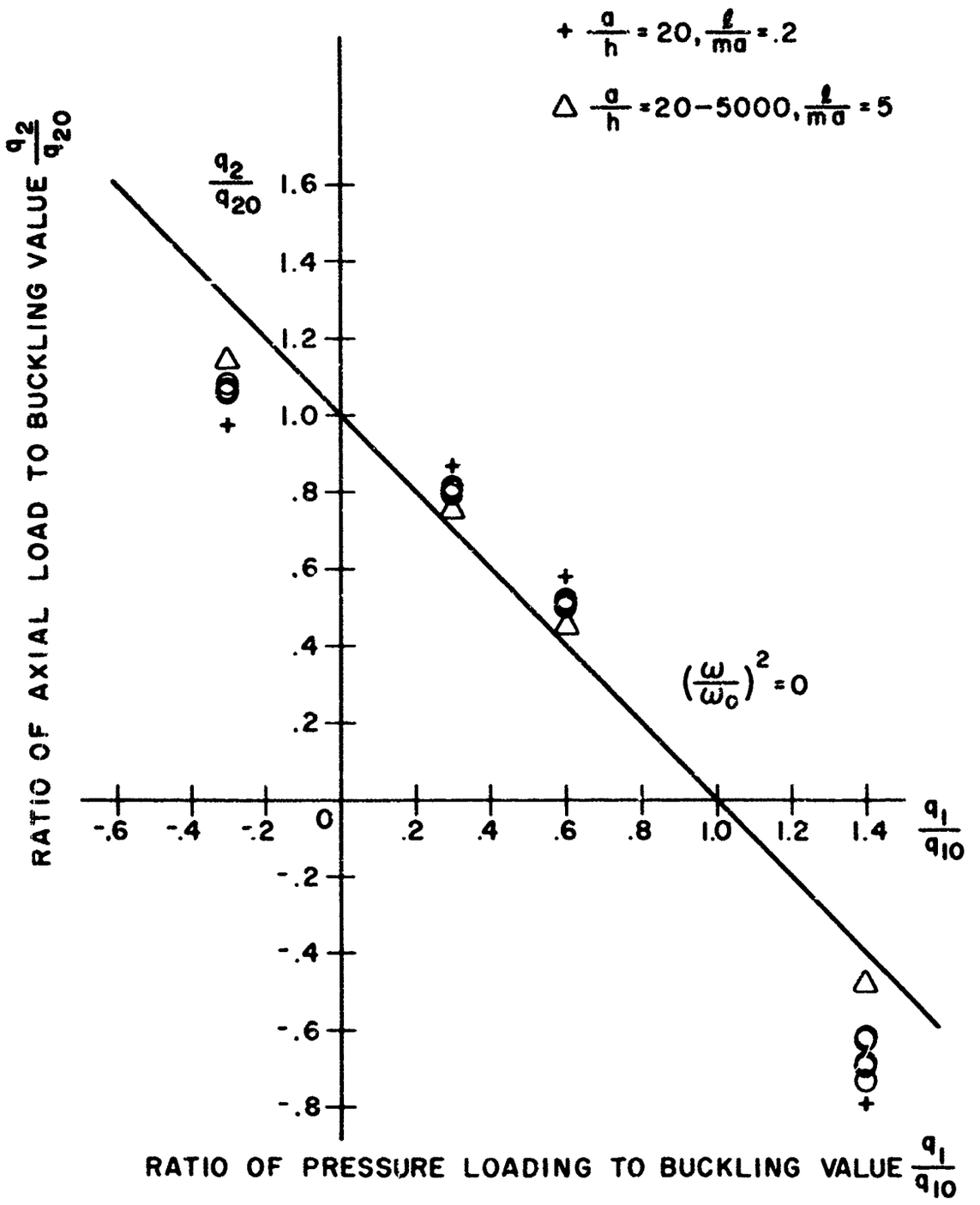

Figure 57. Comparison of Combined Buckling Results for Axisymmetric Modes. (n = 0)

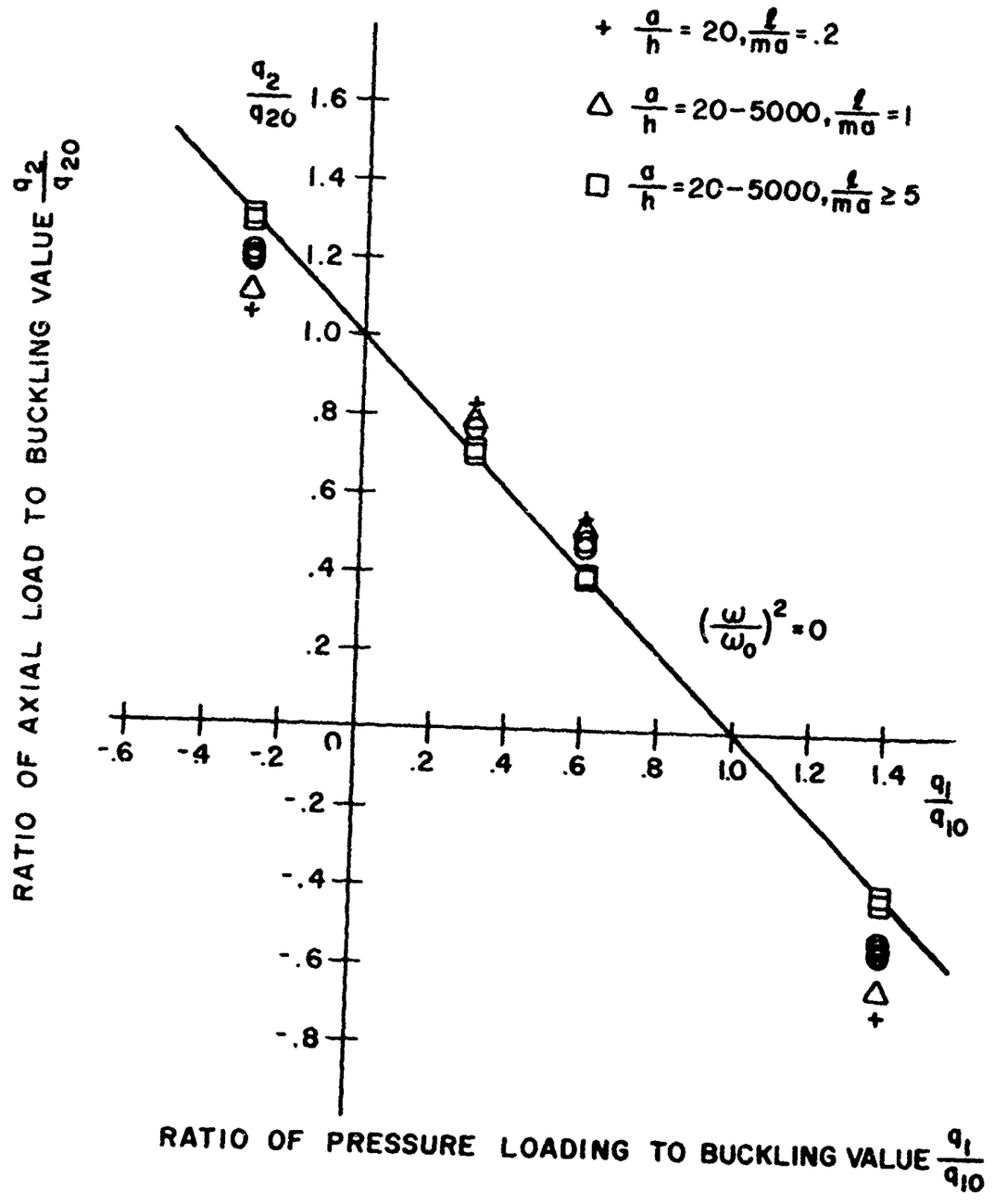

Figure 58. Comparison of Combined Buckling Results for Modes with One Circumferential Wave. (n = 1)

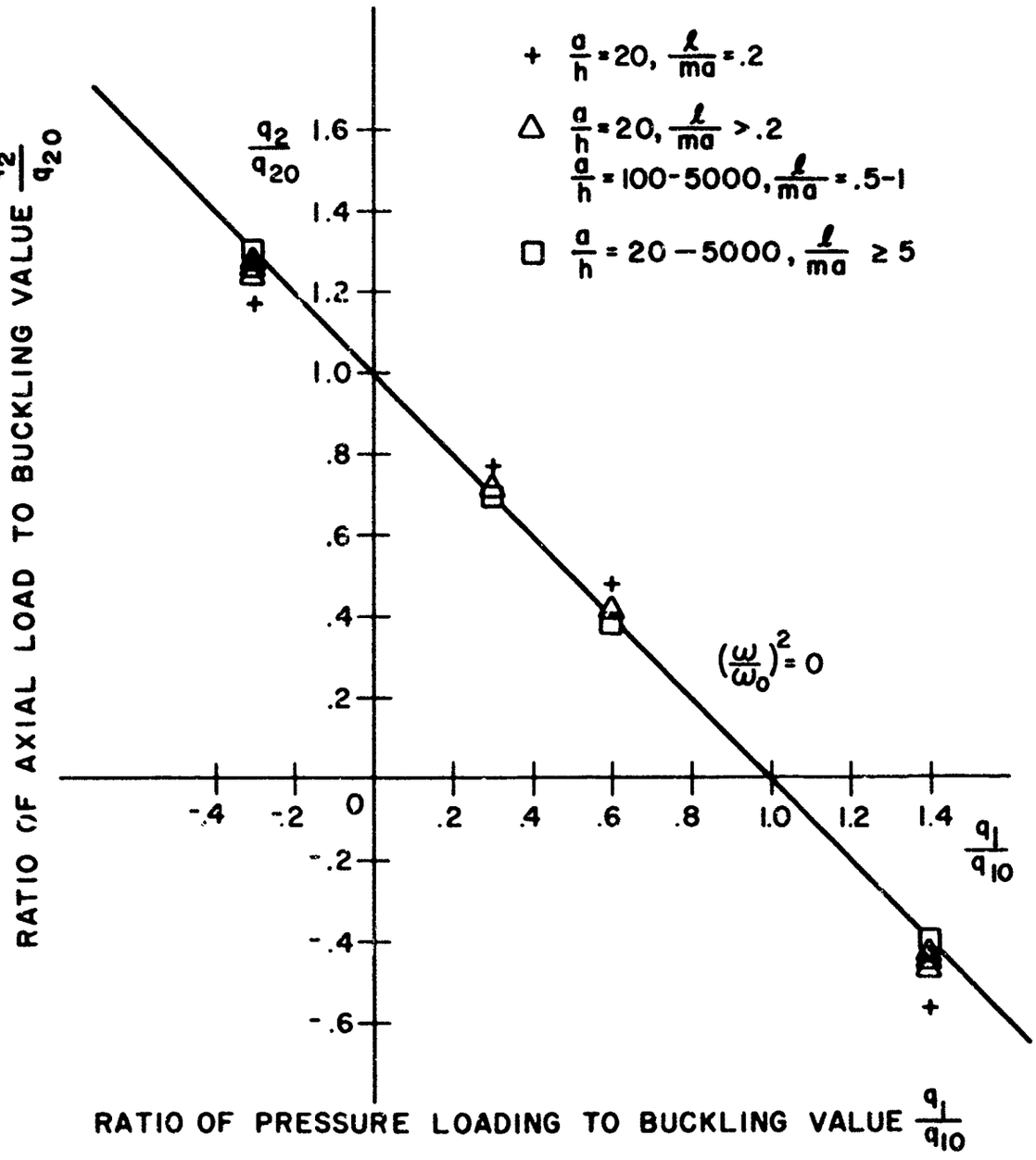

Figure 59. Comparison of Combined Buckling Results for Modes with Two Circumferential Waves (n = 2)

SECTION VII

RESULTS AND CONCLUSIONS

Equations are formulated which can be used to determine the vibration and buckling characteristics of cylindrical shells with various homogeneous boundary conditions under axial loading and a constant external pressure. A method of solution is outlined which makes use of a series of beam functions for the radial, tangential, and axial displacements, which satisfy the appropriate boundary conditions involving these displacements.

Using a series of functions known to be an exact solution to the problem for the freely-supported cylinder the equations reduced to those obtained by Flugge for the buckling of a cylinder subjected to axial loads and a constant external pressure, if the frequency is assumed to be zero. If the axial load and external pressure parameters are assumed to be zero, the equations reduce to a form similar to those obtained by Arnold and Warburton for the natural vibrations of a freely-supported cylinder.

An investigation was made of the vibration and buckling characteristics for the freely-supported cylinder under axial loading and external pressure, since an exact solution was shown to exist for this case. The results discussed in the remainder of this Section are associated with this solution.

The characteristic equations for natural vibrations, buckling due to axial load, and buckling due to external pressure were solved for a range of cylinder radius to thickness ratios from 20 to 5000, for values of the parameter $\frac{\ell}{ma}$ from .2 to 15 and for all circumferential waves from 0 to 20. The vibration and buckling results are presented in a series of figures.

For the freely-supported cylinder the problem reduces to the solution of a cubic characteristic equation, except for the axisymmetric modes, indicating that three eigenvalues exist for each mode. A particular mode involves an integer number of circumferential waves and axial half-waves. These eigenvalues are associated with various amplitude ratios for the radial, axial, and tangential displacements, indicating that these displacements are coupled. For vibration or buckling under axial loading three positive eigenvalues are obtained for a given mode and are associated with deformations which are primarily radial, axial, and torsional. For long cylinders having one circumferential wave the amplitude of the radial and tangential displacement approaches a value of -1 for one of the eigenvalues. This represents the "beam" modes for the cylinder, where the cylinder deflects with little distortion of the circular cross-section.

For buckling due to external pressure a negative eigenvalue is obtained for some modes, which corresponds to buckling due to internal pressure. In this case the negative eigenvalue and one of the positive eigenvalues for that mode are both associated with deformation which is primarily radial.

For the axisymmetric mode ($n = 0$), the tangential displacement uncouples from the axial and and radial displacements. For the natural vibration case and buckling due to axial load, the uncoupled torsional displacement gives rise to a pure torsional vibration or buckling mode. Two eigenvalues are associated with the coupled radial and axial displacements. For buckling due to only external pressure, the uncoupled torsional deformation has only the trivial solution, and only the two eigenvalues associated with coupled radial and axial displacement can be obtained.

The eigenvalues associated with radial deformation were generally dependent on the radius to thickness ratio $\frac{a}{h}$, whereas the eigenvalues associated with axial or torsional deformation were independent of the radius to thickness ratio for values of $\frac{a}{h}$ from 20 to 5000.

The third order characteristic equation, the resulting eigenvalues, and amplitude ratios for the vibration of an unloaded cylinder and for buckling due to axial loads are identical. The eigenvalues $\Delta(\lambda, n)$ represent the frequency parameter $\gamma^2\omega_o^2$ for the unloaded cylinder and $q_{20}\lambda^2$ for the buckling problem.

For the vibration of freely-supported cylinders under axial loads less than the buckling value, the frequency parameter $\gamma^2\omega^2$ and axial load parameter $q_2\lambda^2$ can be combined to form a single eigenvalue expression, $\Delta(\lambda, n) = \gamma^2\omega^2 + q_2\lambda^2$. The eigenvalues can be obtained without specifying a value for axial load. For this problem the square of the vibration frequency for any mode was found to vary linearly with axial load.

The vibration frequency for any mode and axial loading can be obtained by knowing only the vibration frequency of an unloaded cylinder, ω_o, and the value of the buckling parameter q_{20} for that mode. The relationship between these parameters is given by Equation 127

$$\omega^2 = \omega_o^2 \left(1 - \frac{q_2}{q_{20}} \right) \tag{127}$$

The values for ω_o and q_{20} can be obtained from the figures, where both values should be for deformation which is either radial, axial, or torsional. All vibration frequencies decrease for a compressive axial loading and increase for a tensile axial loading. For a given axial loading the relative change in vibration frequency is greatest for those modes having the lowest buckling values q_{20}.

For the non-axisymmetric modes ($n \neq 0$), the lowest natural vibration frequencies and lowest buckling values for axial loading for a given mode were associated with deformation which was radial except for long cylinders and modes with one circumferential wave where the "beam" modes produced the lowest values.

The lowest vibration frequency for the unloaded cylinder has one axial half-wave. This is generally not the case for the lowest buckling mode for a cylinder under axial load. It appears that the lowest natural vibration frequency and the lowest axial buckling load, for a given number of axial half-waves, have the same number of circumferential waves. The number of circumferential waves depends on the value of the parameter $\frac{\ell}{ma}$ and the radius to thickness ratio $\frac{a}{h}$.

The lowest vibration frequencies for the unloaded cylinder for torsional and axial vibration were the axisymmetric modes ($n = 0$) with one axial half-wave. The frequencies increase as the number of circumferential waves and the number of axial half-waves increase.

The lowest natural vibration frequencies for the axisymmetric modes ($n = 0$) are associated with vibration which is radial for values of $\frac{\ell}{ma} < 2$ and pure torsional for values of $\frac{\ell}{ma} > 2$.

The equation for the uncoupled axisymmetric torsional vibration frequency is given by Equation 121.

$$\omega_o = \frac{m\pi}{\ell} \sqrt{\frac{E}{2\rho(1+\nu)}} \qquad m = 1, 2, \cdots \tag{121}$$

The only assumption used to obtain this equation was that the ratio of thickness to radius is small compared to 1.

The lowest axial loading buckling value for axisymmetric modes also involves radial deformation for $\frac{\ell}{ma} < 2$, and pure torsional deformation for $\frac{\ell}{ma} > 2$. The buckling value for the axisymmetric, pure torsional mode is given by Equation 129

$$q_{20} = \frac{P}{D} = \frac{(1-\nu)}{2} \tag{129}$$

with the assumption that the ratio of thickness to radius is small compared to 1. This axial load, q_{20}, is independent of the length of the cylinder and the number of axial half-waves in the mode shape.

For the buckling of a freely-supported cylinder due to a pressure loading, the axisymmetric modes and modes with one circumferential wave have buckling values, q_{10}, which are much higher than those for two or more circumferential waves. For modes having from 0 to 4 circumferential waves, one negative buckling value is obtained, which corresponds to buckling due to internal pressure. For the axisymmetric modes and modes with one circumferential wave, a negative buckling value is obtained for the full range of the parameter $\frac{\ell}{ma}$ from .2 to 15. For modes having two circumferential waves, a buckling value for internal pressure exists only for values of $\frac{\ell}{ma} < 1$. For modes with three circumferential waves, a buckling value for internal pressure exists only for values of $\frac{\ell}{ma} < .4$. For modes with four circumferential waves a buckling value for internal pressure is obtained only for $\frac{\ell}{ma} = .2$. This negative buckling value is quite large.

For modes having one circumferential wave, the lowest buckling value results for external pressure with radial deformation for values of $\frac{\ell}{ma} < \pi$, and internal pressure with a "beam" mode type deformation for values of $\frac{\ell}{ma} > \pi$.

For the buckling of a freely-supported cylinder due to a constant pressure loading in an axisymmetric mode (n = 0) the buckling values q_{10} involving coupled axial and radial deformation are given by Equation 139 for large values of $\frac{\ell}{ma}$.

$$q_{10} = -\nu \pm 1 \tag{139}$$

Numerical calculations for the range of radius to thickness ratios from $\frac{a}{h} = 20$ to 5000 indicate that Equation 139 can be used for values of $\frac{\ell}{ma} > 1$. The deformation associated with these results is radial. Both the positive and negative buckling loads had the same numerical value for the ratio of the radial deformation to axial deformation and were of opposite sign.

For freely-supported cylinders subjected to both axial loads and a pressure loading, the square of the vibration frequency for a given deformation mode was found to vary essentially linearly with the pressure loading as well as the axial load for many modes. This relationship is given by Equation 145,

$$\omega^2 = \omega_o^2 \left(1 - \frac{q_2}{q_{20}} - \frac{q_1}{q_{10}}\right) \tag{145}$$

where ω_o, q_{20}, and q_{10} are the natural frequency of the unloaded shell, buckling value for axial load, and buckling value for a pressure load, for a given deformation mode.

The errors introduced by this linear relationship are evaluated for a wide range of shell modes covering the full range of the shell parameters. Equation 145 was found to give poor results for the axisymmetric modes and modes with one circumferential wave. For modes with two circumferential waves the results were within 7% of the correct values for all modes examined for values of $\frac{\ell}{ma} > .5$. The discrepancy decreases as the number of circumferential waves in the mode shape increases. Buckling values for a combined axial and pressure loading can be obtained by setting ω equal to zero in Equation 145.

For those modes having only positive buckling values for external pressure, external pressure decreases the vibration frequency and internal pressure increases the vibration frequency for that mode. For those modes having negative buckling values corresponding to internal pressure, the vibration frequency appears to increase with external pressure and decreases with internal pressure if the negative buckling value is smaller in magnitude than the other external pressure buckling values for that mode.

SECTION VIII

RECOMMENDATIONS

The figures contained in this report can be used directly to obtain the natural vibration frequencies, buckling values for axial loading, and buckling values for external and internal pressure for freely-supported cylinders. The vibration frequencies can be obtained for cylinders subjected to axial loads, and approximate results can be obtained for freely-supported cylinders subjected to both axial load and external pressure.

Arnold and Warburton (Reference 2) suggest the use of vibration results for the freely-supported cylinder for cylinders with other boundary conditions by relating these to an equivalent freely-supported cylinder. Equivalent wavelength factors were obtained from experimental vibration results for cylinders with different types of supports and are given in Reference 2. Through the use of the concept of an equivalent freely-supported cylinder, the figures and formulas presented could be used to obtain preliminary design values for the vibration frequencies for loaded or unloaded cylinders as well as buckling values for combined loadings for cylinders with various boundary conditions.

If the concept of an equivalent freely-supported cylinder is valid for buckling results as well as for vibration frequencies, the linear approximation between the square of the vibration frequency and axial load and external pressure may also be valid. If this is the case, vibration tests could be conducted in connection with static buckling tests to achieve nondestructive testing. By recording vibration frequencies at various increments of load it may be possible to extrapolate to the buckling values without damaging costly test specimens or actual hardware.

Since the natural vibration frequencies for cylinders are sensitive to both boundary conditions and imperfections, it may be possible to obtain better correlation between buckling tests by using experimental vibration frequencies as an index of imperfection or support restraint.

REFERENCES

1. R. N. Arnold and G. B. Warburton, "Flexural Vibrations of the Walls of Thin Cylindrical Shells Having Freely Supported Ends," Proceedings of the Royal Society (London), Series A, Vol. 197, 1949, p. 238.

2. R. N. Arnold and G B. Warburton, "Flexural Vibrations of Thin Cylinders," Journal and Proceedings of the Institution of Mechanical Engineers (London), Vol. 167, 1953, pp. 62-74.

3. R. P. Felgar, Jr., "Formulas for Integrals Cortaining Characteristic Functions of a Vibrating Beam," Bureau of Engineering Research, Circular No. 14, University of Texas, Austin, Texas, 1950.

4. W. Flugge, Stresses in Shells, Second Printing Springer-Verlag, Berlin 1962.

5. K. Forsberg, "Influence of Boundary Conditions on the Modal Characteristics of Thin Cylindrical Shells". AIAA Journal, Vol. 2, No. 12, 1964, pp. 2150-2157.

6. K. Forsberg, "Axisymmetric and Beam Type Vibrations of Thin Cylindrical Shells", Fourth Aerospace Sciences Meeting, 27-29 June 1966. Preprint No. 66-447.

7. Y C. Fung, "On the Vibration of Thin Cylindrical Shells Under Internal Pressure". Ramo-Wooldridge 6MRD Aeromechanics Section Report No. AM 5-8, September 1955.

8. Y. C. Fung, A. Kaplan and E. E. Sechler, "Experiments on the Vibration of Thin Cylindrical Shells Under Internal Pressurization. The Ramo-Wooldridge Corporation, Aeromechanics Report No. AM 5-9. (AD 607517). December 1955.

9. Y. C. Fung and E. E. Sechler, "Buckling of Thin-Walled Circular Cylinders Under Axial Compression and Internal Pressure". Journal of Aeronautical Sciences.

10. Y. C. Fung, E. E. Sechler and A. Kaplan, "On the Vibration of Thin Cylindrical Shells Under Internal Pressure". Journal of the Aerospace Sciences, Vol. 24, No. 9, September 1957. pp. 650-660.

11. G. Herrmann and J. Shaw, "Vibration of Thin Shells Under Initial Stress", Journal of the Engineering Mecnanics Division, Proceedings of the American Society of Civil Engineers, Vol. 91, No. EMS. October 1965.

12. C. Wang, Applied Elasticity. McGraw Hill Book Company, Inc., New York. 1953.

13. V. I. Weingarten, E. J. Morgan and P. Seide "Elastic Stability of Thin-Walled Cylindrical and Conical Shells under Combined Internal Pressure and Axial Compression". AIAA Journal, Vol. 3, No. 6, 1965. pp. 1118-1125.

UNCLASSIFIED

Security Classification

DOCUMENT CONTROL DATA - R&D

(Security classification of title, body of abstract and indexing annotation must be entered when the overall report is classified)

1 ORIGINATING ACTIVITY (Corporate author) Air Force Flight Dynamics Laboratory (FDDS) Wright-Patterson AFB, Ohio 45433	2a REPORT SECURITY CLASSIFICATION UNCLASSIFIED 2b GROUP NA

3 REPORT TITLE

The Vibration and Buckling Characteristics of Cylindrical Shells Under Axial Load and External Pressure

4 DESCRIPTIVE NOTES (Type of report and inclusive dates)

In-House Report June 1965 - August 1966

5 AUTHOR(S) (Last name, first name, initial)

Bozich, William F., Capt, USAF

6 REPORT DATE	7a TOTAL NO OF PAGES	7b NO OF REFS
May 1967	104	13

8a CONTRACT OR GRANT NO	9a ORIGINATOR'S REPORT NUMBER(S)
b PROJECT NO 1370	AFFDL-TR-67-28
c Task 137003	9b OTHER REPORT NO(S) (Any other numbers that may be assigned this report)
d	None

10 AVAILABILITY/LIMITATION NOTICES

Distribution of this document is unlimited.

11 SUPPLEMENTARY NOTES	12 SPONSORING MILITARY ACTIVITY
None	Air Force Flight Dynamics Laboratory (FDDS) Research and Technology Divisions Wright-Patterson AFB, Ohio 45433

13 ABSTRACT

The Galerkin method is applied to Flugge's differential equations for the vibration of a cylindrical shell under axial load and external pressure to obtain a 3N x 3N characteristic equation in matrix form. N is the number of terms in the assumed series of displacement functions for the u, v, and w displacements which can be selected to satisfy various boundary conditions. For the freely-supported cylinder an exact solution exists, and the various assumed modes uncouple, reducing the problem to the solution of a 3 x 3 characteristic equation for each mode.

The third order characteristic equation for the freely-supported cylinder was solved for a wide range of shell parameters. The natural vibration frequencies and buckling values for axial load and external pressure for all three eigenvalues associated with each mode, are presented in a series of figures. The square of the vibration frequency for any mode was found to vary linearly with axial load, and approximately linearly with a pressure loading for modes with two or more circumferential waves.

DD FORM 1 JAN 64 1473

UNCLASSIFIED

Security Classification

UNCLASSIFIED
Security Classification

14 KEY WORDS	LINK A		LINK B		LINK C	
	ROLE	WT	ROLE	WT	ROLE	WT
Shell Vibration Shell Buckling Shell Dynamics						

INSTRUCTIONS

1. ORIGINATING ACTIVITY: Enter the name and address of the contractor, subcontractor, grantee, Department of Defense activity or other organization *(corporate author)* issuing the report.

2a. REPORT SECURITY CLASSIFICATION: Enter the overall security classification of the report. Indicate whether "Restricted Data" is included. Marking is to be in accordance with appropriate security regulations.

2b. GROUP: Automatic downgrading is specified in DoD Directive 5200.10 and Armed Forces Industrial Manual. Enter the group number. Also, when applicable, show that optional markings have been used for Group 3 and Group 4 as authorized.

3. REPORT TITLE: Enter the complete report title in all capital letters. Titles in all cases should be unclassified. If a meaningful title cannot be selected without classification, show title classification in all capitals in parenthesis immediately following the title.

4. DESCRIPTIVE NOTES: If appropriate, enter the type of report, e.g., interim, progress, summary, annual, or final. Give the inclusive dates when a specific reporting period is covered.

5. AUTHOR(S): Enter the name(s) of author(s) as shown on or in the report. Enter last name, first name, middle initial. If military, show rank and branch of service. The name of the principal author is an absolute minimum requirement.

6. REPORT DATE: Enter the date of the report as day, month, year, or month, year. If more than one date appears on the report, use date of publication.

7a. TOTAL NUMBER OF PAGES: The total page count should follow normal pagination procedures, i.e., enter the number of pages containing information.

7b. NUMBER OF REFERENCES: Enter the total number of references cited in the report.

8a. CONTRACT OR GRANT NUMBER: If appropriate, enter the applicable number of the contract or grant under which the report was written.

8b, 8c, & 8d. PROJECT NUMBER: Enter the appropriate military department identification, such as project number, subproject number, system numbers, task number, etc.

9a. ORIGINATOR'S REPORT NUMBER(S): Enter the official report number by which the document will be identified and controlled by the originating activity. This number must be unique to this report.

9b. OTHER REPORT NUMBER(S): If the report has been assigned any other report numbers *(either by the originator or by the sponsor)*, also enter this number(s).

10. AVAILABILITY/LIMITATION NOTICES: Enter any limitations on further dissemination of the report, other than those imposed by security classification, using standard statements such as:

(1) "Qualified requesters may obtain copies of this report from DDC."

(2) "Foreign announcement and dissemination of this report by DDC is not authorized."

(3) "U. S. Government agencies may obtain copies of this report directly from DDC. Other qualified DDC users shall request through _____."

(4) "U. S. military agencies may obtain copies of this report directly from DDC. Other qualified users shall request through _____."

(5) "All distribution of this report is controlled. Qualified DDC users shall request through _____."

If the report has been furnished to the Office of Technical Services, Department of Commerce, for sale to the public, indicate this fact and enter the price, if known.

11. SUPPLEMENTARY NOTES: Use for additional explanatory notes.

12. SPONSORING MILITARY ACTIVITY: Enter the name of the departmental project office or laboratory sponsoring *(paying for)* the research and development. Include address.

13. ABSTRACT: Enter an abstract giving a brief and factual summary of the document indicative of the report, even though it may also appear elsewhere in the body of the technical report. If additional space is required, a continuation sheet shall be attached.

It is highly desirable that the abstract of classified reports be unclassified. Each paragraph of the abstract shall end with an indication of the military security classification of the information in the paragraph, represented as *(TS), (S), (C), or (U)*

There is no limitation on the length of the abstract. However, the suggested length is from 150 to 225 words.

14 KEY WORDS: Key words are technically meaningful terms or short phrases that characterize a report and may be used as index entries for cataloging the report. Key words must be selected so that no security classification is required. Identifiers, such as equipment model designation, trade name, military project code name, geographic location, may be used as key words but will be followed by an indication of technical context. The assignment of links, rules, and weights is optional.